Experimental Studies on Utilization of Used Transformer Oil as an Alternative Fuel in a DI Diesel Engine

A Thesis

Submitted by

PRITINIKA BEHERA

(Roll Number: 509ME106)

In Partial Fulfillment of
the Requirement for the Degree

of

DOCTOR OF PHILOSOPHY

Department of Mechanical Engineering
National Institute of Technology
Rourkela - 769 008
India
May 2013

Experimental Studies on Utilization of Used Transformer Oil as an Alternative Fuel in a DI Diesel Engine

A Thesis

Submitted by

PRITINIKA BEHERA

(Roll Number: 509ME106)

In Partial Fulfillment of
the Requirement for the Degree

of

DOCTOR OF PHILOSOPHY

Under the Supervision of

PROF. S. MURUGAN

Department of Mechanical Engineering
National Institute of Technology
Rourkela -769 008
India
May 2013

Dedicated to

My Son Tejash Mishra

Department of Mechanical Engineering
National Institute of Technology
Rourkela -769 008
India

BONAFIDE CERTIFICATE

Certified that this thesis titled "**Experimental Studies on Utilization of Used Transformer Oil as an Alternative Fuel in a DI Diesel Engine"** is a bonafide work of Mrs. Pritinika Behera who carried out the research work under my supervision. It is also certified that to the best of my knowledge the work supported here in does not form part of any other thesis or dissertation on the basis of which a degree or award was conferred on an earlier occasion for this or any other candidate.

Supervisor

Prof. S. Murugan
Department of Mechanical Engineering
National Institute of Technology
Rourkela - 769008

ACKNOWLEDGEMENT

I would like to express my heartful and sincere thanks to my supervisor Prof. S. Murugan for giving me an opportunity to work in this interesting research work. I am also thankful his valuable guidance, inspiration, constant encouragement, heartfelt good wishes and support through all the phases my research work.

I am ever grateful to Dr. Sunil Kumar Sarangi, Director who motivated me to do research work and given me a constant support all time during this study. I also sincerely thank Prof. K.P. Maity, Head, Department of Mechanical Engineering and Prof. R.K. Sahoo for his constant encouragement to complete my research work successfully.

I take this opportunity to express my deep sense of gratitude to the members of my Doctoral Scrutiny Committee members, Prof. Pradip Rath, Chemical Engineering Department, Prof. Alok Sathpathy, Mechanical Engineering Department, and Prof. Mithilesh Kumar, Metallurgical and Materials Engineering Department for their valuable suggestion while carrying out this research work. My special thanks to Mr. P.K. Sahu, Assistant Engineer, Electrical Department, Estate Office of NIT Rourkela, for providing used transformer oil for my research work. I am thankful to Dr. S.K. Sahu, Mechanical Department, IIT Indore, for the moral support and inspiration. I would like to thank Mr. N.P. Barik, Mr. Ramkrishna Mandal and Mr. Laxman Kumar Mohanta and other supporting staff for their constant help throughout the work.

I would like to express my gratitude to my research colleagues Mr. R. Prakash and Mrs. Dulari Hansdah for their assistance in my research work. I am also thankful to my other research colleagues for their support and good wishes.

This work is also the outcome of the blessing guidance and support of my father Mr. Dushasan Behera, my mother Mrs. Leela Behera and my brother Mr. Sudeep Behera. This work could have been a distant dream if I did not get the moral support and help from my husband, Mr. Debabrata Mishra, who has equally shared my success and failures with me.

(Pritinika Behera)

ABSTRACT

Reuse and recycling are better options to derive energy or value added products from waste substances and to minimize the disposal problems. Transformer oil is generally used as a coolant in welding transformers, power transformers and electromotive units. After a prolonged use in these devices, the transformer oil becomes waste and is disposed of. The disposal of used transformer oil (UTO) causes an environmental pollution. However, the UTO has properties that are similar to that of diesel fuel with a marginally higher viscosity and lower calorific value. The present investigation is aimed to reuse the UTO as a possible source of energy to run a small powered, single cylinder, four stroke, air cooled, direct injection (DI) diesel engine. Different techniques such as blending, operating the engine with different injection timings, nozzle opening pressures, compression ratios, preheating and dual fuel mode were adopted to study the engine behavior in terms of combustion, performance and emission when the engine is fueled with the UTO. The results are analyzed and compared with diesel operation of the same engine and presented in this thesis.

Initially, UTO and six of its diesel blends on varying the UTO concentration from 10% to 60%, at a regular interval of 10% by volume basis was used. Increase in thermal efficiency with significant improvement in reduction of smoke was observed for UTO and its diesel blends compared to that of diesel. The nitric oxide (NO) emission was found to be higher for UTO and its diesel blends than that of diesel. Ignition delay was marginally shorter for the UTO and its diesel blends than diesel. The higher NO emission was due to advancement of injection timing as a result of bulk modulus characteristics of the UTO.

Secondly, UTO was operated at different injection timings of advanced and retarded injection timings for maximum of 3 degree crank angle (^{o}CA) at a regular interval of 1.5 ^{o}CA from the original injection timings of 23 ^{o}CA bTDC. When compared to the standard injection timing of 23^{o}bTDC and other injection timings tested for UTO, the retarded injection timing of 20^{o}bTDC resulted in a reduction in the NO emission by about 1.4% at an expense of smoke emission and brake specific energy consumption by about 6.7% and 1.1% respectively at full load. The ignition delay of UTO overall

longer by about 1.3 ^{o}CA for retarded injection timings while shorter for advanced injection timings by about 1.8 ^{o}CA than that of diesel operation at maximum brake power.

As the NO emission was lower, and the smoke emission was higher, for the UTO, the engine was operated with UTO at higher nozzle opening pressures varying from 200 bar to 250 bar at a regular interval of 10 bar in the third technique. These results in higher brake thermal efficiency, higher NO emission and lower smoke emissions with UTO230 bar than that of UTO at 200 bar which is a standard nozzle opening pressure set by the manufacturer. The maximum heat release and the maximum cylinder pressure at 230 bar are found to be higher than that of UTO at 200 bar. In comparison with diesel operation, UTO at 230 bar operation gave a higher NO and lower smoke.

Further as a fourth technique, the engine fueled with the UTO was tested at two different lower compression ratio viz 16:1 and 17:1 by varying the clearance volume. The engine was also run at a higher compression ratio of 18.5:1 in addition to the standard compression ratio of the engine. The results indicated that increasing compression ratio increases the thermal efficiency, NO emission and reduced smoke emission. The optimum compression ratio was found to be 18.5:1. With this compression ratio, the NO emission was found to be increased by about 3.1% and 30.6% respectively than that of the UTO and diesel. The smoke emission was found to decrease by about 8.6% and 49% respectively compared to that of the UTO and diesel at maximum brake power.

In the fifth technique, the high viscosity of the UTO was reduced by preheating, before it was allowed into the fuel supply system of the diesel engine. The UTO was preheated at four different temperatures, varying from 80 to 110^{o}C at regular intervals of 10^{o}C. The combustion, performance and exhaust emissions of the engine were evaluated using the UTO (with and without preheating). Preheating the UTO at 90^{o}C gave a better performance and lower smoke emission at a cost of higher NO emission, than other preheating temperatures.

Finally, the engine fueled with UTO was operated on a dual fuel mode attempted in the investigation. Acetylene was inducted as primary at three different flow rates along with the air, to study the combustion, performance and emission behavior of the

diesel engine, while the UTO was injected as pilot fuel with the optimized injection timing. The acetylene flow rates used in the study were 132 g/h, 198 g/h, 264 g/h and 330 g/h and 330 g/h. The experimental results were compared with diesel with acetylene in the dual fuel operation in the same engine. Acetylene aspiration resulted in reduction in ignition delay by about 3 ^{o}CA, and 25% higher cylinder pressure at full load. Smoke was reduced by about 13.7%, in comparison with the UTO operation at maximum brake power. As a whole comparing the results obtained from each technique, it is suggested that the engine fueled with the UTO at 230 bar nozzle opening pressure gave a better performance and lower emissions than the other techniques.

Key words: Used transformer oil, blending, injection timing, injection pressure, compression ratio, preheating, acetylene, combustion, performance and emission.

CONTENTS

LIST OF FIGURES

LIST OF TABLES

NOMENCLATURES

ADC	Analog to digital converter
ASTM	American society for testing and materials
BDC	Bottom dead centre
BP	Brake power
BSEC	Brake specific energy consumption
BSFC	Brake specific fuel consumption
bTDC	Before top dead center
CA	Crank angle
CAGR	Compound annual growth
CI	Compression ignition
CNG	Compressed natural gas
CO	Carbon monoxide
CO_2	Carbon dioxide
DEE	Diethyl ether
DI	Direct injection
DTPO	Distilled tire pyrolysis oil
EGR	Exhaust gas recirculation
EGT	Exhaust gas temperature
FBP	Final boiling point
FT-IR	Fourier transform infrared
GC-MS	Gas chromatography mass spectrometry
GDP	Gross domestic product
GHG	Greenhouse gas
GNP	Gross national product
HC	Hydrocarbon
IBP	Initial boiling point

LED	Light emitting diode
LHV	Lower heating value
LPG	Liquefied petroleum gas
m_a	Mass of air consumption
m_f	Mass of fuel consumption
MgO	Magnesium oxide
MSW	Municipal solid waste
NDIR	Non dispersive infrared
NO	Nitric oxide
O_2	Oxygen
PC	Personal computer
SI	Spark ignition
SMD	Sauter mean diameter
TDC	Top dead centre
TIC	Total ion chromatogram
TPO	Tire pyrolysis oil
ULO	Used lubricating oil
UTO	Used transformer oil
WLO	Waste lubricating oil
WPO	Waste plastic oil

CHAPTER 1
INTRODUCTION

1.1 General

Once man discovered the use of heat in the form of fire, it was just a step to formulate the energy interactions. With this, human beings started to use heat energy for cooking, warming up living spaces, drying and so on. Further, due to the development of civilization and increase in population, man had to move from one place to another. Animals were used as vehicles developed in Sumer between the 4^{th} and 5^{th} centuries BC, and spread to Europe and other countries in the 5^{th} century BC and China in about 1200 BC.

Gradually, man replaced the animals with motive power that was used in transportation. The use of power vehicles began in the late 18^{th} century, with the creation of the steam engine. The early history of the automobiles can be phased into a number of eras, based on the prevalent means of propulsion. The invention of Otto and Diesel cycles in the 19^{th} century transformed the method of propulsion from steam to petroleum fuel. As a result of increased vehicle population and other utilities, like gensets, the use of petroleum fuels becomes necessary. Also, to generate electricity, the use of other fossil fuels was explored by man. Table 1.1 gives the history of automotive vehicles used in land transportation. Gasoline and diesel have been used as primary fuels in automotive, farm and recreational vehicles in the last two centuries.

Table 1.1 Automobiles used in land transportation [1].

Century	Type of vehicles
17^{th}	Steam powered vehicle
18^{th}	Steam-driven artillery tractor
19^{th}	Oil-fired steam car, four-stroke petrol engine, four stroke diesel engine.
20^{th}	Advanced diesel and petrol engine
21^{st}	Modern energy sources controlled with computerized controls, such as advanced electric batteries, fuel cells, photo voltaic, bio-fuels or others.

During the 18th and 19th centuries, the revolution in industrialization necessitated large consumption of energy sources such as coal, crude oil, hydro and nuclear for power generation and automobile applications. Thus, the consumption of energy increased globally in the 20th century.

1.2 Impact of energy consumption in industries

The energy consumption in terms of oil and other energy sources is growing drastically, and it is projected to increase by 36% in the world by the year 2035 [2]. The growing demand is caused by an exponential increase in the population that is predicted to increase further by 25% in the next 20 years, with major population increases, particularly in China and India. Energy in the form of electricity or mechanical energy is used in all the houses in the developed countries and the majority in developing countries [2].

1.2.1 World energy scenario

Figure 1 portrays the percentage of increase in energy and population over the years in the 20th century. It can be observed from the figure that as the population increases, the percentage of energy consumption also increases.

Energy consumption is directly correlated with the gross national product (GNP) and climate, but there is a large difference even between the developed countries. For example, the energy consumption rate is approximately 1.4 kW per person in the USA and it is 6 kW per person in Germany and Japan. In developing countries, particularly those that are sub-tropical or tropical such as India, the per person energy use rate is closer to 0.7 kW. Bangladesh has the lowest consumption rate with 0.2 kW per person. The US consumes about 25% of the world's energy with a share of global gross domestic product (GDP) at 22% and a share of the world population at 4.59%. The most significant growth of energy consumption is currently taking place in China, which has been growing at 5.5% per year over the last 25 years. Its population of 1.3 billion people (19.6% of the world population) is consuming energy at a rate of 1.6 kW per person.

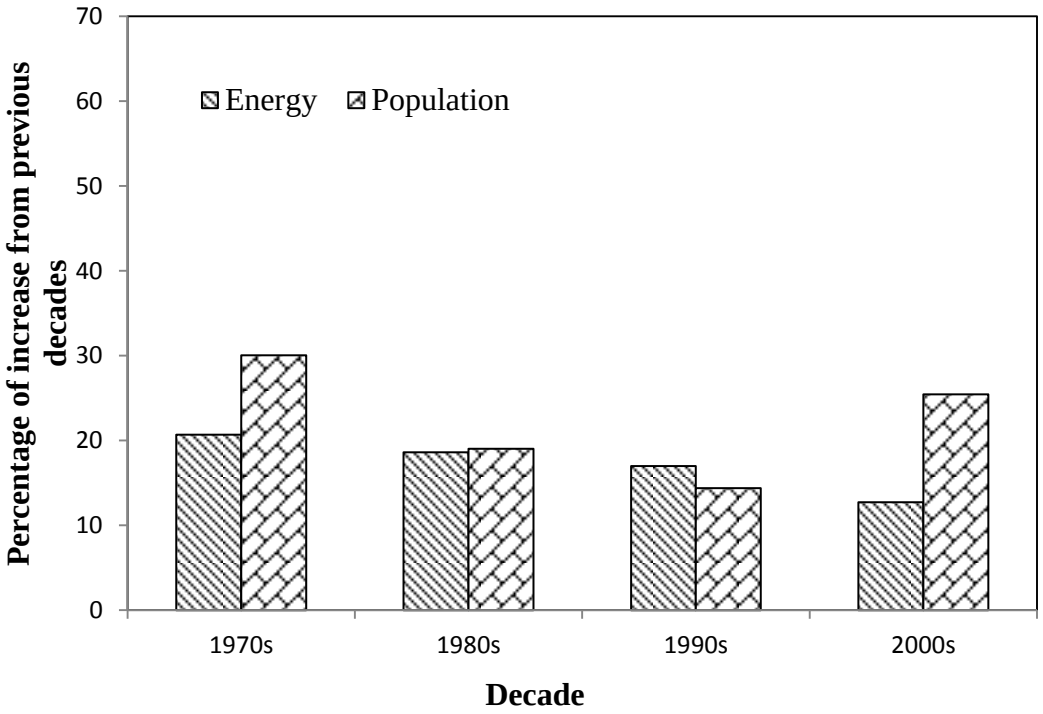

Figure 1.1 Percentage of increase in energy and population with decade variation [3].

Table 1.2 indicates that the consumption of fossil fuels increased progressively from the year 1980 to 2010. If the availability of the fossil fuel is considered, then the gap between the supply and demand is huge.

Table 1.2 Energy consumption of fossil fuel [4]

Fuel type	**Global energy consumption (T/y)**				
	1980	**2004**	**2006**	**2008**	**2010**
Coal	1.46	33.95	45.26	42.71	24.09
Gas	1007.77	1141.36	1107.41	1187.35	1207.79
Oil	1703.46	2006.41	1989.61	1856.39	1793.25
Nuclear power	136.51	409.53	409.17	419.75	420.12
Total	2849.2	3591.25	3551.45	3506.2	3445.25

1.2.2 Energy scenario in India

One measurement of efficiency is energy intensity, which is a measure of the amount of energy it takes a country to produce a dollar of gross domestic product. As India continues to develop, there is a huge demand for energy against the supply. By

the year 2030, India is likely to have a GDP of USD 4 trillion and a population of 1.5 billion. This will increase the demand for critical resources such as coal and oil, with a parallel increase in the greenhouse gas (GHG) emissions. Considering the growth of India by the year 2030, the country needs to enhance its energy security and create a few cleaner technologies, and reduce the emissions from the burning of fossil fuels [5].

With its continuous growth, India's total energy demand is likely to reach around 1.8 billion tones a year in 2030, up from 0.5 billion tones in 2005, even after assuming the efficiency improvements that will occur. This will make India the third largest energy consumer in the world, after the United States and China. This would mean that India's share of world consumption would nearly energy double, and thus India would have to find and secure energy resources much faster than other countries.

This demand growth will greatly increase energy requirements. India's coal demand by 2030 is likely to be 60% higher than the projected domestic production of about 1.5 billion tonnes per annum by the same year. This shortage will have to be met with equivalent coal imports. Further, given India's limited oil reserves, more than 10 times India's domestic supply of oil may have to be imported. Such a high level of energy import will lead to difficulties in ensuring India's energy security. There would also be the challenge of expanding coal mining in India more than three times to reach approximately 1.5 billion tonnes of coal production per annum. The growth in the energy consumption and the resulting increase in the fossil fuel supply, would increase India's GHG emissions. It is reported that the GHG emissions would also increase from roughly 1.6 billion tonnes carbon dioxide equivalent (CO_2) in the year 2005 to 5.0 to 6.5 billion tonnes (CO_2) in the year 2030. The power sector will be the biggest emitter, generating more than 50% of emissions, i.e., 2.9 billion tonnes (CO_2) by 2030, as over 60% of power capacity is likely to remain coal-based [6].

Solutions for reducing the emissions should also increase India's energy security, e.g., a reduction in crude oil consumption would reduce emissions as well as imports. The use of alternative energy sources would substantially reduce the crude oil consumption. Reports indicate that there is a potential for a 40% reduction in crude oil consumption by road transport, correspondingly reducing India's oil imports and

lowering the import bill by around USD 35 billion (at USD 60 barrel) in the year 2030.

1.3 Impact of energy consumption on pollution

1.3.1 Air pollution

Air pollution is the discharge of chemicals, particulates, or biological materials into the atmosphere, causing discomfort, disease, or death to humans, and damage to other living organisms such as food crops, the natural environment or the built environment [6]. A substance in the air that can be harmful to mankind and the environment is known as an air pollutant. The pollutants can be in the form of solid particles, liquid droplets, or gases. They may be natural or man-made. The pollutants can be classified as primary or secondary. Usually, primary pollutants are directly emitted from a process, such as ash from a volcanic eruption, carbon monoxide gas from a motor vehicle exhaust or sulphur dioxide from factories. The secondary pollutants are not emitted directly. Rather, they form in the air when the primary pollutants react or interact. The main sources of air pollution are the thermal power plants, automotive vehicles, refrigeration and air conditioning systems. Apart from these, other sources such as nuclear weapons, rocketry and dust from natural sources, usually large areas of land with little or no vegetation and smoke and carbon monoxide from wild fires etc., also contribute to air pollution [7].

1.3.2 Land pollution

The increase in population creates demand for domestic appliances and many other products which necessitate the establishment of large industries in urban areas. The disposal of solid, liquid or gaseous waste materials in open land or underground can contaminate the soil and ground water, threaten public health, and cause unsightly conditions. The waste materials that cause land pollution are broadly classified as municipal solid waste (MSW, also called municipal refuse), construction and demolition waste (or debris), industrial waste, and hazardous waste. MSW includes non-hazardous garbage, rubbish, and trash from homes, institutions (e.g., schools), commercial establishments, and industrial facilities. Automobile tyres, used oils and chemical fabrics are some of the examples of industrial waste. Garbage contains moist and decomposable (biodegradable) food wastes (e.g., meat and vegetable scraps);

rubbish comprises mostly dry materials such as paper, glass, textiles, and plastic objects; and trash includes bulky waste materials and objects that are not collected routinely for disposal (e.g., discarded mattresses, appliances, and pieces of furniture). Construction and demolition waste (or debris) includes wood and metal objects, wallboard, concrete rubble, asphalt, and other inert materials produced when structures are built, renovated, or demolished. Hazardous wastes include harmful and dangerous substances generated primarily as liquids, but also as solids, sludges, or gases by various chemical manufacturing companies, petroleum refineries, paper mills, smelters, machine shops, dry cleaners, automobile repair shops, and many other industries or commercial facilities. Some of these wastes are recyclable, while others spoil the fertility or nature of the land or create anthropogenic gases that are harmful to the human beings.

1.3.3 Water pollution

Water pollution is the contamination of water bodies. Some of the examples of water bodies are: lakes, rivers, oceans, aquifers and ground water. Water pollution occurs when pollutants or waste disposals are discharged directly or indirectly into water bodies without adequate treatment to remove harmful compounds. Water pollution affects the plants and organisms living in these water bodies.

1.4 Environmental problems

The results of environmental pollution include global warning, ozone depletion, human health problems, death of forests, and infertility of the soil [8]. The major environmental concerns are acid rain and the “death of the forest” [7].

1.5 Need for alternative fuels

One of the most important issues that affect the world economy and politics is the sustainability of energy. The conventional energy sources are mainly considered for heat and power applications. However, due to the depletion of fossil fuels and increased awareness of environmental problems, the world is looking to use alternative fuels in the form of renewable and or non-conventional fuels. Renewable energy sources are derived from natural sources like sun, water, wind and biomass,

while non-conventional fuels may be derived from some other methods such as thermo chemical conversion, thermoelectric or thermionic conversions etc.

Energy can be derived from waste organic substances, which are considered non-conventional fuels. Though, the contribution of energy or fuel derived from waste is not significant, it can reduce the environmental problems considerably.

1.6 Energy through waste management

Waste management is the collection, transport, processing or disposal, management and monitoring of waste materials. The term usually relates to the materials produced by human activity, and the process is generally under taken to reduce their effect on health, environment or aesthetics. Energy can be recovered from waste sub organic substances that are present in municipal, industrial or domestic waste. Several researchers have shown interest in recovering energy from wastes. Some of the examples include gasification of industrial waste to produce power, biogas, production from agriculture and food waste, and liquid fuels from industrial, municipal or agriculture waste by pyrolysis.

1.6.1 Used oils

Waste or used oils represent a considerable portion of the organic waste generated in the world. Used oil is a semi-solid or liquid consisting totally or partially of mineral oil or synthesized hydrocarbons (synthetic oils), oily residues from tanks, and oil-water mixtures and emulsions. Used oils originate from diverse sources, which include petroleum refining operations, including sumps, gravity separators, and the cleaning of storage tanks, the forming and machining of metals, small generators, electrical transformers, welding transformers, and rural farm equipment. These oils are used in various devices for lubrication, hydraulics, heat transfer, electrical insulation (dielectric) or other purposes. The characteristics of these oils change during use, and hence, they become unsuitable for further use in the same applications. Used oils may be of two broad categories from mineral oils, (i) vegetable oil and (ii) synthetic oils. The synthetic oils may cover a wide range of chemicals. The examples are (i) synthetic hydrocarbons (ii) hydrocarbon esters (iii) phosphate esters (iv) glycols (v) chlorinated hydrocarbons and (vi) silicone oils.

Used oils may cause significant detrimental effects on the environment if they are not properly handled, treated or disposed of; used oil primarily contains hydrocarbons. It may also contain chemicals, additives, (i.e: lead) and impurities due to the physical contamination and chemical reactions occurring during its use. The contamination of used oil may also occur from mixing it with other oily fluids or liquid wastes. The processing of used oils has been practised for many years. For example, recycling of engine lubricating oil from vehicle fleets was well established in the 1930s. Certain used oils leaking from oil refinery sites have been stored into "crude ponds" and recycled.

Used oils can be converted into useful energy or value added products by proper waste management methods, which are (i) direct use (ii) reprocessing (iii) reclamation (iv) regeneration and (v) refining [8].

1.6.2 Direct use

It is the simplest way of using oils for recovering heat or value added products, if the oil content is high. Certain types of waste oils, lubricants in particular, can be processed for direct reuse. Some used oils, after treatment; can have high energy content; clean burning fuel; or a lube base stock comparable to highly refined virgin oil. Used oils from synthetic oils are similar in composition to used oils from petroleum based oils but they are synthesized using chemical processes, in which basic carbon and hydrogen compounds are combined. Generally, they are mixed with petroleum distillate feed stocks and used as secondary fuels.

1.6.3 Reprocessing

Reprocessing is the improvement of oil quality by suitable physical and chemical methods. Collecting used oil from non-industrial sources and small generators is very difficult, and requires a well-established and efficient infrastructure. In reprocessing, relatively simple physical/chemical treatments such as settling, dehydration, flash evaporation, filtration, coagulation and centrifugation are applied to remove the basic contaminants in the used oils. The contaminants removed in this process are disposed of in smaller quantities in a proper way. The objective is to clean the oil to the extent necessary for small applications. Direct reprocessing is not feasible for mixed oils;

therefore, the segregation of different used oils is essential. The reprocessed oils are used in several industrial applications.

1.6.4 Reclamation

Reclamation usually involves the treatment to separate solids and water from a variety of used oils. The methods adopted may include heating, filtering, dehydrating and centrifuging. The reclaimed oil is generally used as a fuel or fuel extender. The reclamation of used oils can give a product of quality comparable to the original oil but may contain various contaminants depending on the nature of the process, such as heavy metals, by-products of thermal breakdown and substances associated with specific uses (e.g. lead, corrosion inhibitors).

1.6.5 Regeneration

It is a method of producing base oils from the used oils. In this method, sequences of processes are adopted to remove contaminants, oxidation products and additives for the production of lubricating products. These processes include pre-distillation, treatment with acids, solvent extraction, contact with activated clay and hydro treating. The regeneration of the used oils is widely practised to get the maximum recovery of oil that has a higher commercial value. Besides the economic considerations, the oil regeneration technologies depend on the quality of the used oil. The presence of many oils and chlorinated hydrocarbons can seriously affect the technical performance of the regeneration process, and its ability to produce a good quality of lubricating oil or similar products. All the regeneration processes involve the application of reasonably sophisticated technology, and require care and expertise in their operation.

1.6.6 Re-refining

In this method, the used oil is heated, de-watered and vacuumed distilled into separate grades of distilled oil. These oils may then be hydro-treated to produce a fine clear product. The by-products which have a marginal value include, distillation bottoms (used as an asphalt extender or in fuel oil blending) and demetallized filter cakes (used as road base material). The remainders of the materials are residues or wastes, such as acid tar, spent clay, centrifuged sludge and process water that are

disposed of. As the re-refining process requires sophisticated technology or modern equipment, the overall cost is higher than that of other methods.

The re-refining processes may not be viable for small quantities of motor or used oils. The oil yield and quality differ with respect to the technology employed. The three most commonly used re-refining technologies with respect to the reduction of waste, the energy required for the process, the operating cost and the minimum hazardous material used, are given below:

- the acid/clay re-refining process
- the vacuum distillation/clay process
- hydro treating process (hydro processing)

The above three methods are discussed briefly in the subsequent sections;

1.6.6.1 Acid clay refining process

The acid/clay process has been used for many years. It is not highly sophisticated and is appropriate for a wide range of applications, and therefore, is readily adopted in many countries. However, studies on the use of the byproducts report that the acid/clay process is a poor 'environmental' process compared to the other re-refining processes. The main reason for this is the large quantity of acid tar produced as a byproduct, which cannot be easily disposed of. Hence, it is highly recommended not to use such a process in case there is no or inadequate capacity or facility to treat and dispose of the acid sludges resulting from the process.

1.6.6.2 Vacuum distillation

It is the distillation of oil in the absence of oxygen which lowers the necessary operating temperature and reduces the problems of thermal breakdown. Clays with a high adsorptive capacity are used to remove impurities, such as heavy metals and the breakdown products arising from the use of oil. They are frequently used before distillation to provide a cleaner feed, and also to yield oil with a high degree of refinement.

1.6.6.3 Hydro processing

This requires the presence of hydrogen and an active catalyst. Compared to thermal processes, hydro processing is more flexible, giving higher yields of liquid fractions. An optimum yield of products from hydro processing can be obtained, by properly matching the type of reactor and catalyst with the properties of heavy feeds. Several types of catalytic reactors, i.e., fixed, moving and ebullated-bed reactors are available commercially.Table1.3 gives the information on oils which are refinable and non-refinable.

Only some of the waste oils can be used as secondary fuels. If the fuels from waste or used oils are to be used, then those oils have to be evaluated for the physical properties and the pollutants resulting from them when they are to be used as fuels in combustion devices. Table 1.3 describes about the used oils commonly re-refined by the Canadian association of re-refiners.

Table 1.3 Used oils commonly re-refined by the Canadian association of re-refiners [9]

Re-refinable oils	**Non-Re-refinableoils**
High Viscosity Index Oils	Oils Containing Polychlorinated
All diesel and gasoline crankcase oils	Biphenyls and Polynuclear
	Aromatics
Transmission oils	LVI and MVI oils
Hydraulic oils (non-synthetic)	Halides
Gear oils (non-fatty)	Synthetic oils
Transformer oils	Brake fluids
Dryer Bearing oils	Fatty oils
Compressor oils	Asphaltic oils
Turbine oils	Black oils
Machine oils (non-fatty)	Bunker oils
Grinding oils (non-fatty)	Metal working oils containing fatty acids
Quenching oils (non-fatty)	Form oils
	Rolling oils
	Solvents of any type

The environmental risks associated with the burning of such oils can be reduced through any one of the following methods;

(i) Blending of used oil with petroleum fuels.
(ii) Pretreatment of used oil to meet the established quality specifications (e.g. settling, centrifugation, vacuum distillation, and solvent extraction).
(iii) Installation of exhaust gas emission control devices in the combustion devices.

The important factors considered for the selection of used oil as secondary fuel are as follows;

(i) Type and quality of feedstock.
(ii) Techno economic aspects [4].
(iii) Infrastructure for collection, storage and transportation.
(iv) Public health
(v) Environmental concerns
(vi) Availability of cleaner production methods.

1.7 Present investigation

As mentioned in sections 1.2 and 1.3, energy is consumed on a large-scale at present. Particularly, energy consumption increases day by day. Electrical power generation is expected to increase every year. As a result of this, electrical transformers are used in transmission of power which will lead to increase in number of transformers significantly. Generally, oil cooled transformers are in use. Electrical transformers are also used in welding and electromotive units. The disposal quantity will increase as the number of transformers increases. The energy available in the used transformer oil (UTO) can be trapped by reusing it by an appropriate method in a combustion device particularly for a stationary compression ignition (CI) engines.

The objectives of the present work are as follows:

(a) To characterize the UTO for its use as an alternative fuel for compression ignition (CI) engines by analyzing the physic-chemical properties and compare with diesel properties.
(b) To identify the chemical compounds present in the UTO by Fourier transform infrared (FTIR), Gas chromatography-mass spectrometry (GC-MS), and also to study the Sauter mean diameter of the UTO.

(c) To study the combustion, performance and emission characteristics of a single cylinder, four stroke, air cooled, direct injection (DI) diesel engine to obtain reference data of the test engine.

(d) To study the combustion, performance and emission characteristics of a single cylinder four stroke, air cooled, DI diesel engine fueled with the UTO and diesel blends. The blend percentage of the UTO was varied from 0% to 60% on a volume basis in the blend. Also, to find the optimum blend ratio of the UTO and its diesel blends by comparing the results with diesel operation in the same engine.

(e) To study the combustion, performance and emission characteristics of a single cylinder four stroke, air cooled, DI diesel engine fueled with the UTO by three different engine modifications viz, (i) Operating the engine with the UTO at different injection timings. (ii) Operating the engine fueled with the UTO at different nozzle opening pressures (iii) Operating the engine with the UTO at different compression ratios.

(f) Further to study the combustion, performance and emission characteristic of the diesel engine fueled with the UTO at different preheating temperatures.

(g) To study the combustion, performance and emission characteristic of the diesel engine fueled with the UTO on dual fuel mode by inducting acetylene at different flow rates.

(h) To compare the results of combustion, performance and emissions obtained from the engine fueled with UTO at different conditions, with fuel and engine modifications.

1.8 Organization of thesis

Chapter 1 gives the introduction to the importance of energy, environmental pollution, need for alternative fuels, and conversion of waste to energy.

Chapter 2 presents the literature survey on diesel engine fuels and waste oils.

Chapter 3 discusses the characterization of the UTO. It also includes the FT-IR and GCMS analyses of the UTO.

Chapter 4 details the experimental investigation adopted in this study.

Chapter 5 presents the methodologies of this work, and the different techniques adopted, such as blending, change of injection timing, injection pressure compression ratio, preheating and converting a diesel engine to the dual fuel mode with acetylene.

Chapter 6 discusses the results that are obtained for the combustion, performance and emission parameters of the UTO fueled engine at different operating conditions in comparison with diesel operation of the same engine.

Chapter 7 discusses the conclusions drawn from the above studies, and the scope for future work.

CHAPTER 2
LITERATURE SURVEY

2.1 General

This present study is novel in its field. Hence, as a consequence, the available literature in this field is limited. The researcher has gone through various research articles and documents that are useful to understand development of the CI engine, the theory related to the use of alternative fuels in CI engines and apply them in the research work. This chapter discusses the review of previous literature available, pertaining to the development of alternative fuels and their use in CI engines.

2.2 Development of CI engines

CI engines are used largely in different sectors such as transportation, power generation, industrial and commercial, because of their higher thermal efficiency and durability than the spark ignition (SI) engines [10]. However, due to an increase in fuel consumption, there is a steep rise in fuel costs. Hence, the use of alternative fuels may be beneficial in reducing dependency on diesel fuel.

Akroyd-Stuart [11] developed a vaporizer engine in 1891, which was the first oil engine to run without a spark for ignition, relying on an externally heated vaporizer in the cylinder head to start the engine. External heating was only needed for starting, as the combustion maintained the vaporizer at a high temperature while the engine was running. A patent was registered in the year 1890, describing that there was no risk of premature ignition of an explosive mixture. Near the end of the compression stroke, liquid fuel was sprayed onto the heated vaporizer, where it vaporized and mixed with the hot air, igniting automatically and propelling the piston on its-power stroke.

The diesel engine was invented by Dr. Rudolf Diesel [12]; it could be run on a variety of fuels. In the beginning, diesel engines were used in industrial, marine and railway installations in isolated locations across the world. Shortage of gasoline in Germany after the year 1918, stimulated developments of CI engines in that country. Interest spread to

European countries, stimulating development of diesel engines specifically for road transport. By the year 1930, there were significant numbers of diesel powered trucks and buses in service.

In the year 1939, the automotive diesel was well established in Europe, but had limited use in the military. Ricardo Comet patented in 1931 a new design of engine whose operation and freedom from smoke was a significant improvement on previous designs of diesel engine and was adopted by a number of British diesel engine manufactures. Europe and Japan have experienced a significant growth in the number of passenger cars fitted with diesel engines in the last 30 years. Today, diesel engines are ubiquitous.

2.3 Phenomenon of combustion in diesel engines and the effect of fuel properties

The CI engine is a heat engine in which the chemical energy possessed by the fuel is converted into heat energy by combustion process and further converted into mechanical power by the piston displacement [7]. The complex heterogeneous combustion process occurs in the combustion chamber with a series of small explosions called combustions, as the fuel reacts chemically with oxygen from the air, and ignites. Once the fuel-air mixture is ignited, the hot combustion gases expand, driving the piston downward, producing mechanical work and subsequently leaving the cylinder of the engine.

CI engine behaviour depends on the fuel properties, combustion and engine geometry etc., Properties such as Cetane number, viscosity, density, heating value, sulphur content, aromatic content, flash and fire point, pour point, cloud point and distillation range are responsible for variation in the combustion behaviour of CI engine fuels [13]. When the fuel is injected in to a hot compressed air stream in a closed volume, the fuel evaporates, becomes vapour, mixes with air and then starts to ignite. There is a little time duration in crank angle in which a mixture preparation of fuel and air takes place which is known as delay period. Fuel with a higher Cetane number and low self-ignition temperature ignites more readily, providing a shorter ignition delay period. The recommended Cetane number of diesel fuel is in the range of 40-50 [14]. Fuel structure also plays an important role that affects the fuel properties which in turn influence the combustion. Viscosity and density of fuel predominantly affect the fuel supply system and fuel spray patterns. The

viscosity of diesel fuel should neither be too low nor too high. Fuels of lower viscosity can result in power loss due to the injector or pump leakage while the highly viscous fuels may result in higher pump resistance, filter clogging, carbon deposit, wear and tear of engine components and poor spray patterns. It is recommended to have the kinematic viscosity of a diesel fuel in the range of 1.9 to 4.1 centistoke (cSt) at 40^{o}C for diesel fuel [15]. The fuel consumption, power output, engine wear and the exhaust smoke are greatly influenced by density of the fuel [16].

Higher viscosity fuel affects the atomization of the fuel and spray formation [17]. The heating value or heat of combustion of diesel fuel is the measured amount of available energy content from a known quantity of fuel and is directly proportional to the fuel density. If a fuel has a higher heating value that may result in higher power output and increased economy. Two factors can be altered to change the heating values result in higher power output and increased fuel economy. The heating value of a fuel is affected by (i) carbon-hydrogen ratio, (ii) aromatic content, and (iii) distillation profile of fuel. The aromatic content of fuel also affects Cetane number. However, the aromatic content is limited by the minimum Cetane number requirement. The higher the aromatic content in the fuel the lower the Cetane number. The flash point of the fuel affects the boiling point of the fuel [18]. But, it is not related directly to engine performance. As per American Society for Testing and Materials (ASTM) D 975 the flash point of a fuel affects the storage and handling issues. The flash point should be minimum of 52^{o}C for diesel fuel. A lower flash point may result in sudden ignition when a fuel is transported in high temperature conditions.

In a CI engine, the spray formation is influenced by the volatility of fuel. The greater the volatility the better the mixing of fuel with air and, hence better combustion. The fuel volatility depends on boiling point, density and aromatic content [6]. The distillation temperature at 90% evaporation of fuels (T90) indicates the volatility of a fuel. As per ASTM procedure, the T90 of diesel fuel must be in the range of 282 to 338^{o}C. The boiling point of fuel influences some parameters that are important for combustion of diesel fuel. Changing the boiling point may affect more than one fuel property. Low boiling point temperatures may affect properties such as pour point, cloud point, flash

point and Cetane number [19]. High boiling point fuel can result in an increased smoke emission and choking of the injection nozzle. Varying the aromatic content, Cetane number and distillation temperature simultaneously may result in more nitric oxide (NO) formation and particulates in diesel engine [20].

2.4 Investigations on alternative Fuels

After continuous design and development of CI engines, improvements were carried out in order to achieve a good performance and lower emissions by varying injection pressure, injection timing, preheating, air flow, combustion chamber geometry and exhaust gas recirculation [21]. Research works carried out on the diesel fuel properties, spray characteristics, mixture formation and combustion process which are key factors [22-24]. In later development, with the introduction of alternative fuels, the diesel engines were investigated with different fuels; biodiesel and alcohols. Investigations were carried out with gaseous fuels such as Hydrogen, Acetylene, Liquefied petroleum gas (LPG), Compressed natural gas (CNG), Biogas and Producer gas with diesel fuel on dual fuel mode [25-37].

2.4.1 Vegetable oils

Detailed investigations on utilization of vegetable oils of edible and non-edible oil as alternative fuels in CI engines were investigated by several researchers [38-43]. They carried out the research works with fuel and engine modifications etc. It was reported that the raw plant oils showed a drop in power output, while some of them showed a marginal increase compared to diesel fuel. The BSFC with vegetable oils were found to be higher by about 2 to 15% in comparison with diesel fuel. The carbon dioxide emission (CO_2) were found unchanged or increased in plant oil, while the oxides of nitrogen (NO_x) emissions were found to be lower. The use of raw vegetable oils showed long term durability issues such as carbon deposition, lubrication oil dilution or thickening, piston ring sticking and injector nozzle coking. High flash point and viscosity were said to be the reasons for this. Further, researchers have adopted various techniques such as blending, emulsification and transesterification to obtain better performance, emission and durability of the CI engines. They have carriedout modifications in the engine that

include changes in injection timing, injection pressure, compression ratio, use of separate combustion chamber and exhaust gas recirculation. The use of raw vegetable oils in diesel engines were said to be successful for short term use [21, 44-46].

2.4.2 Esters of vegetable oils

Transesterification is found to be a technically feasible for utilising the vegetable oil as a CI engine fuel to a greater extent. Numerous documents are available on utilisation of biodiesel from edible and non-edible vegetable oils that were investigated by many researchers [47-65]. In summary, it was reported by many researchers that the use of biodiesel results in a reduction in engine power because of the lower heating value of biodiesel compared to diesel. The high viscosity and high lubricity of biodiesel exhibited certain effects on engine power. The injection pressure and injection timing also showed an impact on engine power. The use of a turbocharger in the engine or low heat engine exhibited an improvement in biodiesel engine economy. On durability issues, the biodiesel fueled engine was found to be better than vegetable oil fueled engines. It was mentioned that the use of biodiesel favours to improve the durability of engine due to lower soot formation and inherent lubricity in comparison with diesel. From an emission point of view, it was reported that the particulate emissions of biodiesel were found to be significantly reduced compared to diesel. The reduction was found to be smaller with the reduction of biodiesel production in the blended fuel. The reason for lower particulate emissions with biodiesel was due to a lower aromatic content, lower amount of sulphur compounds, higher cetane number, and moreover because of higher oxygen content. Many comparative studies have been performed to study the effect of biodiesel on the NO_x emissions including blended fuels [46] , three blend fuels [60] and more blends [66], Many literatures showed that the NO_x emissions increased with increase in content of biodiesel. Some of them reported that the NO_x emissions were found to be lower compared to diesel. It was reported that the content of unsaturated compounds in a biodiesel showed a greater impact on the NO_x emissions. Some researchers have investigated the effect of exhaust gas recirculation (EGR) on the NO_x emissions of biodiesel fueled engine. It was also reported that the use of EGR could reduce the NO_x emission, but they are also affected by typical increase in particulate emissions, engine

overheating, acid wear on engine etc. the change of combustion characteristics [6]. Water injection, emulsions of biodiesel with water was also investigated by few researchers [7].

2.4.3 Alcohols

Although alcohols have lower Cetane numbers, they have merits such as they are renewable in nature, oxygenated and easily producible. Considering these merits many researchers have investigated the use of alcohols (i.e., methanol, ethanol and butanol) in CI engines. They have investigated the use of alcohol with diesel and different biodiesels in the form of emulsions, solutions, dual fuel mode, surface ignition etc. [67]

Wang et al. [68] have applied methanol in diesel engines for achieving fuel diversity and reduction of engine emissions. Dual fuel application is the most promising method, but its combustion characteristics have been less extensively studied. The authors have measured the cylinder pressures of the operational engine using both diesel and dual fuel (methanol-diesel) and the engine combustion characteristics were investigated. The high methanol mass fraction showed a reduction in the smoke and NO_x emissions under all the operating conditions, whereas the carbon monoxide (CO) and unburnt hydrocarbon (HC) emissions were found to increase emissions.

Kowalewicz and Pajaczek [69] have used ethanol in a CI engine with diesel fuel, which was injected into the inlet manifold. The CO_2 and NO_x were found to decrease with increasing amount of ethanol. The optimization of the energy ratio of both fuels and injection timing of diesel fuel were also studied in the investigation.

2.4.4 Pyrolysis oils

Pyrolysis is a method of deriving alternative fuels from different feed stocks that may be available in the form of solid or liquids. It is a method of thermal degradation of the organic substance into value added products such as pyrolysis oil, pyro gas and char or carbon black. Some of the research works have been documented on the use of pyrolysis oil in CI engines. Different feed stocks such as wood, tyre, plastic, mixture of vegetable oil etc., were tried to derive pyrolysis oil [70].

Some of the common problems reported by several researchers [71-75] with the use of the pyrolysis oil or bio oil in CI engines are: (i) difficulty in starting the engine due to the poor ignition quality of pyrolysis oil or bio oil, and subsequent unstable operation, (ii) HC, CO and smoke emissions were found to be higher due to the complex hydrocarbon chain or higher aromatic content present in the pyrolysis oil, (iii) engine parts are affected due to corrosion and erosion and (iv) inferior combustion compared to diesel or coking operation.

Murugan et al. [76] have carried out tests to evaluate the performance and emission characteristics of a single cylinder, four stroke, air cooled, direct injection, diesel engine fueled with 10, 30 and 50% blends of tire pyrolysis oil (TPO) with diesel. TPO was derived from waste automobile tires through vacuum pyrolysis in one kg batch pyrolysis unit. Results indicated that the brake thermal efficiency of the engine fueled by TPO-diesel blends increased with increase in blend concentration and higher than diesel at full load. The HC, CO and smoke emissions were found to be higher at higher loads due to high aromatic content and longer ignition delay at original injection timing. The cylinder peak pressure increased from 71.4 to 73.8 bar. The ignition delays were longer than diesel.

Murugan et al. [77] have taken 80% and 90% of distilled tire pyrolysis oil (DTPO) blended with 20% and 10% diesel respectively and conducted investigations in a four stroke, single cylinder, air cooled, diesel engine without any engine modification. The performance, emission and combustion characteristics of a single cylinder, four stroke, air cooled, DI diesel engine running with the DTPO-diesel blends at higher concentrations were studied. There was approximately 3% reduction in the brake thermal efficiency. The NO emissions were found to be lower by about 18% and smoke emissions were found to be higher by about 38% compared to that of diesel at full load.

Murugan et al. [78] have done experimental investigation for TPO as an alternative fuel in a diesel engine. TPO was desulphurised and then distilled through vacuum distillation. Also, two DTPO-diesel blends at lower (20% DTPO) and higher concentrations (90% DTPO) were used as fuels in a four stroke, single cylinder, air

cooled, diesel engine without any engine modification. The results were compared with the diesel fuel (DF) operation of the same engine. Results indicated that the engine can run with 90% DTPO and 10% diesel fuel.

Hariharan et al. [79] have conducted experiments on a single cylinder, four stroke, DI diesel engine using TPO as a main fuel. Results indicated that the engine performs better and with lower emissions when DEE was admitted at the rate of 170 g/h with TPO and NO emission in TPO-DEE operation reduced by 5% compared to diesel fuel operation. The HC, CO and smoke emissions were higher for the TPO-DEE operation by 2%, 4.5% and 38% than diesel mode.

Dogana et al. [80] have studied the effect of tire-derived fuel (TDF) on engine performance and exhaust emissions in a diesel engine. The authors tested the TDF in a single cylinder, four stroke, unmodified, and naturally aspirated DI high speed diesel engine at full load and four engine speeds (1400, 2000, 2600 and 3200 rpm) by using six test fuels. The experimental test results showed that the DI diesel engine can run with the TDF fuel blends up to TDF90. The smoke opacity, HC, and CO emissions reduced while the NO_x emissions increased with the increasing TDF content in the fuel blends.

2.5 Waste oils

Literature review reveals that oils such as waste lubricating oil (WLO), waste plastic oil (WPO) have also been investigated for their use as alternative fuels in CI engines.

Arpa et al. [81] have examined WLO as an alternative fuel in a single cylinder, four-stroke, air cooled, naturally aspirated, direct injection diesel engine developing a maximum power of 10 kW at 2000 rpm. Results of the investigation indicated that there was a marginal increase in the brake thermal efficiency, brake mean effective pressure and exhaust gas temperature obtained for WLO at full load. The brake specific fuel consumption for WLO was found to be marginally lower compared to that of diesel fuel. In terms of emissions; the CO, NO and sulphur dioxide increases by about 14.7, 12.7, 22.5% whereas oxygen decreases by about 11.4%.

Tajima et al. [82] carried out an experimental investigation to utilize the used lubricating oil (ULO) as an alternative fuel in a diesel generator plant. The combustion characteristics of a diesel engine were determined by observing the burning flames in the engine, while on a test run. The results were compared with heavy fuel oil. The ULO showed better ignition quality and the smoke emission was found to be lower by about 64.71% compared to heavy fuel oil operation. However, a thick deposit of combustion products was noticed in the combustion chamber after a short run. It was suggested that a process was required to remove the additives from ULO, before utilizing it as a fuel in diesel engines.

Waste plastic oil was used an alternative fuel in a small powered diesel engine [83]. The influence of the injection timing on the performance, emission and combustion characteristics of a single cylinder, four stroke, direct injection diesel engine was studied using WPO as a fuel, at four different injection timings (23, 20, 17 and 14^{o}bTDC). In comparison with standard injection timing of 23^{o}bTDC the retarded injection timing of 14^{o}bTDC, the WPO fueled engine gave a reduction in NO_x, CO and HC emissions by about 4.4%, 25% and 30% respectively at full load. The brake thermal efficiency was found to be higher by about 4% for the WPO compared to that of diesel operation at full load. It was also noticed that the smoke emission was found to be higher by 35% for WPO than that of diesel at full load.

Mani et al. [84] have analysed the properties of WPO and compared with the petroleum products they reported that it had properties similar to that of diesel. After the analysis of oil, the WPO was used as an alternate fuel in a DI diesel engine without any engine modification. They also conducted an experimental investigation to study the performance, emission and combustion characteristics of a single cylinder, four-stroke, air cooled DI diesel engine fueled with the WPO. They analysed the results in comparison with diesel operation throughout engine operation. The experimental results have also showed a stable operation and comparable brake thermal efficiency for the WPO with that of diesel. The unburnt HC emission from the WPO fueled engine was found to be higher by about 15% compared to that of diesel operation at full load. The

CO emission for the WPO was noticed higher by about 5% than that of diesel at full load. Smoke was found to be reduced by about 40% for the WPO at all loads.

2.6. Summary

Much research work has been carried out using different alternative fuels, with different engine and fuel modifications in the CI engines. Reviewing the literature, there seem to be little work in the area of used transformer oil (UTO) as an alternative fuel in CI engines. This review would suggest that this area of investigation, whilst promising, requires further work in order to demonstrate the viability of UTO as a diesel oil substitute in CI engines.

CHAPTER 3
USED TRANSFORMER OIL

3.1 General

The electrical transformer is an essential piece of equipment used in the transmission and distribution of the electrical energy that is installed in small, medium and large electrical distributing stations. It is also used in arc welding equipment and the electromotive units in trains. The performance and the life of an electrical transformer depend on the effective insulation and cooling. Mineral oil, synthetic ester and silicone oils are traditionally used as the feed stocks for the production of transformer oils. The mineral oil is composed of the hydrocarbons of paraffinic, aromatic or naphthenic structure that are obtained by the fractional distillation of crude petroleum [85]. The conventional transformer oils are obtained from the different feed stocks or base materials. Table 3.1 gives the comparison of the properties specified for transformer oil obtained from different base oils [86 - 91]. Figure 3.1 shows the sample of the pure transformer oil used in power transformer or welding equipment.

Figure 3.1 Pure transformer oil

Table 3.1 Comparison of the transformer oil with different base oils

Name	**Dielectric Strength (kV)**	**Pour Point (°C)**	**Flash Point (°C)**	**Moisture Content (mg/kg)**	**Viscosity (cSt) at 40°C**	**Density (kg/m^3)**
Mineral oil	45	-50	147	-	9.2	800
Sunflower oil		-15	73	-	58.50[a]	918
Soyabean oil		-12.2	254	-	65.40[a]	914
Coconut oil	60	-40	234	1	50.1	912
Palm oil		-31.7	267	-	39.6	918

a-@27^0C

The transformer oil serves both for electrical insulation and heat dissipation. The transformer oil suffers from continuous deterioration and degradation due to the electric and cyclic thermal stresses due to the loading and climatic conditions. This may affect the electrical equipment and installation. Therefore, a continuous monitoring of the transformer oil characteristics is essential to avoid the deterioration of the oil characteristics under working conditions, and eventual breakdown of both oil and transformers.

After long use, the transformer oil becomes unusable and is disposed off. The life of the waste or used transformer oil is determined by important properties, such as dielectric strength, pour point, flash point, moisture content, viscosity and density [85]. Recently, samples of UTO with mineral oil as a base have been characterized for their physico-chemical properties and dielectric strength. The sample had a dielectric strength which indicates that it could not be used further. However, the sample could be characterized as suitable as a fuel.

3.2 Degradation of transformer oil

The transformer oil will deteriorate rapidly at high temperatures and moisture acts as a catalyst for its aging. There are also other substances and metals present in a

transformer that are responsible for oil degradation. These include copper, paint, varnish and oxygen. The principal mechanism of transformer oil aging is oxidation which results in acids and other polar compounds being formed [92].

When a transformer is subjected to thermal and electrical stresses in an oxidizing atmosphere, it gradually loses its stability and becomes decomposed and oxidized, its acidity increases, and finally, it begins to produce mud. This is the degradation mechanism of the oil.

By detecting the color, transformer oil is considered to be scrapped. There is no direct correlation between a change in the color of the oil and a specific problem within the equipment [92]. The changes normally occur over long periods of time. Empirical values exist with respect to condemning limits for operation of the equipment, as well as relative condition [93].

A visual test should be performed, following ASTM D 1524-84. The condition of the transformer oil is determined by the ASTM color comparator, which is given in Table 3.2

Table 3.2 Condition of transformer oil

Color comparator number	**ASTM color**	**Transformer oil condition**
0.0-0.5	Clear	New oil
0.5-1.0	Pale yellow	Good oil
1.0-2.5	Yellow	Service-aged oil
2.5-4.0	Bright yellow	Marginal condition
4.4-5.5	Amber	Bad condition
5.5-7.0	Brown	Severe condition (reclaim oil)
7.0-8.5	Dark brown	Extreme condition (scrap oil)

Although the actual service life varies widely depending on the manufacturer design, quality of assembly, materials used, maintenance, and operating conditions, the expected life of a transformer is about 40 years [94]. The quantity of UTO, that is

disposed of annually is quite difficult to estimate from the referred statistics, but day by day more transformers are installed and old transformer oils have to be scrapped. The overall installed capacity of the transformers has grown at a compound annual growth rate (CAGR) of 11.7% over the years 1998 to 2007 and a CAGR of 22.9% between the years 2007 and 2010. In 2012, more than 3,50,000 power transformers are installed in India [95]. Figure 3.2 depicts the increase in the number of transformers installed over time.

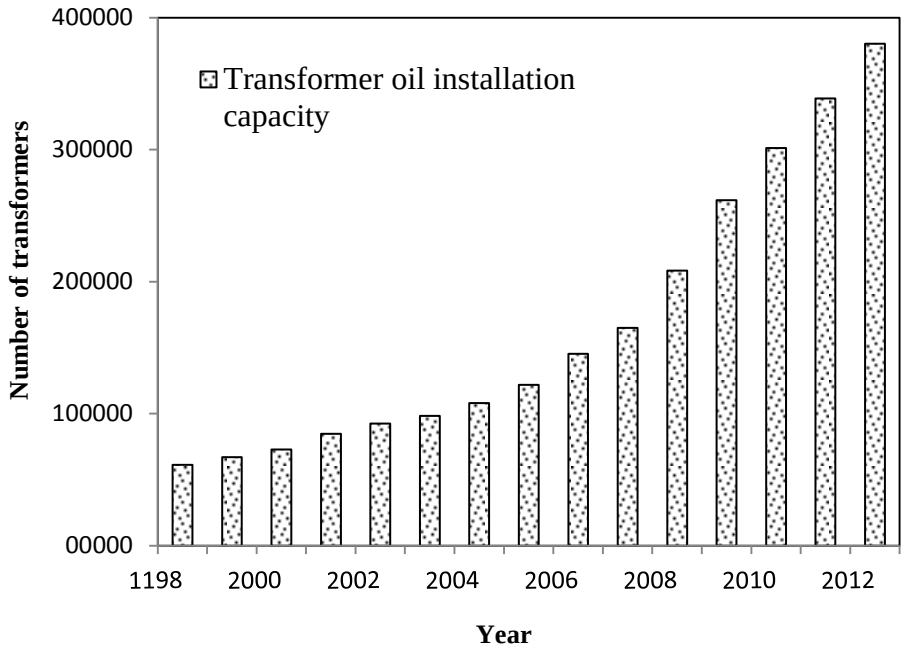

Figure 3.2 Number of installed transformers versus time

3.3 Filtering of the used transformer oil

Figure 3.3 shows the schematic of the steps involved in the disposal of the UTO from transformer oil. Once the life of the oil was determined, the transformer oil was removed from the transformers and sent for settling.

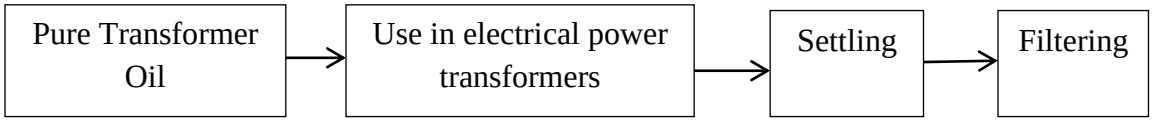

Figure 3.3 Disposal of the UTO from transformer oil

Now the disposed transformer oil has been categorized as UTO, a further two processes are involved in processing the oil (a) settling and (b) filtering. The processes are discussed below;

(a) Settling: Foreign particles and sediments of the UTO settle at the bottom of the oil tank. The settling works better in warm conditions and over a number of days or weeks. The settled UTO was drained from the oil tank.

(b) Filtering: Fine filters may be required depending on the application. For this study, the UTO was filtered with the help of a fabric filter of size 30 microns. Figure 3.4 shows the photographic view of the UTO sample.

Figure 3.4 Photograph of the UTO sample after procuring

3.4 Group compounds of the UTO

The chemical compounds present in an organic or inorganic substance can be determined using FT-IR Spectroscopy. It is a measurement technique where spectra are collected, based on the measurements of the coherence of a radiative source, using the time-domain or space-domain measurements of infrared radiation. The FT-IR test was carried out with the Perkin Elmer Spectrum ONE equipment, which has a scan range of 450-4000 cm^{-1} with a resolution of 1.0 cm^{-1}. The FT-IR absorption is related to covalent bonds, and it provides detailed information about the structure of molecular compounds. The results of the FT-IR analysis are in the form of a graph plotted between the wave

length and percentage of transmittance which will give information about the position of various bond vibrations, distinguished by several modes of vibration such as stretching, distortion, bending etc. Figure 3.5 shows the comparison of FT-IR analysis of diesel and UTO. The bonds found with the diesel and UTO are listed in Table 3.3 and 3.4.

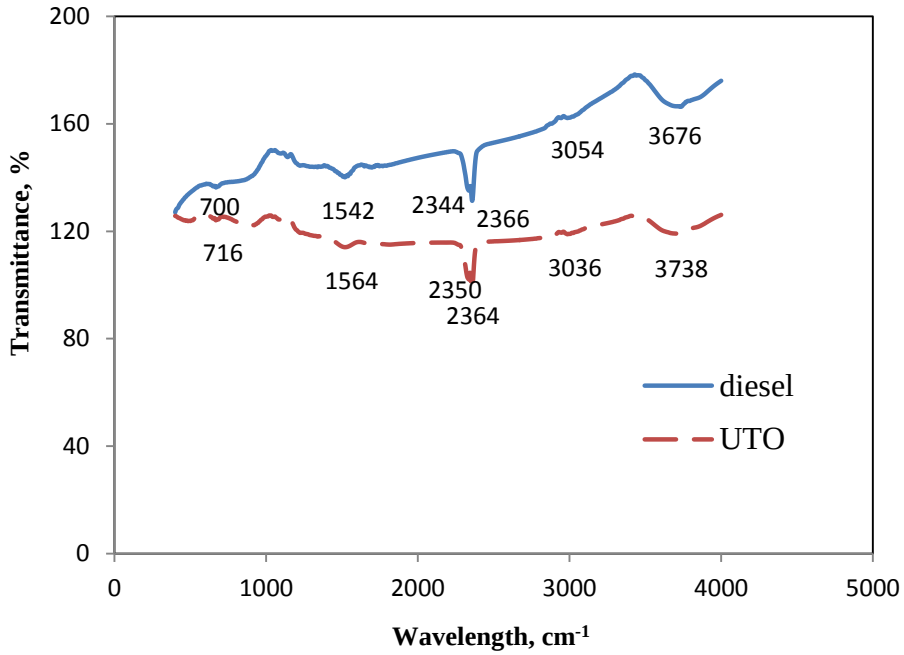

Figure 3.5 FT-IR analysis of diesel and UTO

Table 3.3 FT-IR analysis of diesel

Wave number (cm^{-1})	**Type of vibration**	**Wavelength, µm**	**Compound group present**
700	$C\text{-}H_{Rocking}$	6.9-7.1	alkanes
1542	$N\text{-}H_{Bending}$	6.1-6.7, 5.9-6.3, 5.4-6.1	amines
2344	$C{\equiv}C_{Stretch,}$ $C{\equiv}N_{Stretch}$	4.2-4.8	alkenes/aromatics, nitriles
2366	$C{\equiv}C_{Stretch,}C{\equiv}N_{Stretch}$	3-3.7	alkenes/aromatics, nitriles
3054	$C\text{-}H_{Stretch,}$ $O\text{-}H_{Stretch,}$ $N\text{-}H_{Stretch}$	3-3.7	carboxylic acids alcohols and
3676	$O\text{-}H_{Stretch}$	2.7-3.3	phenols

According to the wavelength present in UTO, the compounds present are alkenes, aromatics, alcohols, phenols and carboxylic acids, which are similar to the compounds present in diesel respectively.

Table 3.4 FT-IR analysis of UTO

Wave number (cm^{-1})	**Type of vibration**	**Wavelength, µm**	**Compound group present**
484	Carbonates	6.9-7.1	Carbonates
1632	$N\text{-}H_{Bending,}$ $C{=}C_{Stretch}$, $C{=}O_{Stretch}$	6.1-6.7, 5.9-6.3, 5.4-6.1	alkenes/aromatic, aldehydes and ketones
2372	$C{\equiv}C_{Stretch,}C{\equiv}N_{Stretch}$	4.2-4.8	alkenes/aromatis
2902	$C\text{-}H_{Stretch}$	3-3.7	carboxylic acids
2956	$C\text{-}H_{Stretch}$	3-3.7	carboxylic acids
3616	$O\text{-}H_{Stretch}$	2.7-3.3	alcohols and phenols

3.5 GCMS analysis

The percentage of different compounds present in the UTO was determined by gas chromatography-mass spectrometry (GCMS). The compounds present in the UTO were identified and compared with the standard chromatogram data available for diesel. Table 3.5 gives the data obtained from the chromatogram for diesel. The data for the UTO obtained from GCMS is given in Table 3.6. From the comparison, it has been observed that although diesel contains around 83 compounds, while the UTO contains 23 compounds, taking into account the area percentage, the highest peak areas of total ion chromatogram (TIC) of the compounds were n-hexadecane, pentadecane, n-tetradecane, hexadecane and n-tridecane for diesel, and hexadecane, Eicosane, Octadecane, Heneicosane and Heptadecane for the UTO.

N-hexadecane ignites very easily under compression; hence, it serves as a reference for fuel mixtures, and occupies the highest area of 5.91% in diesel. Pentadecane occupies

11.48% of the area and also represents an alkane hydrocarbon. N-tetradecane, hexadecane and n-tridecane represented the linear alkanes groups [7]. The UTO contains alkanes and phenols groups. All the compounds were characterised by an increase in the retention time.

Table 3.5 Chemical compounds in diesel obtained from GCMS analysis

R. time	**Area %**	**Compound Name**	**Formula**
3.065	0.98	1-Ethyl-2-methylcyclohexane	C_9H_{18}
3.240	0.57	(2E)-2-Tridecen-1-ol	$C_{13}H_{26}O$
3.304	0.63	3-Methylnonane	$C_{10}H_{22}$
3.359	1.06	Propylcyclohexane	C_9H_{18}
3.682	0.75	2,2,3,3-Tetramethylpentane	C_9H_{20}
3.737	0.84	2-Methylnonane	$C_{10}H_{22}$
3.782	1.04	m-Ethylmethylbenzene	C_9H_{12}
3.831	0.95	5-Ethyl-2-methylheptane	$C_{10}H_{22}$
3.903	0.48	1,2,3-Trimethylbenzene	C_9H_{12}
4.094	0.74	1-Methyl-2-Pentylcyclohexane	$C_{12}H_{24}$
4.274	3.51	Decane	$C_{10}H_{22}$
4.588	0.45	4-Methyldecane	$C_{11}H_{24}$
4.839	0.59	Decane, 2-cyclohexyl-	$C_{16}H_{32}$
5.080	0.44	1,3-Diethylbenzene	$C_{10}H_14$
5.126	0.81	Malonic acid, 4-methylpent-2-yl tetradecyl ester	$C_{23}H_{44}O_4$
5.233	0.53	Benzenepropanal	$C_9H_{10}O$
5.250	0.75	2-Methyldecane	$C_{11}H_{24}$
5.351	0.95	3-Methyldecane	$C_{11}H_24$
5.822	2.14	n-Undecane	$C_{11}H_{24}$
5.979	0.42	Benzene, (1-Ethyloctadecyl)-	$C_{26}H_{46}$
6.054	0.55	1-Chlorooctadecane	$C_{18}H_{37}Cl$

Table is continued on next page

R. time	**Area %**	**Compound Name**	**Formula**
6.167	0.80	Cyclohexanone, 5-Methyl-2-(1-Methylethylidene)-, (R)-	$C_{10}H_{16}O$
6.222	0.63	1,2,3,4-Tetramethylbenzene	$C_{10}H_{14}$
6.425	0.68	Cyclohexane, 1,1'-(1,2-Ethanediyl)BIS	$C_{17}H_{32}$
6.549	0.45	1-Methyl-2-Isopropenylbenzene	$C_{10}H_{12}$
6.715	0.98	1,7,7-Trimethyl-2-Vinylbicyclo[2.2.1]Hept-2-ene	$C_{12}H_{18}$
6.799	0.98	1-Iodo-2-Methylundecane	$C_{12}H_{25}I$
6.894	0.81	3-Methylundecane	$C_{12}H_{26}$
7.199	0.44	1-(Cyclohexylmethyl)-2-methylcyclohexane	$C_{14}H_{26}$
7.250	0.46	1,7,7-Trimethyl-2-vinylbicyclo[2.2.1]hept-2-ene	$C_{12}H_{18}$
7.356	2.71	Dodecane	$C_{12}H_{26}$
7.525	0.84	2,6-Dimethylundecane	$C_{13}H_{28}$
7.741	0.66	1-Octadecanesulphonyl chloride	$C_{18}H_{37}ClO_2S$
8.004	0.56	Octane, 2-cyclohexyl-	$C_{14}H_{28}$
8.197	0.70	4-Methyldodecane	$C_{13}H_{28}$
8.279	0.85	2-Methyldodecane	$C_{13}H_{28}$
8.380	1.36	6-Ethylundecane	$C_{13}H_{28}$
8.467	0.53	1,2,3,4-Tetrahydro-5-Methylnaphthalene	$C_{11}H_{14}$
8.814	4.07	n-Tridecane	$C_{13}H_{28}$
8.942	0.75	3,4-Difluorobenzoic acid, pentadecyl ester	$C_{22}H_{34}F_2O_2$
9.023	0.50	n-Dodecane	$C_{12}H_{26}$
9.171	0.50	Phosphorous acid, tris(decyl) ester	$C_{30}H_{63}O_3P$
9.236	0.51	1,2,3,4-Tetrahydro-2,6-dimethylnaphthalene	$C_{12}H_{16}$
9.477	0.81	2-Butyl-1-Octanol	$C_{12}H_{26}O$
9.525	0.49	2,4-Dimethyldodecane	$C_{14}H_{30}$
9.677	0.70	2-Methyltridecane	$C_{14}H_{30}$
9.766	0.84	2-Bromo dodecane	$C_{12}H_{25}Br$

Table is continued on next page

R. time	Area %	Compound Name	Formula
9.826	0.83	2,6,10-Trimethyldodecane	$C_{15}H_{32}$
10.189	4.45	n-Tetradecane	$C_{14}H_{30}$
10.787	0.77	7-Methylpentadecane	$C_{16}H_{34}$
10.940	1.64	n-Hexadecane	$C_{16}H_{34}$
10.994	0.74	2-Methyltetradecane	$C_{15}H_{32}$
11.083	0.62	3-Methyltetradecane	$C_{15}H_{32}$
11.480	4.87	Pentadecane	$C_{15}H_{32}$
11.961	0.44	3-(2-Methyl-propenyl)-1H-indene	$C_{13}H_{14}$
12.025	0.49	Furazan-3-carboxamide, 4-amino-N-(2-tetrahydrofurfuryl)-	$C_8H_{12}N_4O_3$
12.039	0.50	6-Amino-1-methyl-2,4-dioxo-1,2,3,4-tetrahydro-5-pyrimidinyl(methyl)formamide	$C_7H_{10}N_4O_3$
12.080	0.51	Tetradecane	$C_{14}H_{30}$
12.154	0.84	4-Methylpentadecane	$C_{16}H_{34}$
12.229	1.16	6-Propyltridecane	$C_{16}H_{34}$
12.317	0.80	3-Methylpentadecane	$C_{16}H_{34}$
12.690	4.35	Hexadecane	$C_{16}H_{34}$
12.741	0.71	Octadecane	$C_{18}H_{38}$
13.197	1.83	2,6,10-Trimethylpentadecane	$C_{18}H_{38}$
13.400	0.77	2-Methylhexadecane	$C_{17}H_{36}$
13.484	0.45	3-Methylhexadecane	$C_{17}H_{36}$
13.844	5.91	n-Hexadecane	$C_{16}H_{34}$
14.279	0.62	n-Nonadecane	$C_{19}H_{40}$
14.508	0.61	8-n-Hexylpentadecane	$C_{21}H_{44}$
14.925	3.83	n-Octadecane	$C_{18}H_{38}$
14.972	1.40	2,6,10,14-Tetramethylhexadecane	$C_{20}H_{42}$
15.334	0.73	n-Hexadecane	$C_{16}H_{34}$

Table is continued on the next page

R. time	Area %	Compound Name	Formula
15.334	0.73	n-Hexadecane	$C_{16}H_{34}$
15.648	0.61	3-Methyloctadecane	$C_{19}H_{40}$
15.959	3.38	n-Hexadecane	$C_{16}H_{34}$
16.336	0.62	n-Hexadecane	$C_{16}H_{34}$
16.945	3.04	Octadecane	$C_{18}H_{38}$
17.293	0.76	Octadecane	$C_{18}H_{38}$
17.607	0.56	3-Methylicosane	$C_{21}H_{44}$
17.885	2.57	Octadecane	$C_{18}H_{38}$
18.784	2.01	n-Octacosane	$C_{28}H_{58}$
19.648	1.61	Octacosane	$C_{28}H_{58}$
20.476	1.35	Tetracosane	$C_{24}H_{50}$
21.269	0.85	n-Octacosane	$C_{28}H_{58}$

Table 3.6 Chemical compounds in the UTO obtained from GCMS analysis

R. time	Area %	Compound Name	Formula
9.103	0.82	Tridecane	$C_{13}H_{28}$
10.159	0.41	2, 6, 10, 14-Tetramethylhexadecane	$C_{20}H_{42}$
10.468	2.39	Tetradecane	$C_{14}H_{30}$
11.280	1.32	Hexadecane	$C_{16}H_{34}$
11.390	0.68	14B-Pregane	$C_{21}H_{36}$
11.514	0.54	3, 7, 11, 15,- Tetramethyl-2-Hexadecen-1-OL	$C_{20}H_{40}O$
11.755	4.51	Pentadecane	$C_{15}H_{32}$
12.97	7.38	Hexadecane	$C_{16}H_{34}$
13.539	2.08	2, 6, 10- Tetramethylpentadecane	$C_{18}H_{38}$
14.122	10.09	Heptadecane	$C_{17}H_{36}$
14.189	6.23	2, 6, 10, 14- Tetramethylpentadecane	$C_{19}H_{40}$

Table is continued on next page

R. time	Area %	Compound Name	Formula
15.319	4.79	2, 6, 10, 14- Tetramethylhexadecane	$C_{20}H_{42}$
16.255	11.70	Hexadecane	$C_{16}H_{34}$
17.245	11.09	Eicosane	$C_{20}H_{42}$
18.193	10.47	Heneicosane	$C_{21}H_{44}$
19.098	5.19	Docosane	$C_{22}H_{46}$
19.966	3.47	Tricosane	$C_{23}H_{48}$
20.800	2.52	Tetracosane	$C_{24}H_{50}$
21.601	1.27	Docosane	$C_{22}H_{46}$
22.373	1.15	Nonacosane	$C_{29}H_{60}$
23.118	0.55	Eicosane	$C_{20}H_{42}$
23.835	0.36	Nonacosane	$C_{29}H_{60}$

Hexadecane has, with the highest area of 11.7% represents the linear alkane groups. The alkanes are easier to transport as liquids, and are highly flammable. They vaporize easily on entry into the combustion chamber without forming droplets, showing the uniformity of the combustion; they are much less prone to premature ignition; and are anti-corrosive agents. The presence of Eicosane shows higher melting points, which may cause problems at low temperatures, where the UTO becomes too thick to flow smoothly. All these properties are similar to diesel fuel, hence UTO may be investigated as an alternative fuel for a CI engine.

3.6 Physico-chemical properties of the UTO

A comparison of the ultimate analysis of the UTO and diesel is given in Table 3.7. The chemical composition of the UTO indicates that the fuel has carbon equal to that of diesel fuel. The hydrogen present in the UTO is 1.5 times less than that of diesel. It is also clear from the table that the UTO has considerable oxygen present.

The kinematic viscosity of the UTO is approximately 6 fold higher than that of the diesel. Table 3.8 gives the comparison of the physico-chemical properties of the UTO with diesel, in accordance with ASTM standards.

Table 3.7 Ultimate analysis of diesel and UTO

Description	**diesel**	**UTO**
C, %	86.5	89.95
H, %	13.2	9.19
N, %	0.18	0.03
S, %	0.3	0.35
O by difference, %	0	0.44
C/H ratio	5.437	9.7
Carbon residue, %	0.02	0.02

Table 3.8 Properties of the UTO and diesel

Property	**ASTM Test method**	**diesel**	**UTO**
Kinematic viscosity, cSt@ 27^{o}C	D-0445	2.4	13
Flash point, °C	D0093-02A	50	150
Fire point, °C	-	56	172
Pour point, °C	D0097-05A	-16	-16.7
Density, kg/m^3	D-1298	860	890
Lower calorific value kJ/kg	D-4809	44800	39270
Sulphur content, %	D129-00R05	0.05	0.020
Cetane number	-	51*	43.6*
Surface tension, mN/m	D 971	26.7	29.6
T10, °C		210	320
T50, °C		230	340
T90, °C		260	370
T100, °C		350	360

* Calculation for Cetane number is done using the equation A6.1, given in Appendix A6

The distillation curve of the UTO obtained by decomposing of the waste oil sample and diesel are displayed in Fig 3.6. The distillation curve of a fuel is important and that defines the presence of low and high boiling point compounds in a fuel. Initial boiling

point (IBP) of the UTO is higher than diesel whereas the final boiling point (FBP) is closer to each other. IBP is higher in UTO which signifies a higher flash point than diesel, and impacts the safety of transportation. The higher IBP indicates the lower volatility of UTO. Volatility of the fuels effects crank case dilution, cold start characteristics of the engine, warm-up time of the engine, and running performance and acceleration behavior of the engine [96]. One of the most important characteristics of a fuel is lower heating value (LHV), which is tested under laboratory conditions and the value is 39270 kJ/kg. It is closer to LHV of diesel with a value of 43,800 kJ/kg.

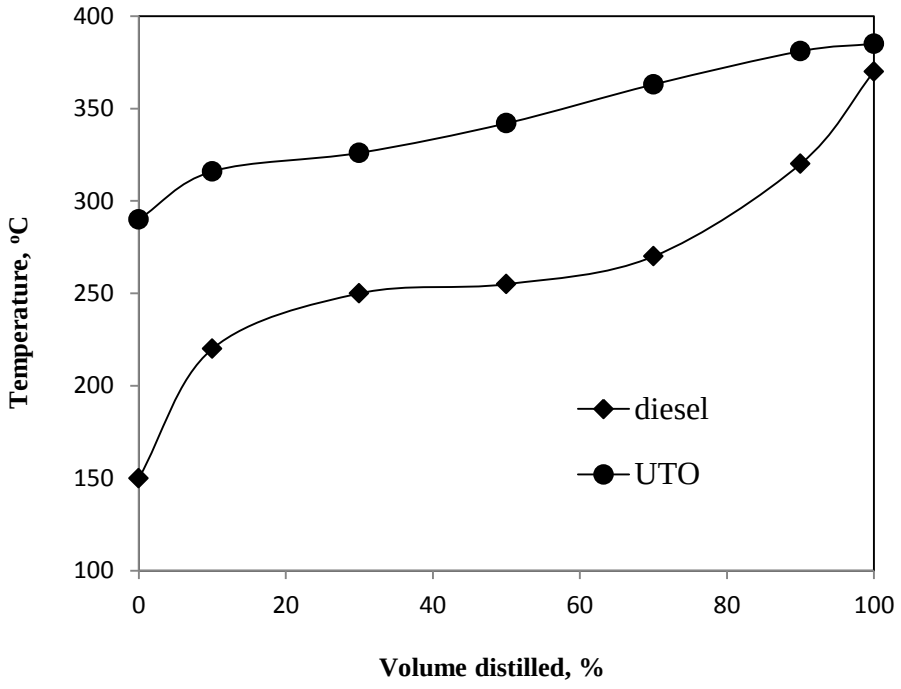

Figure 3.6 Boiling range of UTO and diesel

3.7 Determination of Sauter mean diameter

Modern engine manufacturers in the world have recently focused more on improving the thermal efficiency of their engines, in order to meet both the economic and environmental standards [97]. Incomplete combustion produces various air pollutants, such as CO, NO, and nitrogen dioxide. Factors such as fuel droplet size, injection rate, injection quantity and injection timing etc., play an important role in improving the

thermal efficiency of the CI engines [98]. The droplet size of the fuel is directly related to the design and quality of the fuel injector. The more effective a fuel injector is, the smaller the droplets produced, thus increasing the fuel surface and evaporation rates, improving the burning range results in a higher power output and lower exhaust emission [99].

The Sauter mean diameter (SMD) is an average of the particle size of a liquid or fuel. The finer and more homogeneous the atomization, the more complete will be the physical preparation of the fuel, and more easily effective the combustion. Studies include the measurement of the droplet size using an age-old magenesium oxide (MgO) coating technique, and converting it into the more sophisticated Laser beam technique. Though the MgO technique is erroneous, it is simple and can be attempted in any laboratory environment compared to alternative methods that are more sophisticated and very costly. The Malvern particle analyzer is out of reach for many researchers. Therefore, the authors attempted to collect the raw data using the MgO technique, and converted it into the more useful equivalent Malvern particle data.

The experimental set up employed to collect the spray is shown in Fig 3.7. In this study, the MgO coated plates were introduced before the fuel spray. The distance between the MgO coated plate and the nozzle tip was 762 mm. The impressions of the droplet created on the coating of the plate were seen through a 10X microscope, choosing different regions on the plate. In order to minimize the error, two samples were selected from the spray collected on a glass plate, and were manually counted, as given in Table 3.9. The numbers of droplets of different sizes were manually counted, viewing through the microscope and recorded. The injection pressure was fixed at 200 bar and the fuel samples of the UTO were tested and compared with the diesel sample. The crude data was converted into the more sophisticated measure used by the Laser Beam technique from Malvern particle analyzer data, using an empirical equation [100].

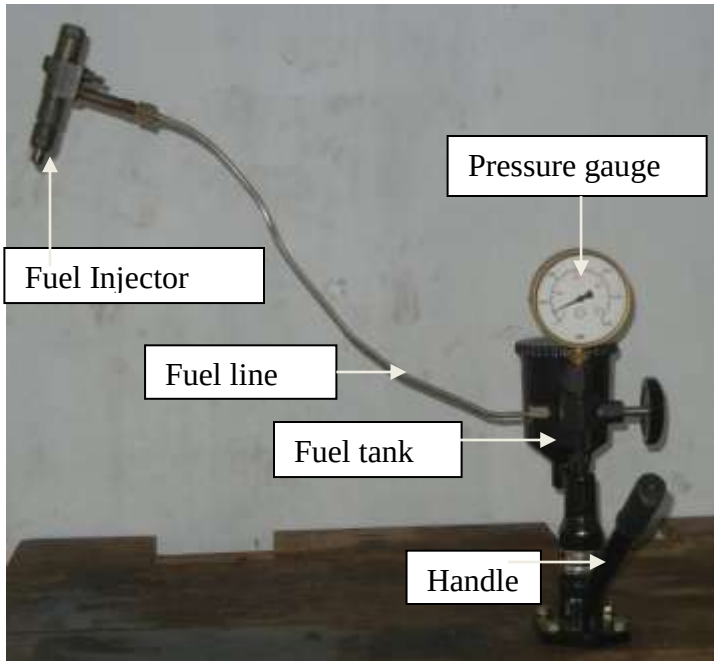

Figure 3.7 Photographic view of the injector test bench

Table 3.9 presents the sample study of the measurement of the droplet size of the UTO and diesel, using the MgO technique at a room temperature of 27^{o}C.
The SMD was determined using the following empirical equation [100]:

$$(\mathrm{SMD})_{\mathrm{Mgo}} = \frac{\frac{4\pi}{3}\left[N_1\left(D_1/2\right)^3 + N_2\left(D_2/2\right)^3 + N_3\left(D_3/2\right)^3 + \cdots\ldots\ldots\ldots\ldots\right]}{4\pi\left[N_1\left(D_1/2\right)^2 + N_1\left(D_1/2\right)^2 + N_1\left(D_1/2\right)^2 + \cdots\ldots\ldots\ldots\ldots\right]} \quad (3.1)$$

where, N_1, N_2, N_3……are the numbers of droplets collected on the coated glass plate.

D_1, D_2, D_3……...are the respective diameters of those droplets.

Figure 3.8 (a) and (b) show the images obtained by the MgO plates after sprayed with diesel and UTO respectively. Due to higher viscosity and surface tension of the UTO, it has fewer and larger droplets.

Table 3.10 gives the SMD values of a given sample, that are determined by adopting the magnesium oxide technique, and converting them into SMD data using the following equation:

$$(\mathrm{SMD})_{\mathrm{laser}} = 37 - 0.1739\,(\mathrm{SMD})_{\mathrm{MgO}} \quad (3.2)$$

Table 3.9 Droplet size of diesel and UTO

Sl.No	Range of Droplet Diameter, Micron	diesel oil Sample I Number	diesel oil Sample II Number	UTO Sample I Number	UTO Sample II Number
1	<15	1580	1724	1040	1056
2	15-30	164	132	144	116
3	30-45	72	56	60	52
4	45-60	24	21	23	14
5	60-75	15	6	9	5

Injection pressure =200 bar; Single hole injector

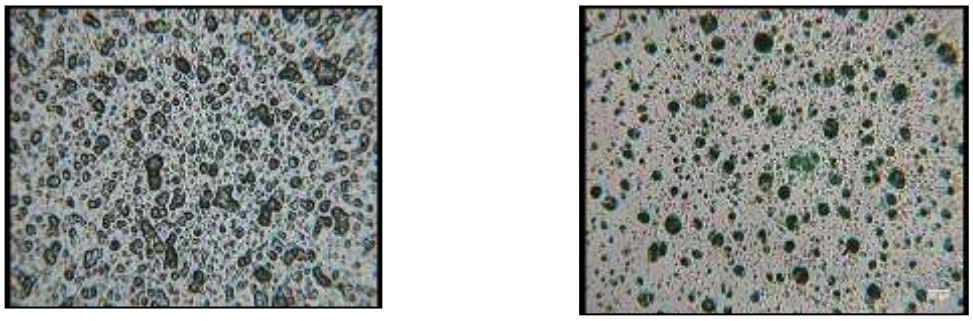

diesel UTO

Figure 3.8 Droplet size of diesel and UTO

Table 3.10 SMD of the diesel and UTO

Sl No.	Sample oil	MgO	Laser
1	Diesel	5.74365	35.97105
3	UTO	5.0865	36.115

CHAPTER 4
EXPERIMENTATION

4.1 General

Before starting the investigation on the use of any alternative fuel in a CI engine, it is essential to plan for the selection of engine and instrumentation to be provided. The knowledge and the methodology to be adopted in each technique and calculations for determining different parameters are also required. Similarly, modification of the engine has to be carried out for the investigation. This chapter describes the preparatory work carried out before the start of the investigation; experimental set up; experimental procedure and method of calculating the parameters.

4.2 Preparatory work for investigation

The following preparatory steps were carried out before starting the investigation:

1. The required UTO for the study was collected from the electrical maintenance department of the institute. The impurities and foreign particles in the oil were removed by settling and filtering. A 20 micron fabric filter was used for filtration.
2. The fuel consumption would be higher if a multi cylinder engine would be used for the investigation. As this is an early stage investigation of UTO as a fuel for DI engines, a single cylinder, four stroke, air cooled, DI diesel engine developing power of 4.4 kW at a rated speed of 1500 rpm was selected for the investigation.
3. An experimental setup was developed to conduct experiments with fuel or engine modifications to evaluate the combustion, performance and emission parameters at different power outputs of the engine. The necessary fuel and air measuring instruments were selected and incorporated in the experimental set up which are discussed in the subsequent sections.
4. A piezo-electric pressure transducer was flush mounted on the cylinder head to obtain the pressure data of the engine. A top dead center marker was mounted on the flywheel for obtaining the every crank angle of the piston. The description of

the pressure sensor and top dead center marker are described in the subsequent section 4.3.3.

4.3 Experimental set up

Figure 4.1 shows the overall schematic diagram of the experimental set up used for all the experiments conducted in the investigation. A photographic view of the experimental setup is shown in Fig. 4.2.

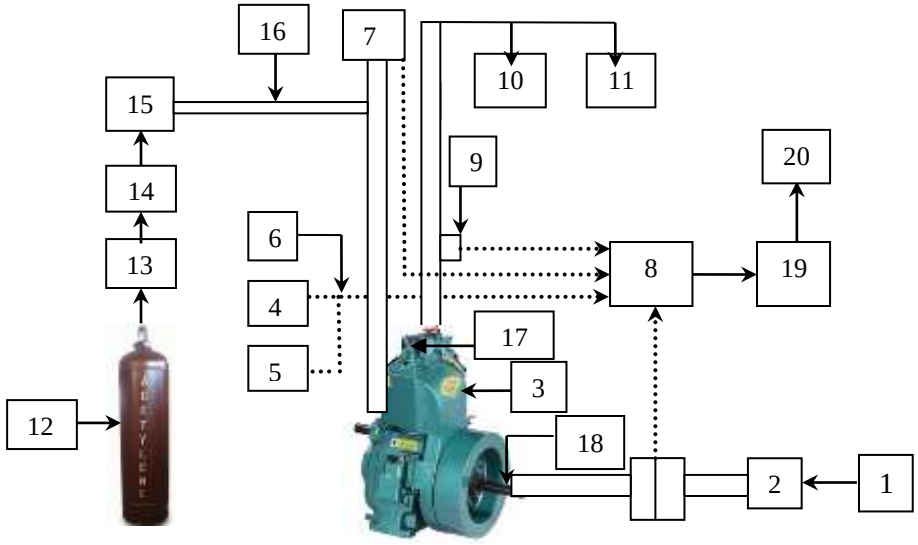

1. Load cell	2. Alternator	3. Engine
4. Fuel tank A	5. Fuel tank B	6. Two way valve
7. Air box	8. Data receiver unit	9. Exhaust gas temperature indicator
10. Exhaust gas analyzer	11. Smoke meter	12. Acetylene cylinder
13.Flow meter	14. Flash back arrestor	15. Pressure regulator
16. Hose Pipe	17. Pressure transducer	18. Top dead center marker
19. Data acquisition system	20. PC with monitor	

Figure 4.1 Schematic diagram of the experimental setup

The details of the overall engine set up and other instrumentation provided for the study are discussed in the following subsections.

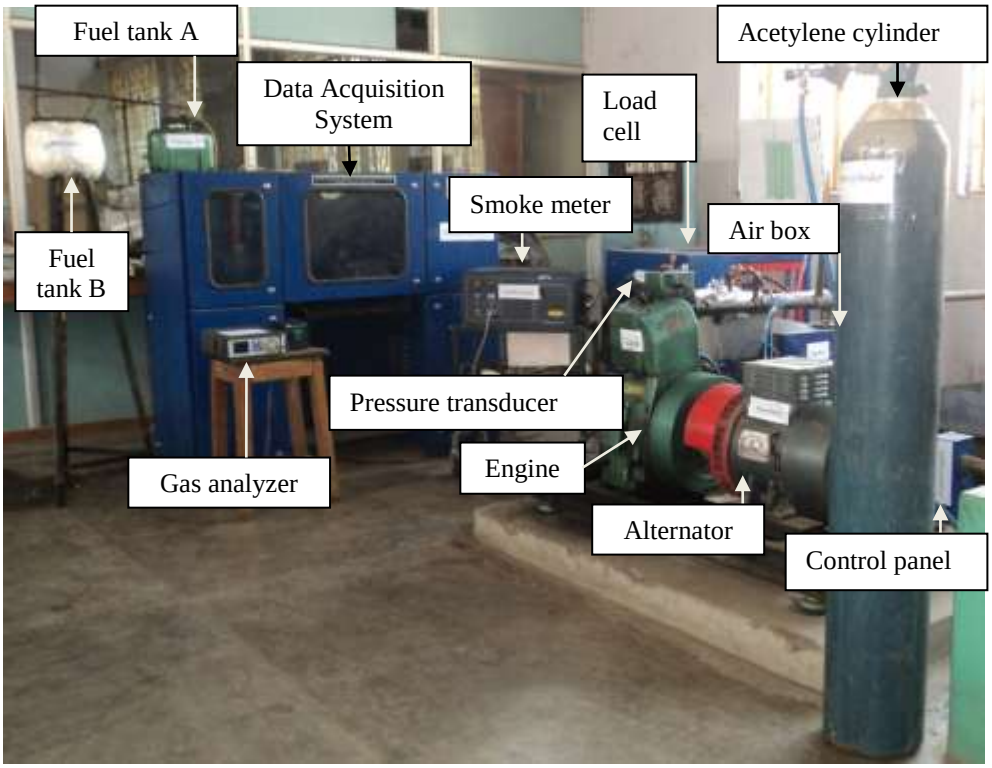

Figure 4.2 Photographic view of the experimental setup

4.3.1 Test Engine

The test engine with loading device used in this investigation was a Kirolaskar TAF-1 single cylinder, four-stroke, air cooled, constant speed direct injection diesel engine. The technical specifications of the engine are given in Appendix A1. The general experimental setup provided in the study is discussed below;

A control panel (1) was fitted with an alternator (2) to provide the load to the engine (3) in constant speed mode. The engine output was varied by controlling the field current. The dynamometer was calibrated statically by applying a known current. The load was measured by the dynamometer with the help of a strain gauge type of load cell mounted between the stator base and the frame. A burette and a fuel sensor were included in the fuel circuit to measure the fuel consumption and give the input to the computer. The

burette was fitted with a two way valve. When the valve was set at position "1" the fuel from the fuel tank was sent to the engine directly and in position "2" the fuel contained in the burette was sent to the engine. For the measurement of fuel flow rate of the engine, the valve was set at position "2". The fuel flow rate was measured on the volume basis. The fuel sensor sensed the time for a definite flow and gave an input to the data acquisition system to calculate the total fuel consumption and it was displayed in the monitor of the computer. Two different fuel tanks A and B were used in the investigation. Fuel tank A (4) was a conventional one while fuel tank B (5) was provided for alternative fuel. The UTO was used in fuel tank B which was insulated and also provided with electrical coil. A separate electrical line was connected to the fuel tank B from the power line with a switch and a temperature controller. Whenever the electrical switch was on the electrical coil around the fuel tank heated up the UTO and filled up fuel tank B. Both the fuel tanks were connected to the fuel supply system through a two way valve. When the valve was set at position "a" only diesel from the fuel tank A flows into the fuel supply system. When the position was set at "b" the fuel from fuel tank B enters into the fuel supply system. In the fuel line a fuel filter and fuel pump were also connected. Atmospheric air entered into the intake manifold of the engine through an air filter and an airbox (7) which was used to avoid pressure fluctuation at the inlet. Care was taken to avoid air leakage from the airbox. An air flow sensor fitted in the airbox measured the air consumption which was recorded by the data acquisition system, stored in a computer and displayed on a monitor. All the inputs such as engine brake power, air and fuel consumption were recorded via the data acquisition system, stored in a computer and displayed on the monitor. The data obtained from the air flow and fuel flow sensors were given as inputs to the data receiver unit (8). A Chromel Alumel (K-Type) thermocouple and a temperature indicator (9) were connected at the exhaust pipe that indicated the exhaust gas temperature.

4.3.2 Exhaust gas measurements

An AVL DiGas444 exhaust gas analyzer (10) was used to measure the pollutants; HC, CO, CO_2 and NO emissions, and also oxygen from the engine exhaust. The HC, CO, CO_2 were measured with the help of sensors working on non-dispersive infrared (NDIR)

principle and NO was measured with a photochemical sensor. A photographic view of the exhaust gas analyzer is shown in Fig. 4.3. The detailed specifications of the AVL five gas analyzer are presented in Appendix A2.

The recommended periodic calibration of the gas analyzer was carried out in order to ensure the accuracy of measurement. The gas analyzer's electronics, optics and its response to environmental factors were checked through calibration. The calibration procedure involved injection of calibration gases of known concentration and validating the response. The composition of CO, CO_2 and HC gases were; 3.5% volume of CO, 14% volume of CO_2, 2000 ppm volume of propane and remainder nitrogen, whereas calibration gas for the NO component is 2200 to 3000 ppm volume of the NO and the remainder N_2. Instrument outputs were then adjusted to the known inputs to correct for variations in electronic response due to temperature effects, drift or other, interferences. Thus the accuracy of the analyser was assured and an accurate response to the sampled gas was achieved after caliberation.

Figure 4.3 Photographic view of the exhaust gas analyzer

The smoke density of the exhaust was measured with the help of an AVL 437 diesel smoke meter (11). This measuring instrument consists of a sampling probe that sucks a specific quantity of exhaust sample through a white filter paper fitted in the smoke meter. The reflectivity of the filter paper was measured by the smoke meter. This consisted of a light source which and an annular photo detector illuminate the fitter paper to measure the reflected light. Before every sample, it was ensured that the exhaust from the previous measurement was completely driven off from the tube and pump. A photographic view of the diesel smoke meter is shown in Fig. 4.4. The detailed specifications of the diesel

smoke meter are presented in Appendix A3. Calibration of the smoke meter was done periodically. The method of calibrating the smoke meter adopted in the investigation is also described in next paragraph.

Smoke meter calibration was done by warming the heating elements up to 70^{o}C. The heating was designed to prevent the temperature falling below dew point and thus to avoid measurement error. Fresh air was allowed to enter the measurement chamber which is drawn through the fitter paper, undergoes measurement and sets the zero point for calibration. The halogen bulb current irradiates the column of fresh air volume and the signal from the detector are measured by the microprocessor and set as the reference value for 0% opacity. The linearity can be checked by gently pushing the linearity check knob down up to its dead position. The calibration plate was thus measured in front of the detector and the measured opacity value was indicated and printed on the protocol print out. The probe of the exhaust gas analyzer was inserted at end of the exhaust pipe during measurement of emissions. Once the engine reached stable operation, the probe was inserted into the exhaust pipe and the measurements were taken. A flow meter (13), flash back arrestor and (14) pressure regulator (15) were incorporated for the dual fuel mode operation.

Figure 4.4 Photographic view of the smoke meter

4.3.3 Combustion parameters

It is necessary to study the combustion parameters such as ignition delay, heat release rate, combustion duration, rate of pressure rise etc for the efficiency of the engine and suitability of the fuel used. In order to evaluate such parameters, it is essential to collect

the pressure values corresponding to each crank angle diagram. This was achieved by mounting a pressure transducer (17) on the engine head and top dead center marker (18) on the flywheel of the engine. A photographic view of the Kistler pressure transducer is shown in Fig. 4.5.

The specifications of the pressure transducer and the charge amplifier are given in Appendix A4. The model of the Kistler pressure transducer was 6613A which has the advantage of a good frequency response and linear operating range. The piezoelectric transducer produces a charge output, which is proportional to the in-cylinder pressure. A photographic view of the pressure transducer mounted on cylinder head is shown in Fig. 4.6

Figure 4.5 Photographic view of Kistler pressure transducer

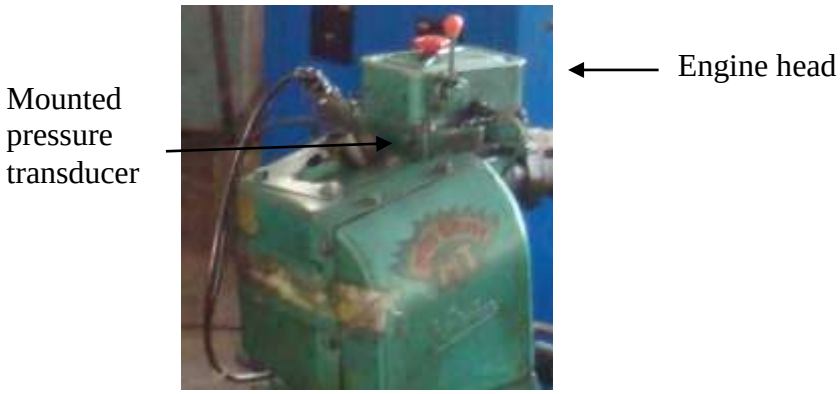

Figure 4.6 Pressure transducer mounted on the engine head

A continuous circulation of air was maintained to cool the transducer using fins to maintain the required temperature. The cylinder pressure data were acquired for 50

consecutive cycles and then averaged in order to eliminate the effect of cycle-to-cycle variations. The personal computer (PC), through an analog to digital converter (ADC) reads the output of the charge amplifier. There was a small drift in the voltage measured (-2 mV/s) due to charge leakage in the pressure transducer. Since the signal from a piezoelectric transducer indicated only relative pressures, it was necessary to have a means of determining the absolute pressure at some point in the cycle. Hence, the differential pressure had to be compared to a reference. This was done by assuming that the cylinder pressure at suction bottom dead center (BDC) was equal to the mean intake manifold pressure. The top dead center marker on the flywheel of the engine was connected to the output shaft to record the crank angle. Figure 4.7 shows the photographic view of the top dead center cut away marker on the fly wheel of the test engine and the corresponding sensor.

Figure 4.7 Top dead center marker

A hole was drilled at top dead center (TDC) and used to indicate the position of TDC by providing a voltage pulse exactly when the TDC position was reached. This sensor consisted of a matched pair of infrared diode and phototransistor so that infrared rays emitted from the diode would fall on the phototransistor when it was not interrupted. A continuous disc with a small cut at the TDC position with respect to sensor point was made to get the signal when the piston reaches TDC exactly. At this point, the output voltage from photo-transistor rises to 5 volts and at all other points it is approximately zero. Voltage signals from the optical sensor were fed to the ADC and then to the data acquisition system along with pressure signals for recording. The engine cylinder

pressure and the TDC signal were acquired using a digital data acquisition system and stored on a high speed computer. A 12 bit ADC was used to convert analog signals to digital signals. The analog to digital card had both an external and internal trigger facility. The pressure and crank angle data were collected in an excel spreadsheet installed in the data acquisition system (19).

The instantaneous experimental data were acquired over several cycles. For averaging, pressure data of approximately 50 thermodynamic cycles were chosen. The first in the voltage signal due to TDC indicator was taken as a TDC position. The clock frequency of the data acquisition card was 100 kHz, approximately 370-380 pressure-voltage readings were acquired by the PC for each rotation of the crank shaft. By interpolation, the pressure-voltage readings were arranged at a spacing of 1 ^{o}CA. The interpolation was more accurate if done through spline fitting. Since the engine was four stroke type, 720 such interpolated data points correspond to one complete thermodynamic cycle (intake, compression, combustion and exhaust) of the engine. The interpolated data were corrected for the transducer drift by subtracting from them, a linearly increasing voltage (≈2 mV/s). Subsequently, these data were multiplied by the constant "B" to obtain it in relative pressure values at each instant. These pressure data were required to be referenced using a particular known pressure hence pressure at inlet BDC was taken equal to the inlet manifold pressure. This was because at this instant, the inlet valve was completely open and the cylinder pressure was considered in equilibrium with the inlet manifold pressure, which was atmospheric pressure in the naturally aspirated engine case. After the pressure and crank angle were obtained at every load, other combustion parameters such as ignition delay, heat release rate and combustion duration were calculated using the necessary formulae or empirical calculations. The methods of calculation are described in the subsequent paragraphs. The value of calibration constant for the pressure transducer was found to be 9.9831 bar/volt and the linear curve fit equation between pressure and voltage yields:

Pressure (bar) = 9.9831 (charge amplifier voltage in volts) – 0.0263 (4.1)

Ignition delay is the time lag between the start of injection to the start of combustion. From the pressure crank angle diagram the ignition delay was calculated using an empirical relationship, which is given below;

$$\text{Ignition delay} = 3.45 \exp^{\left(\frac{2100}{T_m}\right)} p_m{}^{-1.02} \quad (4.2)$$

Where; T_m and p_m are the mean temperature and pressure of the ambient during ignition delay respectively.

Along with the pressure signal, the TDC position signal was also acquired by the ADC installed in the data acquisition system. These voltage signals were stored in two columns in a file at uniform time intervals. Since a piezo-electric pressure transducer provided only relative pressures, it was necessary to know the absolute pressure at some point in the cycle so that the pressure at all other points could be determined. For this, the cylinder pressure at suction BDC was assumed to be equal to mean manifold pressure [101].

The rate at which combustion occurs i.e., the rate of heat release affects the efficiency, power output and emissions of an engine. The heat release rate curve provides an idea about the combustion process that takes place in the engine. A set of empirical relations and equations was used to compute the heat release rate based on the first law of thermodynamics. This was done with the help of an excel spreadsheet. The heat release rate analysis is given in the Appendix A5. The combustion duration in a particular power output was calculated as the crank angle duration at which 90% the heat release rate curve covered. The crank angle at which there is a sudden rise in heat release rate was taken as the start of combustion. End of combustion was determined from the cumulative heat release curve. It was taken as the point where 90% of heat release had occurred.

CHAPTER 5
METHODOLOGY OF THE PRESENT WORK

5.1 General

From the physico chemical properties of the UTO, it is understood that the viscosity of the UTO is higher than that of diesel. In order to investigate the use of the UTO as an alternative fuel in a CI engine, a few fuel and engine modifications were adopted. The techniques adopted are discussed in the following subsections.

5.2 Investigation on the UTO-diesel blends

Blending is the simplest method of using a high viscous fuel as an alternative fuel in a CI engine by mixing it with a diesel fuel or low viscous fuel [104]. For the experimental investigation, the UTO was blended with diesel in different proportions on a volume from 10% to 60% in regular steps of 10%. The blend was denoted as the UTO, followed by the numerical value, which represents the percentage of the UTO in the blend. For example, the numerical value in the blend UTO10 indicates 10% of UTO. Similarly, other blends were denoted as UTO20, UTO30, UTO40, UTO50, UTO60 and UTO. The blend was stirred well with the help of a mechanical agitator, to get a homogeneous stable mixture. Figure 5.1 shows the photographic view of the mechanical agitator used for stirring in this investigation.

Figure 5.1 Photographic view of the mechanical agitator

Samples of different fuel blends were kept in the open atmosphere and observed for their miscibility, deposits or surface reactions after several weeks of monitoring. The samples of the UTO-diesel blends are shown in Fig. 5.2.

UTO 10 UTO 20 UTO 30 UTO 40 UTO 50 UTO60

Figure 5.2 Photographic view of the UTO-diesel samples

The comparison of the density, viscosity and gross calorific value of the blends with diesel are given in Table 5.1.

Table 5.1 Properties of test fuels

Fuel	**Fuel blend ratio (% vol)**	**Density, kg/m^3**	**Viscosity, cSt@27^{o}C**	**Lower calorific value, kJ/kg**
diesel	0/100	860	2.4	44800
UTO10	10/100	835.3	3.4	43626.45
UTO20	20/100	841	3.76	43584.58
UTO30	30/100	847.4	4.03	43542.72
UTO40	40/100	851.8	4.47	43542.72
UTO50	50/100	856.9	5.1	43458.98
UTO60	60/100	862.4	5.88	43417.11
UTO	100/0	890	13	39270

All the tests were conducted by starting the engine with diesel only. After the engine was warmed up, it was switched to the UTO operation. At the end of the test, the fuel was switched back to diesel, and the engine was kept running for a while, before shut-down, to flush the UTO from the fuel line and the injection system. All the tests were conducted at the rated speed of 1500 rpm. All readings were taken only after the engine attained stable operation. The gas analyzers were switched on before starting the experiments to stabilize them before starting the measurements. All the instruments were periodically calibrated. The injector opening pressure and injection timing were kept constant at the rated value during this phase of the study.

The engine output was varied from no load to full load in steps of 25%, 50%, 75% and 100% in the normal operation of the engine. At each load the fuel flow rate, air flow rate, exhaust gas temperature, emissions of carbon monoxide, hydrocarbon and oxides of nitrogen, and smoke readings were recorded. The pressure crank angle history of 50 cycles was also recorded, by using the data acquisition system and stored in the personal computer. The data was processed to get the average pressure crank angle variation and used for further calculations.

5.3 Investigations with the UTO at different injection timings

Before starting this study, the fuel pump was dismantled to change the injection timing. The number of shims placed above the plunger in the fuel pump was three. Each shim has a thickness of 0.5 mm. To get an advancement of injection timing, the shim was removed from the pump. By removing one shim 1.5 ^{o}CA injection timing was advanced. Similarly, by inserting a shim 1.5 ^{o}CA was retarded. Figure 5.3 shows the photographic view of the shim and the fuel pump.

Experiments were conducted with three different advanced injection timings and retarded injection timings from 18.5 ^{o}CA to 27.5 ^{o}CA at regular intervals of 1.5 ^{o}CA in the engine fueled with the UTO. The combustion, performance and emission study was conducted throughout the full range from minimum brake power to maximum brake power to ascertain the behaviour over the entire range. After finishing each set of experiments, every injection timing was restored to the original timing, and the next

injection timing was set. The optimum injection timing was determined by analysing the results of the UTO, and comparing them with the diesel data. At the end of the test, the fuel was switched back to diesel and the engine was kept running for a while at standard injection timing, before shut-down, to flush the UTO from the fuel line and the injection system.

Figure 5.3 Photographic view of the shim (a) and the fuel pump (b)

5.4 Investigations with the UTO at different fuel nozzle opening pressures

From the analysis of the results on running the injection timing, it was found that 20 ^{o}CA (retarded timing) was found to be the optimum injection timing based on the performance and emission parameters. At optimum injection timing, the engine fueled with the UTO gave a lower thermal efficiency and higher smoke emissions compared to diesel operation. Several studies reported that operating the engine with higher nozzle opening pressures might yield a better performance and lower emissions, if the fuel has a higher viscosity [102].

The main aim of this module is to evaluate the combustion, performance and emission characteristics of the engine fueled with the UTO at different fuel nozzle opening pressures. The nozzle opening pressures were varied from 200 bar to 250 bar at regular intervals of 10 bar, with an optimum injection timing of 20^{o}bTDC. Initially, the data were collected at 0%, 25%, 50%, 75% and 100% loads for diesel operation to get the baseline data. After that, the engine was warmed with UTO for 30 minutes and then the data was collected. Before starting the test for higher nozzle opening pressures, the fuel

injector was removed from the engine head, and the injector was dismandled. The adjustable screw located in the top of the injector was adjusted to get the required nozzle opening pressure. The nozzle opening pressure was tested with the help of the nozzle pressure tester, as shown in Fig. 5.4. Then, the injector was inserted into the cylinder head and mounted. The experiments were conducted at that particular nozzle opening pressure.

Figure 5.4 Nozzle pressure tester

5.5 Investigations with the UTO at different compression ratios

The engine fueled with the UTO was subjected to different compression ratios. The method of varying the compression ratio is discussed in this section. There are different methods to change the compression ratio in a CI [103] they are given below:

(a) moving the cylinder head
(b) variation of combustion chamber volume
(c) variation of piston deck height
(d) modification of the connecting rod geometry (usually by means of some intermediate member)
(e) moving the crankpin within the crankshaft (effectively varying the stroke)
(f) moving the crankshaft axis

In the present investigation, the change in the clearance volume was achieved by placing gaskets of different thicknesses between the cylinder and the cylinder head. Figures 5.5 (a and b) show the photographic views before and after changing the compression ratio respectively. The tests were conducted with four different compression ratios (16:1, 17:1, 17.5:1 and 18.5:1) at a predetermined optimum injection timing (20^{o}bTDC) and optimum injection pressure (230 bar). The calculated clearance volume and the volume of the gasket are given in Table 5.2 corresponding to the compression ratio.

Figure 5.5 Photographic view of dismantled engine head (a) and head gasket (b)

Table 5.2 Clearance volume and gasket volume for different compression ratio

Compression ratio	Total clearance volume (cm^3)	Gasket volume (cm^3)
18.5	37.77	3.37
17.5	40.01	5.6
17	42	7.6
16	44.12	9.67

5.6 Investigations with the UTO at different preheating temperatures

Preheating is one of the techniques to reduce the viscosity of fuel if the viscous fuel has to be used as an alternative fuel in a CI engine [104].

In this technique, the viscosity was reduced by preheating the UTO, and measured in the range of 15-120^{o}C. Variations of the kinematic viscosity of the UTO at different temperatures were measured with the help of the Petro test kinematic viscometer. The kinematic viscosity of the UTO at different temperatures was calculated, using the following formula.

$$v = c \times t \quad (5.1)$$

Where, v = kinematic viscosity, cSt , c = constant, t = time

Figure 5.6 portrays the variation of the kinematic viscosity with temperature for the UTO and diesel. The test results showed that heating the UTO to a temperature above 100^{o}C brings its physical properties closer to those of diesel. Figure 5.7 shows the photographic view of the preheater set up used in the investigation.

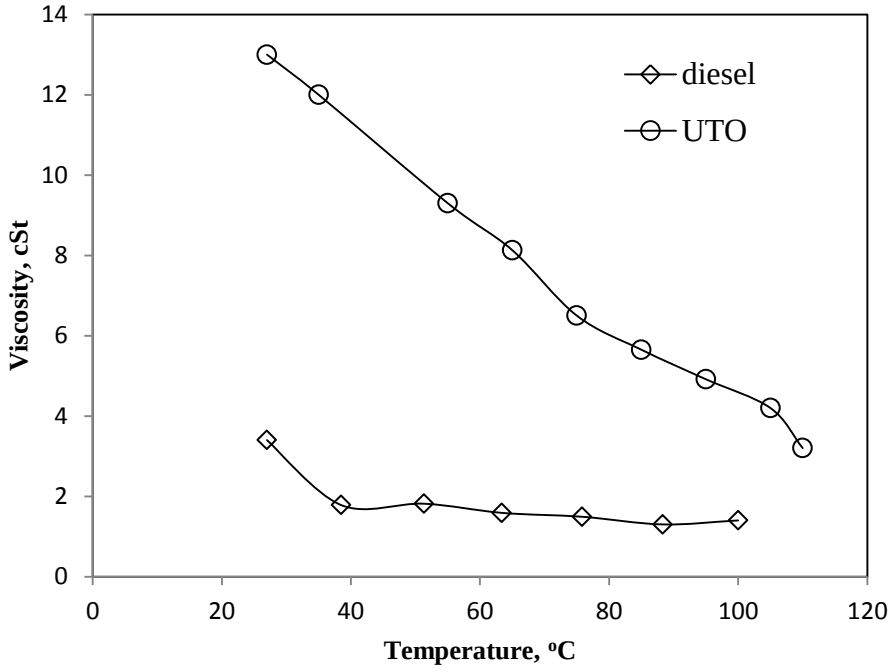

Figure 5.6 Variation of viscosity with temperature for the UTO and diesel

Experiments were conducted with the unheated UTO, and the UTO at four different preheating temperatures, varying from 80^{o}C to 110^{o}C at regular increments of 10^{o}C at optimum injection timing. The distance between the preheating chamber and the fuel

filter of the engine is about 600 mm. It was assumed that the atmosphere did not have much effect on the oil.

Figure 5.7 Photographic view of the preheated (Fuel tank B) set up

The tests were conducted for at least three hours at each preheating temperature. The load was applied at 30 minutes intervals. To ascertain the results, the tests were repeated three times, and the average values of each parameter in the three tests was calculated and used for data generation. The combustion performance and emission study was conducted throughout the full range from minimum brake power to maximum brake power, to examine the behaviour of the engine.

5.7 Investigations with the UTO and acetylene in dual fuel mode

The brake thermal efficiency of the engine fueled with the UTO at optimum injection timing was found to be lower than that of diesel operation in the same engine. The smoke emission was found to be higher with the UTO at full load. Studies report that dual fuel offers an improvement in the thermal efficiency and reduction in smoke emission, when high viscous fuel was used as an alternative fuel in a CI engine [29-33]. In this section, an attempt was made to study the effect of acetylene induction on the combustion, performance and emission behaviour of the engine filled with the UTO. The engine was modified to work in the dual fuel mode, by inducting acetylene in the intake pipe at a proper distance to avoid overheating in the intake port. The acetylene stored in a high-pressure storage tank at a pressure of 15 bar was reduced to a pressure of 1 bar by a pressure regulator. The flow of acetylene was controlled by a needle valve, and measured by a calibrated gas flow meter and flame trap. Acetylene enters the combustion chamber

through a non return valve, a flash back arrestor and flame trap, used to quench the back fire from the engine. Table 5.3 gives the comparison of physical and combustion properties of acetylene, with LPG and diesel. The acetylene flow rates were varied as 132, 198, 264, 330 g/h. Table 5.3 shows the energy share of acetylene required for the stable combustion of diesel and the UTO at different loads. The photographic view of the acetylene cylinder, pressure regulator, flow meter, flash back arrestor for the dual fuel mode is shown in Fig. 5.8.

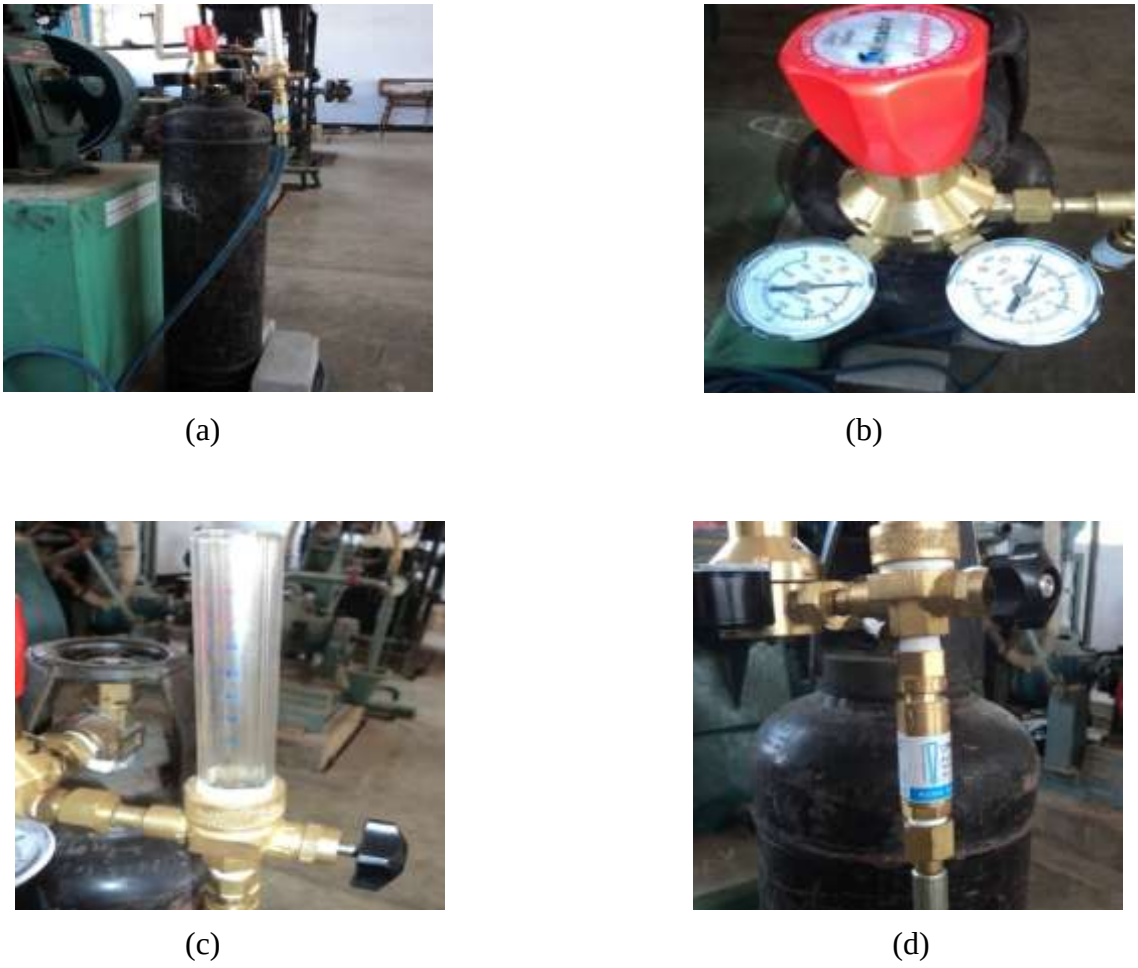

(a) (b)

(c) (d)

Figure 5.8 Photographic view of (a) the acetylene cylinder (b) pressure regulator (c) flow meter (d) flash back arrestor of the dual fuel mode

From Table 5.4, it can be observed that the acetylene required at no load is higher than that required at full load. The increase in the energy share of acetylene at no load

may be due to the lower combustion chamber temperatures, and also due to the mixing of the primary fuel, with the residual gases present inside the engine cylinder from the previous cycle. The empirical relation for the energy share of acetylene with UTO is given in Appendix A6. The test matrix indicating all the experiments conducted is given in Table 5.5.

Table 5.3 Comparison of physical and combustion properties of acetylene with diesel

Properties	**Acetylene**	**Diesel**
Formula	C_2H_2	C_8-C_{20}
Density at 1.01325 bar & and 293 K kg/m_3)	1.092	840
Auto-ignition temperature (K)	578	527
Stoichiometric air fuel ratio (kg/kg)	13.2	14.5
Flammability limits (volume %)	2.5-81	0.6-5.5
Flame speed(m/s)	1.5	0.3
Adiabatic flame temperature (K)	2500	2200
Lower calorific value (kJ/kg)	48,225	42,500
Ignition energy (mJ)	0.019	-

Table 5.4 Energy share of acetylene

Acetylene inducted at different flow rates (g/h)	**Load (%)**	**Energy share of acetylene when diesel as primary fuel**	**Energy share of acetylene when UTO as primary fuel**
132	0	27	29
	25	21	24
	50	17	18
	75	13	13
	100	11	12

Acetylene inducted at different flow rates (g/h)	Load (%)	Energy share of acetylene when diesel as primary fuel	Energy share of acetylene when UTO as primary fuel
198	0	41	38
	25	36	33
	50	29	28
	75	23	23
	100	18	19
264	0	54	62
	25	46	52
	50	39	44
	75	24	39
	100	24	29
330	0	60	80
	25	57	62
	50	50	50
	75	37	44
	100	30	36

Table 5.5 Test matrix

Sl No.	Variables	Fuels used	Objective
1.Normal operation with diesel			
	Minimum to maximum Brake power at rated speed of 1500 rpm	diesel	Base line data generation for combustion, performance and emission parameters

Sl No.	Variables	Fuels used	Objective
2. UTO and its diesel blends			
	Minimum to maximum Brake power at rated speed of 1500 rpm	UTO, UTO10, UTO20, UTO30, UTO40, UTO50, UTO60	Evaluation of combustion, performance and emission parameters
3. UTO at different injection timings			
	Minimum to maximum Brake power at rated speed of 1500 rpm Injection timing used: 18.5, 20, 21.5, 24.5, 26 and 27.5 ^{o}bTDC	UTO	Evaluation of combustion, performance and emission parameters
	Minimum to maximum Brake power at rated speed of 1500 rpm Injection timing used: 18.5, 20, 21.5, 24.5, 26 and 27.5 ^{o}bTDC	UTO	Evaluation of combustion, performance and emission parameters
4. UTO at different nozzle opening pressures			
	Minimum to maximum Brake power at rated speed of 1500 rpm Nozzle opening pressure used: 200,	UTO	Evaluation of combustion, performance and emission parameters

	210, 220, 230, 240 and 250 bar		
5. **UTO at different compression ratio**			
	Minimum to maximum Brake power at rated speed of 1500 rpm Compression ratio used: 16:1, 17:1, 17.5:1 and 18.5:1	UTO	Evaluation of combustion, performance and emission parameters
5. **UTO at different preheating temperatures**			
	Minimum to maximum Brake power at rated speed of 1500 rpm Preheted temperature used: 80, 90. 100, 110 ^{o}C	UTO	Evaluation of combustion, performance and emission parameters
5. **Diesel on dual fuel mode**			
	Minimum to maximum Brake power at rated speed of 1500 rpm	diesel, diesel + Acetylene 132 g/h, diesel + Acetylene 198 g/h, diesel + Acetylene 264 g/h, diesel + Acetylene 330 g/h	Evaluation of combustion, performance and emission parameters
6. **UTO on dual fuel mode**			
	Minimum to maximum Brake power at rated speed of 1500 rpm	UTO, UTO + Acetylene 132 g/h, UTO + Acetylene 198 g/h, UTO + Acetylene 264 g/h, UTO + Acetylene 330 g/h	Evaluation of combustion, performance and emission parameters

5.8 Analysis and procedure

During the investigation the humidity of the atmospheric air was measured with the help of the hygrometer, and it was 41%.

Three performance parameters viz, the brake specific fuel consumption (BSFC) and exhaust gas temperature were determined for diesel operation. The BSFC is not a reliable parameter if fuels of different viscosity and density are used. Brake specific energy consumption (BSEC) is a product of BSFC and the calorific value of fuel at a particular load. Therefore, the BSEC rather than BSFC is discussed in results and discussions. The calculations used for determining the BSEC from BSFC are given in Appendix A6.

The emission parameter such as HC, CO and NO, were directly obtained with the help of exhaust gas analyzer. The units of these emissions were measured in ppm, %vol and ppm respectively. These values were converted into g/kWh. The conversation formulae are given in Appendix A6. Smoke values are directly obtained with the help of smoke meter.

5.9 Uncertainty analysis

Any measurement, irrespective of the type of instrument used, possesses a certain amount of uncertainty or error. Some of these errors are of a random nature and need a device to specify consistently the uncertainty in an analytical form. Hence, a brief attempt was made to estimate the uncertainty of various measurements by theoretical methods. An uncertainty analysis was performed using the method described by Holman [105]. The range, accuracy and percentage of the uncertainty of each instrument is given in Appendix A7. The procedure used for the uncertainty analysis is given in Appendix A8.

CHAPTER 6
RESULTS AND DISCUSSION

6.1 General

This chapter presents a detailed discussion on the results obtained for combustion, performance and emission of a single cylinder, four stroke, air cooled, DI diesel engine, fueled with the UTO using different techniques. Two fuel modification techniques; viz, (i) blending the UTO at different percentages with diesel and (ii) preheating the UTO at different temperatures, were adopted. Four engine modifications viz, (i) Operating the engine with the UTO at different injection timings, (ii) Runnig the engine with the UTO at higher nozzle opening pressures, (iii) Operating the engine with different compression ratios and (iv) Operating the engine in the dual fuel mode with the UTO, and acetylene, were also adopted.

6.2 UTO and its diesel blends

As mentioned in the chapter "Experimental methodology", the UTO was blended with diesel from 10% to 60% on volume basis and the blends were tested. In this section the results of the combustion, performance and emission parameters of the engine fueled with UTO and its diesel blends are analyzed, compared with those of diesel operation of the same engine and presented. The numerical value after 'UTO' refers to the percentage of UTO in the blend. For example, UTO10, is composed of 10% UTO and 90% diesel.

6.2.1 Combustion analysis

6.2.1.1 Pressure crank angle diagram

The pressure variation in the cycle is important in the analysis of the performance characteristics of any fuel. The pressure variations of UTO and its diesel blends with respect to the crank angle at maximum brake power are shown in Fig. 6.1. It can be observed from the figure that the ignition of UTO10, UTO20, UTO30, UTO40, UTO50, UTO60 and UTO occurs 2, 1, 3, 1.5, 2.5, 3 and 1 ^{o}CA earlier than that of diesel at maximum brake power. The early

occurrence of ignition in UTO and its diesel blends is attributed to the increased cetane number of UTO and its diesel blends [106].

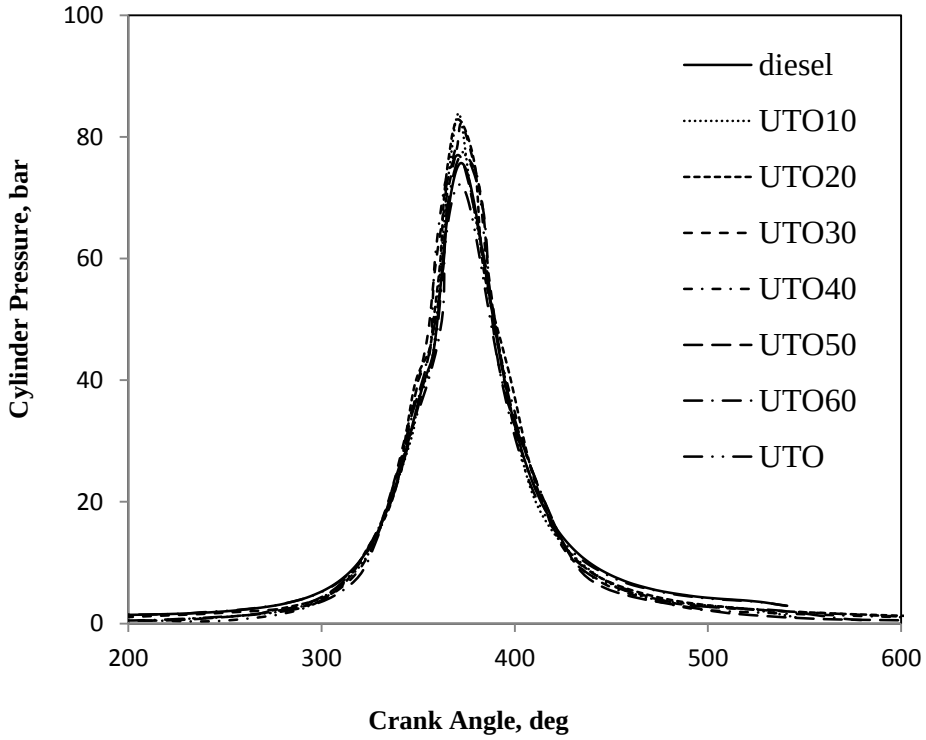

Figure 6.1 Variation of the cylinder pressure with crank angle at maximum brake power for the UTO and its diesel blends

6.2.1.2 Ignition delay

Ignition delay is the time difference measured in the degree of the crank angle between the start of injection and the start of ignition of a fuel in a diesel engine. The value of ignition delay helps to determine the heat release, maximum pressure and rate of pressure rise [107]. The variation of the ignition delay for the UTO, its diesel blends and diesel with respect to brake power is presented in Fig. 6.2. The ignition delay of the tested fuels in this study decreases as the brake power increases. This trend is genuine, because as the brake power increases the heat prevailing inside the cylinder increases, and helps the fuel air mixture to ignite sooner. It can also be observed from the figure that the ignition delay is found to decrease with an increase in the UTO in the blends. The ignition delay for diesel is about 11.4 ^{o}CA at maximum brake power, whereas for the UTO, it is 10.1 ^{o}CA at maximum brake power.

In the case of UTO10, UTO20, UTO30, there is not much deviation in the ignition delay and the value is noticed as 11.2 ^{o}CA at maximum brake power. The value of ignition delay for the UTO40, UTO50 and UTO60 is 10.7, 10.6, 10.5 ^{o}CA respectively at maximum brake power. The reason for the shorter ignition delay may be the chemical reactions during the injection of the UTO and its blends at high temperature which might result in the breakdown of the higher molecular weight compounds into products of lower molecular weight. These complex chemical reactions led to the formation of gases of lower molecular weight on the peripheral region with a very dense inner core of liquids of higher molecular weight. The rapid vaporization of this lighter oil at the fringe of the spray spread out the jet, and thus the volatile combustible compounds ignited earlier and reduced the ignition delay.

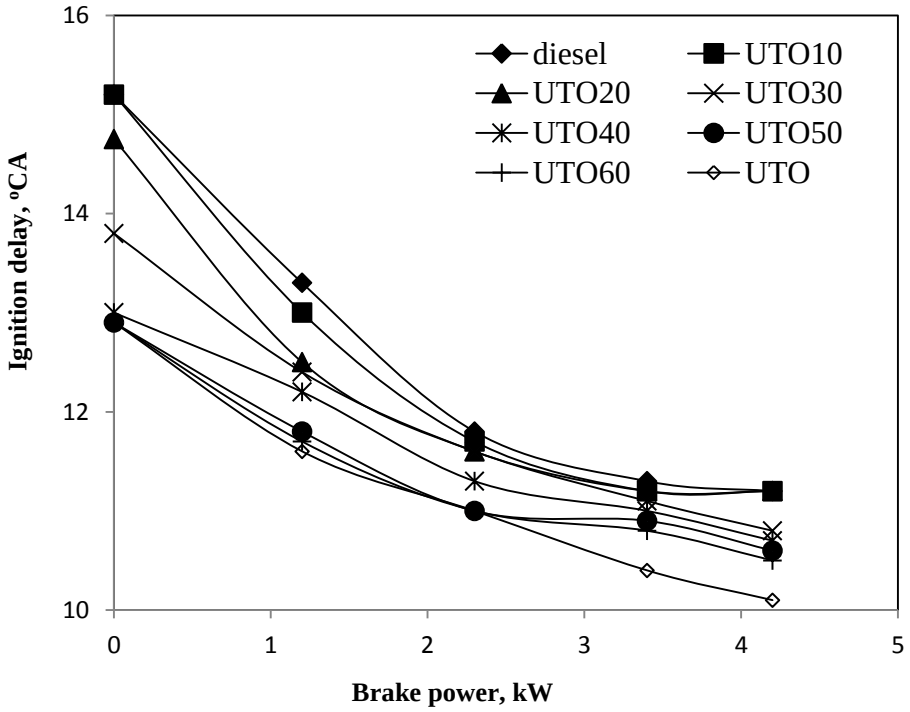

Figure 6.2 Variation of the ignition delay with brake power for the UTO and its diesel blends

6.2.1.3 Heat release rate

The heat release rate corresponding to every crank angle for the UTO, diesel blends and diesel at maximum brake power is shown in Fig. 6.3. Heywood [107] reported that the heat release rate in the premixed combustion phase depends on the ignition delay, mixture formation

and the combustion rate in the initial stages of combustion. It is also reported that the heat release rate may or may not reach the second peak in the diffusion combustion phase. It can be observed from the figure that the second peak does not appear significantly in the diffusion combustion phase.

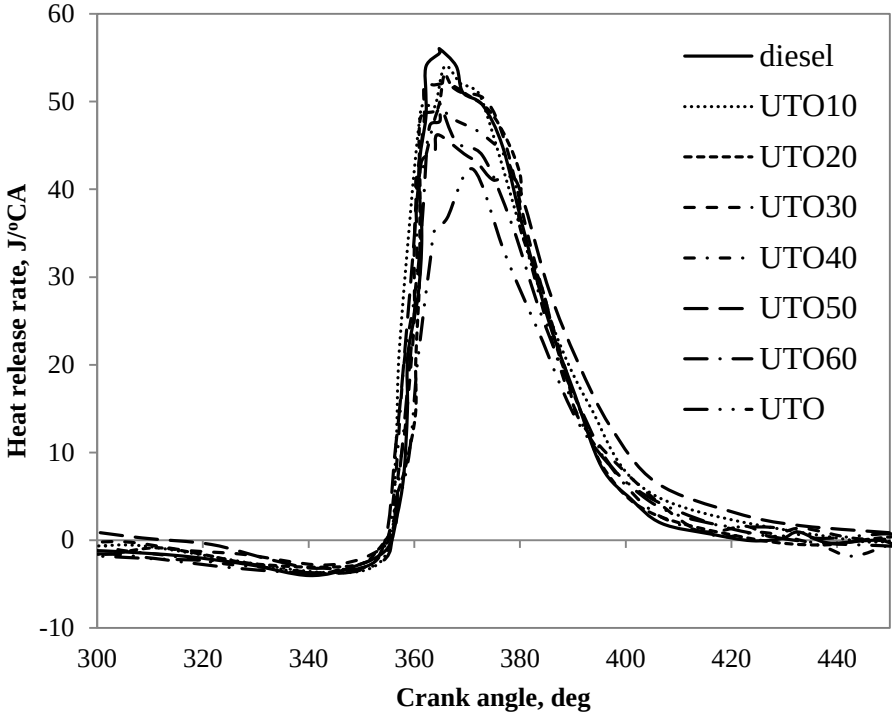

Figure.6.3 Variation of the heat release rate with crank angle at maximum brake power for the UTO and its diesel blends

It can also be observed that the occurrence of the maximum heat release rate is found to be a little earlier for the UTO and its diesel blends than that of diesel at maximum brake power, as a result of the bulk modulus characteristic of UTO. The maximum heat release for the UTO and diesel occurred at 371 ^{o}CA and 364.78 ^{o}CA at maximum brake power. The occurrence of the maximum heat release rate for the UTO10, UTO20, UTO30, UTO40, UTO50 and UTO60 is at 365.7, 365.6, 366.2, 364.15, 364.44 and 364.85 ^{o}CA respectively, at maximum brake power. As the percentage of UTO in the blend increases, the maximum heat release rate decreased and the crank angle at which it takes place advanced.

6.2.1.4 Combustion duration

Figure 6.4 portrays the variation of the combustion duration with brake power for the UTO, diesel blends and diesel.

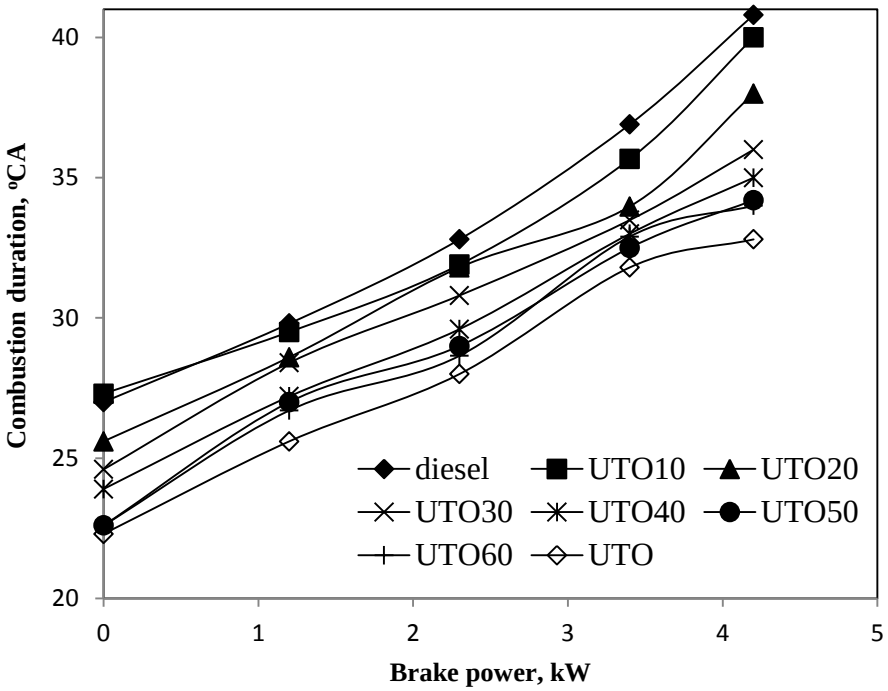

Figure.6.4 Variation of the combustion duration with brake power for the UTO and its diesel blends

The combustion duration increases with increase in the engine brake power for all the fuels tested. The combustion duration of UTO and its diesel blends is found to be lower than that of diesel fuel at maximum brake power. The combustion duration of diesel, UTO10, UTO20, UTO30, UTO40, UTO50, UTO60 and UTO is 40.8, 40, 38, 36, 35, 34.2, 34 and 32.8 ^{o}CA respectively, at maximum brake power. The combustion duration decreases as the percentage of UTO increases in the blend. This may be due to the promotion of combustion as a result of the oxygen content present in the UTO.

6.2.1.5 Maximum cylinder pressure

Figure 6.5 shows the variation of the maximum cylinder pressure with the brake power for the UTO, UTO-diesel blends and diesel. The maximum cylinder pressure of a CI engine depends

mainly on the amount of fuel accumulated in the delay period, and the combustion rate in the initial stages of premixed combustion [108]. The maximum cylinder pressure for diesel and the UTO at maximum brake power is 78.1 and 85.9 bar, respectively whereas for the UTO10, UTO20, UTO30, UTO40, UTO50 and UTO60 blends it is 79.9, 81.7, 82.5, 83, 84.1 and 84.5 bar. When compared to diesel, the values of the maximum cylinder pressure for the UTO and its diesel blends are found to be higher than that of diesel at maximum brake power. The maximum cylinder pressure for the UTO and its diesel blends is owing to the higher heat released in the premixed combustion phase. In the case of UTO the maximum cylinder pressure is found to be higher than that of diesel and UTO60, at maximum brake power.

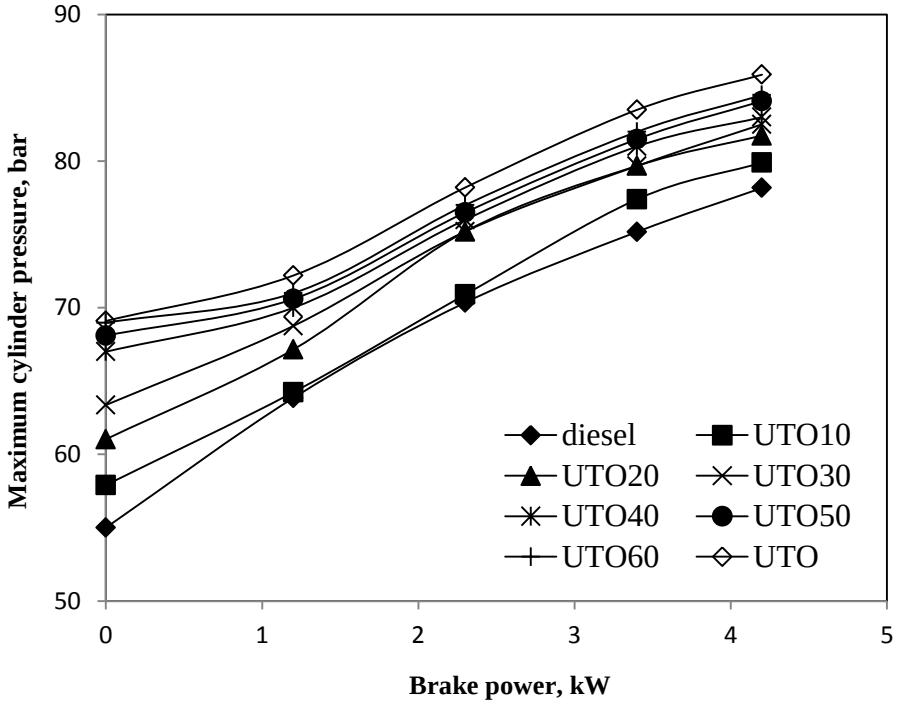

Figure 6.5 Variation of the maximum cylinder pressure with brake power for the UTO and its diesel blends

6.2.1.6 Maximum rate of pressure rise

Figure 6.6 portrays the comparison of the maximum rate of pressure rise with respect to the engine brake power for the UTO, its diesel blends and diesel. The maximum rate of pressure rise defines the rate at which the pressure imposed at every crank angle during the combustion

process on the cylinder head and other components. The rate of pressure rise depends on the amount of heat released in the initial stages of combustion and the fuel quality [107]. The higher the maximum rate of pressure rise, the higher the brake power on the piston and other components, which may lead to severe damage of the parts [76].The maximum rate of pressure rise for diesel and UTO are found to be 5.34 and 4.5 bar/^{o}CA respectively at maximum brake power, whereas for the UTO10, UTO20, UTO30, UTO40, UTO50 and UTO60, it is 5.2, 5.19, 5.14, 5, 4.7 and 4.6 bar/^{o}CA respectively. The maximum rate of pressure rise for diesel is the highest compared to those of UTO and its diesel blends, as a result of longer ignition delay of diesel. As the rates of pressure rise for the UTO and its diesel blends are lower than that of diesel, the engine piston will not be affected by the pressure imposed in it.

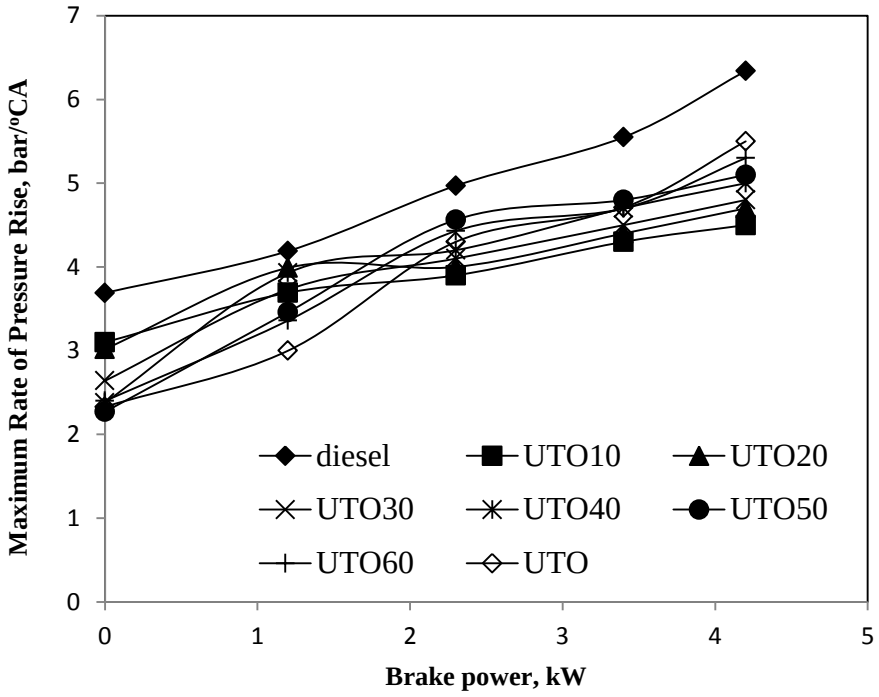

Figure 6.6 Variation in the maximum rate of pressure rise with brake power for the UTO and its diesel blends

6.2.2 Performance parameters

6.2.2.1 Brake specific energy consumption

Figure 6.7 illustrates the variation of the BSEC with engine brake power for the UTO, its diesel blends and diesel. The energy consumption of all the tested fuels decreases with an

increase in the brake power as expected. The BSEC is found to be the lowest for UTO (11.3 MJ/kWh) among all the tested fuels in this study, throughout the engine operation. As the percentage of UTO increases up to 40% in the blend the combustion duration decreases due to oxygen content present in the UTO. This may be attributed to more and better complete combustion of UTO-diesel blends, thus BSEC decreases. The UTO40 blend shows the lowest value of the BSEC at the maximum brake power. UTO50, UTO60 and UTO exhibited higher specific energy consumption than that of UTO40.

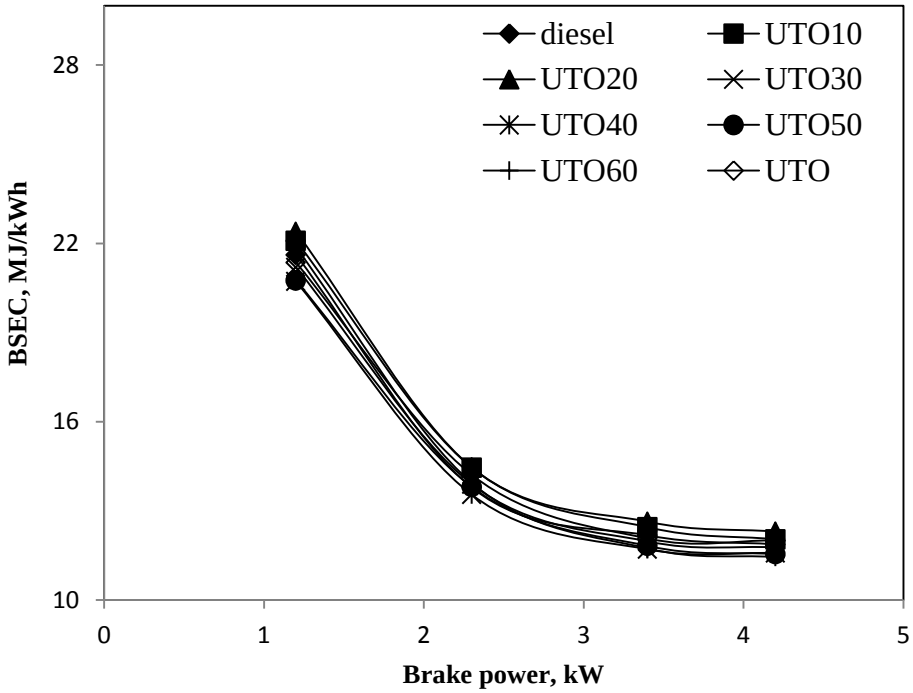

Figure 6.7 Variation in the BSEC with brake power for the UTO and its diesel blends

The fuel spray formed by UTO50, UTO60 and UTO may be poorer as a result of the high viscosity of the blend. Hence, more energy may be required to produce the same power output compared to that of diesel. The values for diesel and UTO are 11.8 and 11.3 MJ/kWh, whereas for the UTO10, UTO20, UTO30, UTO40, UTO50 and UTO60, they are 12.04, 12.3, 11.7, 11.58, 11.54, 12 and 11.44 MJ/kWh respectively, at the maximum brake power.

6.2.2.2 Exhaust gas temperature

The exhaust gas temperature of an engine is an indication of the effective energy conversion from heat into mechanical work [48]. Figure 6.8 portrays the variation of the exhaust gas

temperature with brake power for different tested fuels. The exhaust gas temperature increases with an increase in the engine brake power for the UTO, and its diesel blends and diesel. The exhaust gas temperature for the UTO and its diesel blends is found to be higher than that of diesel in the entire engine operation, as a result of the higher viscosity and density of UTO.

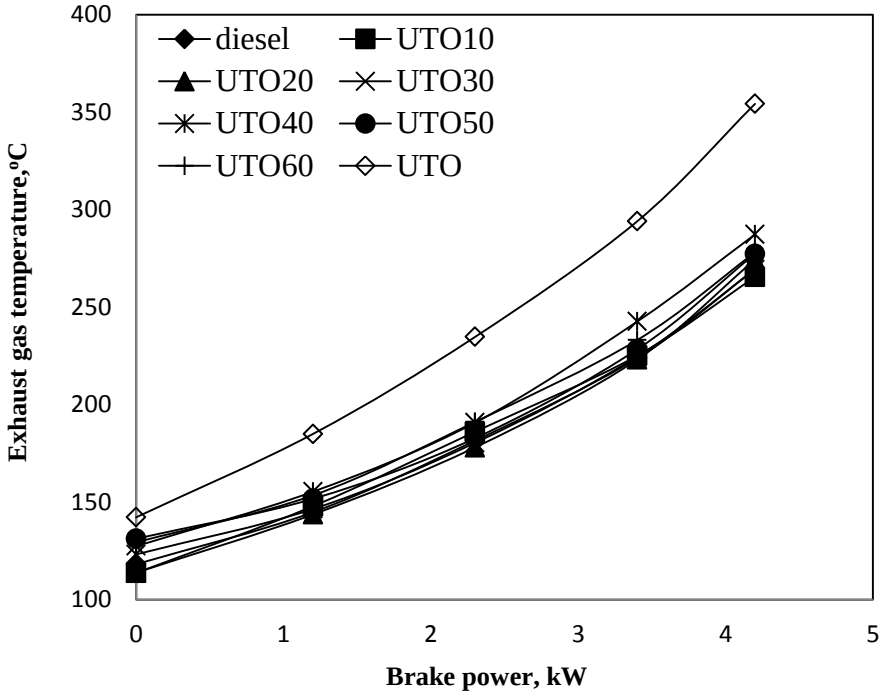

Figure 6.8 Variation of the exhaust gas temperature with brake power for the UTO and its diesel blends

Among the UTO-diesel blends the exhaust gas temperatures of UTO40, UTO60, UTO50, UTO20, UTO30 and UTO10 are found to be sequentially lower than that of UTO, but higher than that of diesel at the maximum brake power. The exhaust gas temperatures of diesel and UTO are 269.5 and 354.2^{o}C, whereas for the UTO10, UTO20, UTO30, UTO40, UTO50 and UTO60, they are 265.4, 274.44, 269.2, 287.3, 277.4 and 278.1^{o}C respectively at maximum brake power.

6.2.3 Emission parameters

6.2.3.1 Nitric oxide emission

The NO emission in a CI engine depends strongly on the combustion temperature and oxygen availability. The variation of the NO emission for the UTO, diesel blends and diesel for

different engine brake power, is shown in Fig. 6.9. The NO emissions of diesel and UTO at maximum brake power are 5.6 and 5.8 g/kWh respectively, whereas for the UTO10, UTO20, UTO30, UTO40, UTO50 and UTO60, the NO emission are 5.81, 6.07, 6.62, 6.9, 7 and 7.09 g/kWh respectively, at maximum brake power. The NO emission for the UTO and its diesel blends are noticed higher compared to that of diesel for a given power output. The higher NO emission for the UTO and its diesel blends may be associated with higher combustion temperatures and presence of oxygen in the UTO.

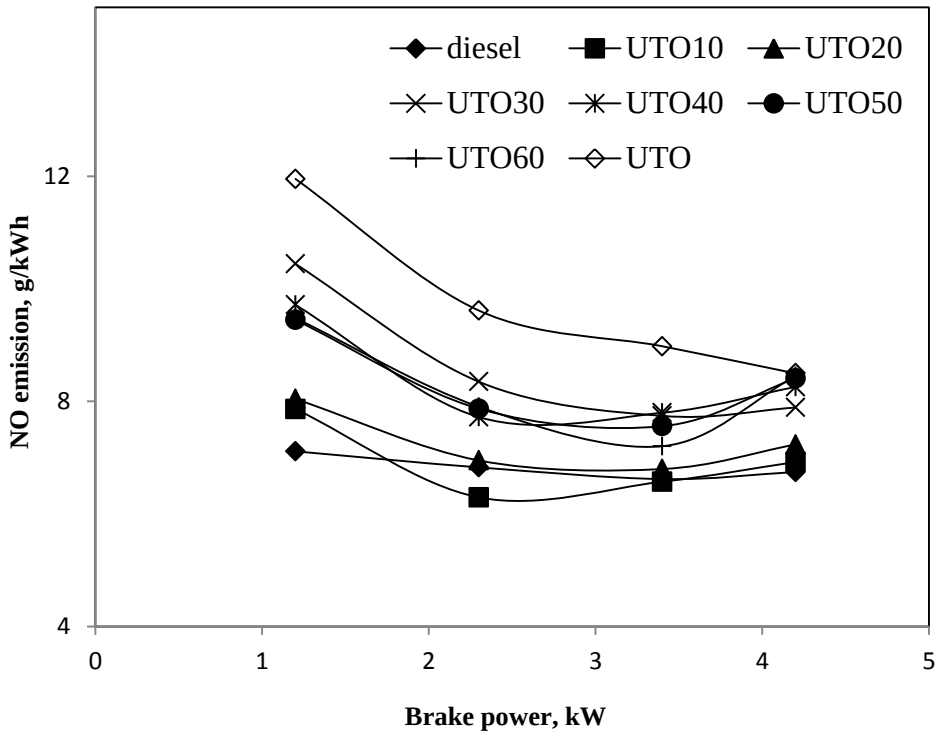

Figure 6.9 Variation of the NO emission with brake power for the UTO and its diesel blends

6.2.3.2 Carbon monoxide emission

The CO emission in a CI engine is quite negligible compared to that of SI engines, as the former is operated with excess air. The variation of the CO emission for the UTO, diesel blends and diesel for different engine brake powers is shown in Fig. 6.10. The CO emissions for diesel, UTO, UTO10, UTO20, UTO30, UTO40, UTO50 and UTO60 are 0.0023, 0.0046, 0.0024, 0.0028, 0.003, 0.0034, 0.004 and 0.0043 g/kWh respectively at maximum brake power. It can be observed from the figure that the CO emission is marginally higher for the UTO-diesel blends

compared to that of diesel at maximum brake power. The CO values are the lowest for diesel and the highest for the UTO, at maximum brake power. The higher CO emissions for the UTO may be attributed to local rich regions and poor mixture formation in some locations of the combustion chamber [109].

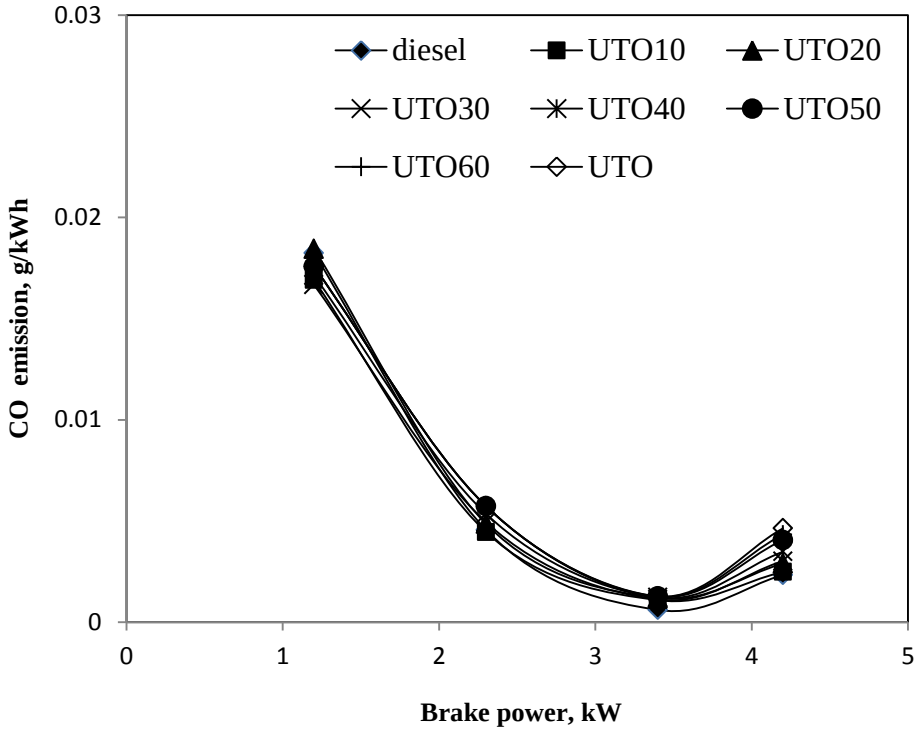

Figure 6.10 Variation of CO emission with brake power for the UTO and its diesel blends

6.2.3.3 Hydrocarbon emission

Pundir [110] mentioned that the CI engines are capable of converting the fuel-air mixture into products of combustion by about 98%. The variation of the unburned HC emission for the UTO, its diesel blends and diesel for different brake powers is shown in Fig. 6.11.

The HC emission for diesel and UTO are 0.005 and 0.01 g/kWh respectively at maximum brake power, whereas for the UTO10, UTO20, UTO30, UTO40, UTO50 and UTO60 they are 0.0058, 0.0067, 0.0073, 0.0097, 0.0098 and 0.01 g/kWh respectively at maximum brake power. The UTO-diesel blends generate higher unburned HC compared to that of diesel. The HC emission for the UTO and its diesel blends are found to be higher as a result of higher viscosity, density and poor mixture formation. It can be observed that the lowest and highest values of HC

emission are recorded with diesel and UTO respectively. However the HC emission for the UTO and its blends are close to that of diesel at maximum brake power.

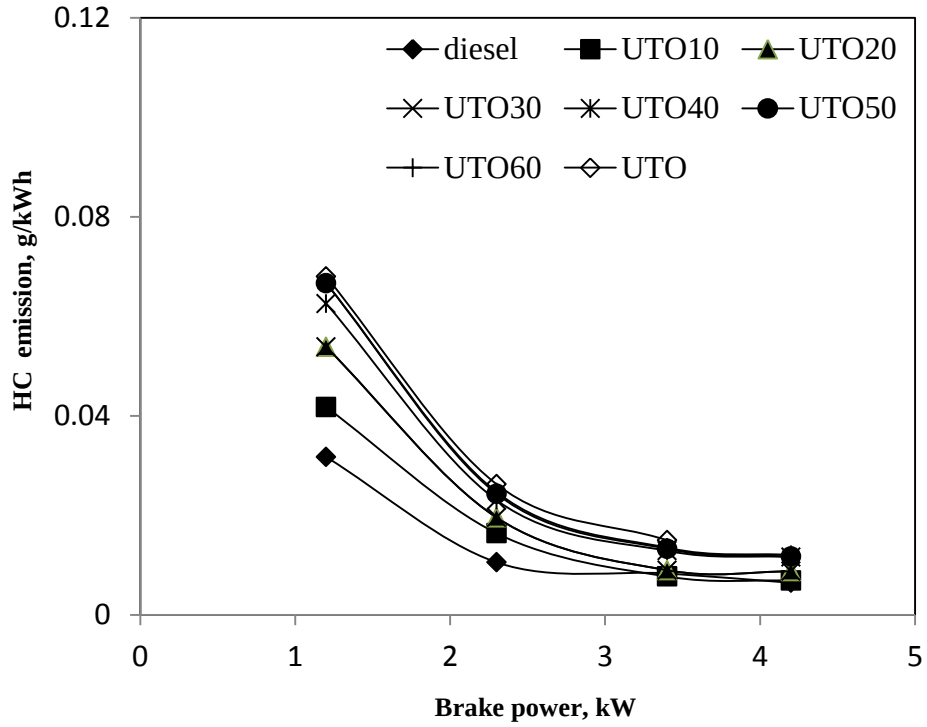

Figure. 6.11 Variation of HC emission with brake power for the UTO and its diesel blends

6.2.3.4 Smoke density

The smoke density is higher when a fuel's ratio of hydrogen to carbon is less than two. Figure 6.12 compares the smoke density of UTO, its diesel blends and diesel at different brake powers. It can be observed that the smoke density increases with an increase in the brake power as expected. The hydrogen to carbon ratio of UTO is found to be lower by about 49% than that of diesel. The smoke density of UTO-diesel blends decreases as the concentration of UTO increases from 20%. The diesel and UTO10 exhibit the highest smoke density among all the fuels tested whereas UTO shows the lowest smoke density. The smoke densities of diesel, UTO, UTO10, UTO20, UTO30, UTO40, UTO50 and UTO60 are 24, 19.2, 24, 22.2, 21.4, 20.1, 19.5 and 19.3% respectively, at maximum brake power.

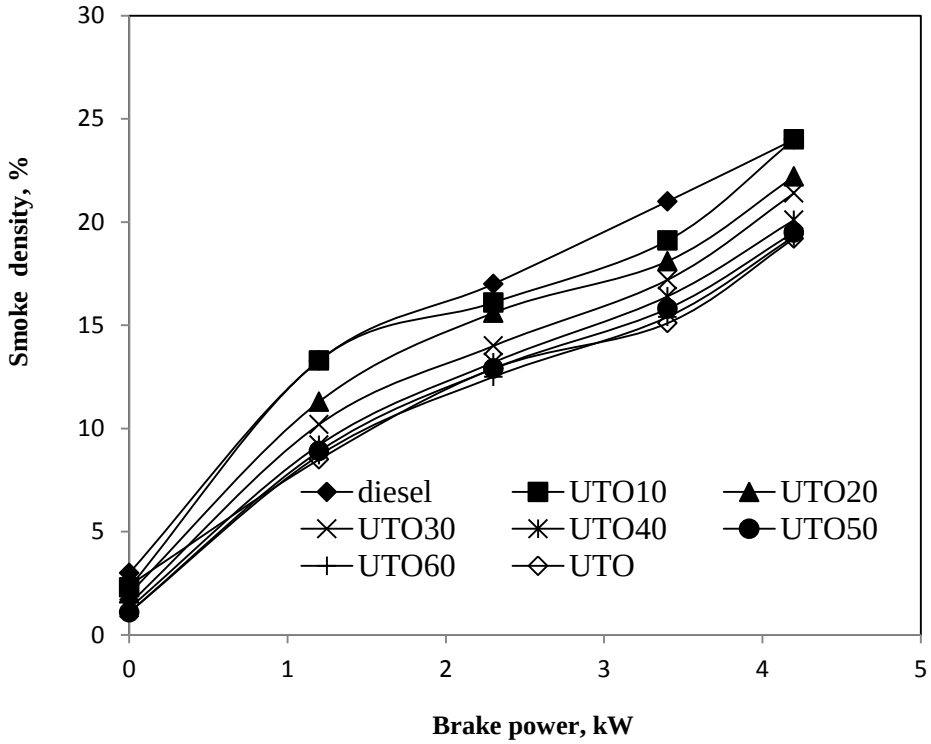

Figure. 6.12 Variation of smoke density with brake power for the UTO and its diesel blends

The percentage increase or decrease in the values of the combustion, performance and emissions at maximum brake power for the tested fuel is given in Table 6.1.

6.2.4 Closure

The results of the investigation reveal that the engine can run with sole UTO or in a blended form with diesel, without any engine modification. From the analysis of the combustion, performance and emission of the engine fueled with the UTO and its blends, UTO40 gave a better performance and lower emissions than the other blends and diesel. The NO emission increased with increase in blend percentage even though the viscosity increases. This is due to advancement of injection of UTO owing to its bulk modulus characteristics. Thus the effect of injection timing on the behavior of the engine fuelled with UTO was checked. This is discussed in the next chapter.

Table 6.1 Percentage variation of UTO and its diesel blends in comparison with diesel at maximum power output

Si.No	**Parameter**	**UTO10**	**UTO20**	**UTO30**	**UTO40**	**UTO50**	**UTO60**	**UTO**
Combustion Parameters								
1.	Occurrence of ignition	0.52	0.26	0.99	0.46	0.82	0.99	0.65
2.	Ignition delay	0	0	-3.5	-4.4	-5.3	-6.25	-9.82
4.	Combustion duration	-1.96	-6.86	-11.76	-14.21	-16.17	-16.66	-19.6
5.	Maximum heat release	-3.58	-5.37	-7.17	-12.35	-17.47	-11.28	-24.49
6.	Maximum cylinder pressure	2.21	4.56	5.55	6.17	7.58	8.09	9.88
Performance parameters								
1.	Brake specific energy consumption	1.43	3.62	-0.84	-2.44	-2.78	-3.62	1.09
2.	Exhaust gas temperature	-1.5	1.81	-1.57	6.59	2.91	3.17	31.4
Emission parameters								
1.	HC emission	6.59	24.3	35.2	79.7	80.85	86.24	91.35
2.	CO emission	6.57	24.35	29.55	49.31	74.19	85.65	99.05
3.	NO emission	2.65	7.24	16.97	22.41	24.69	25.25	25.96
4.	Smoke density	0	-7.5	-10.83	-16.25	-18.75	-19.58	-20

"+" indicates increasing percentage; "-" indicates decreasing percentage.

6.3 UTO at different Injection timings

6.3.1 General

Since the engine was able to run with the sole UTO, further investigations were carried out to study the effect of varying the injection timing of the engine fueled with the UTO. The results of combustion, performance and emission parameters of engine fueled with the UTO at different injection timing are analyzed, compared with diesel fuel and presented. The standard injection timing of the engine is 23^{o}bTDC. The injection timing of the engine was set at 24.5, 26 and 27.5^{o}bTDC for advancing while the injection timing was set at 18.5, 20, 21.5^{o}bTDC injection for retardment. The injection timing given in the markers in all the figures in this section presents the injection timing of UTO.

6.3.2. Combustion Analysis

6.3.2.1 Pressure crank angle diagram

Figure 6.13 shows the comparison of cylinder pressure histories of UTO at different injection timings with diesel operation at maximum brake power condition.

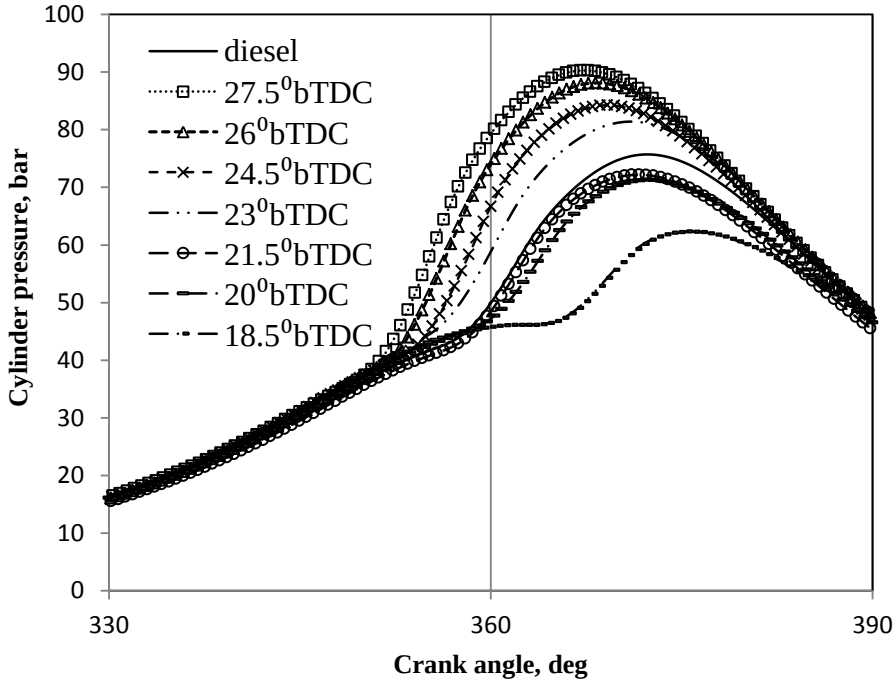

Figure 6.13 Variation of cylinder pressure with crank angle for engine fueled with UTO at different injection timings

At advanced injection timing of 27.5 ^{o}CA, the UTO ignites earlier at 3 ^{o}CA than the UTO at standard injection timing of 23^{o}bTDC. Retarded injection timing results later ignition. Thus UTO at 18.5^{o}bTDC injection timing exhibits ignition with 5 ^{o}CA later, than UTO.

6.3.2.2 Ignition delay

The variation of the ignition delay for diesel and the UTO at different injection timings with brake power is illustrated in Fig. 6.14. The ignition delay is found to be the shortest for the UTO at the advance injection timing of 24.5^{o}bTDC at the maximum power output.

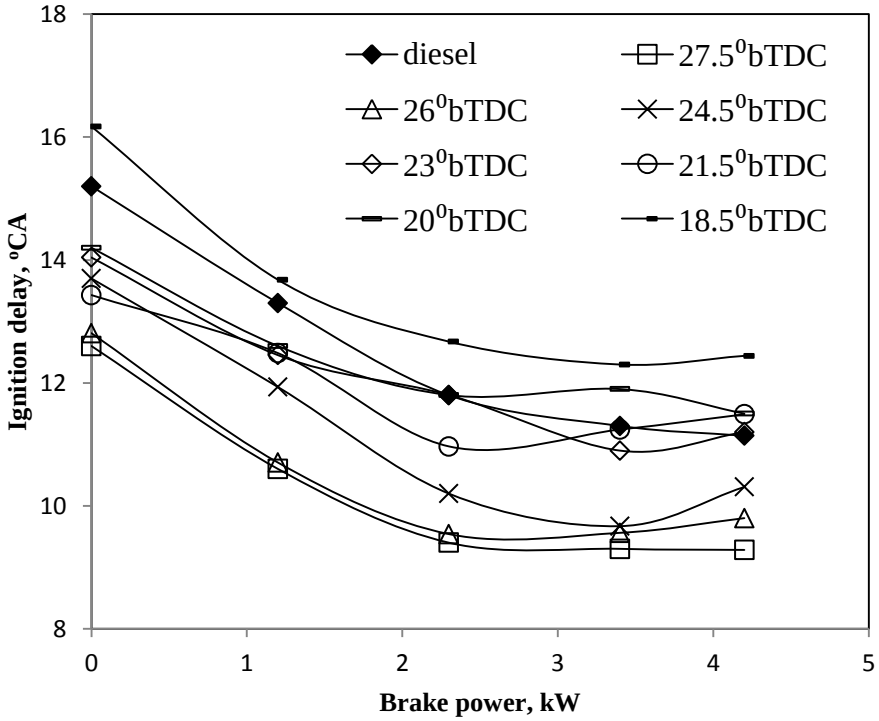

Figure 6.14 Variation of ignition delay with brake power for engine fueled with UTO at different injection timings

With the three advanced injection timings, the ignition delay is found to be shorter for the UTO than at original injection timing and diesel, while retarding the injection timing, the ignition delay becomes longer. The more viscous UTO has a complex molecular compound that may produce larger spray angles and shorter penetrations compared with those of diesel. Similar results have been reported by Jacob [111]; Ryan et al., [112]. The lighter compounds might have ignited earlier, resulting in shorter ignition delay. At maximum brake power the ignition delay

values for the UTO with 18.5, 20, 21.5, 24.5 and 27.5^{o}bTDC are 12.4, 11.1, 11.4, 9.2, 10.3 and 10.6 ^{o}CA respectively at maximum brake power.

6.3.2.3 Heat Release Rate

Heat release in a CI engine predominantly affected by ignition delay, density, adiabatic flame temperature and bulk modulus characteristics [113-118]. At original injection timing of 23 ^{o}CA bTDC for the UTO, the heat release rate is found to be highest at 364 ^{o}CA, while diesel has the maximum heat release rate highest at 52 J/^{o}CA at 367 ^{o}CA. The higher heat release rate of UTO at original injection timing may be due to bulk modulus characteristics of the fuel or different adiabatic flame temperatures of the constituents of UTO.

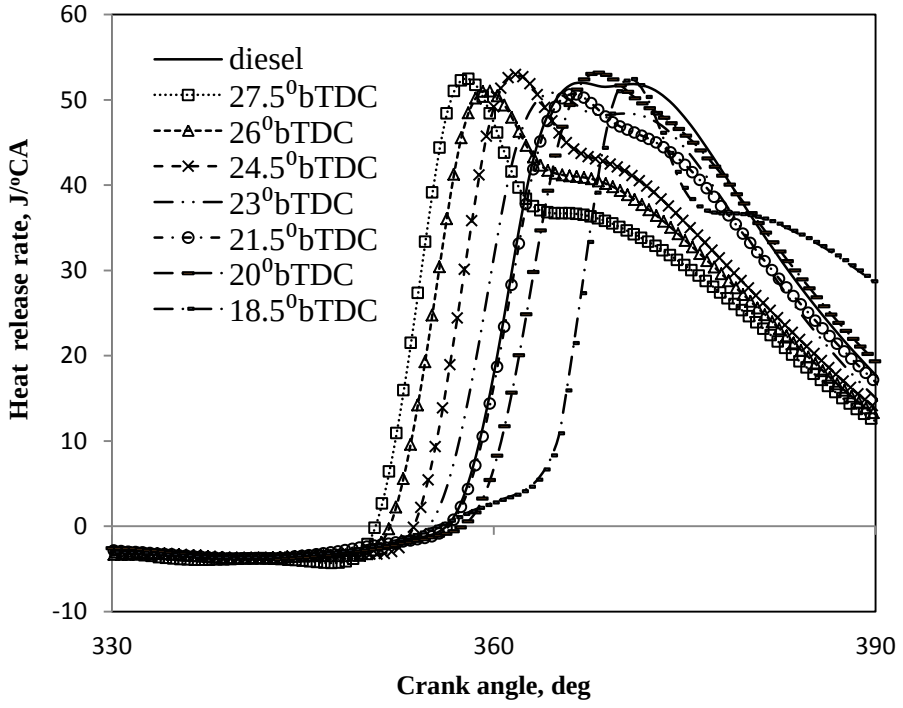

Figure 6.15 Variation of heat release rate with crank angle at maximum brake power for engine fueled with UTO at different injection timings

The heat release rate at every crank angle for the diesel and UTO at different injection timing at maximum brake power is shown in Fig. 6.15. Advancing the injection timing further results in increased heat release rate for the UTO at maximum brake power. The values of the maximum heat release rate for the UTO at advanced injection timing of 24.5, 26 and 27.5 ^{o}CA bTDC are

53, 51 and 52 J/^{o}CA that occurred at 362, 360 and 358 ^{o}CA at maximum brake power due to more fuel accumulated in the combustion chamber which increases the heat release rate. By retarding the injection timing from the original injection timing of 23 ^{o}CA bTDC to 20 ^{o}CA bTDC the heat release rate for premixed combustion gets reduced. Further retarding the injection timing to 18.5 ^{o}CA, the heat release rate decreased significantly to 52 J/^{o}CA than other injection timings that occurred at 370 ^{o}CA at maximum brake power. This is because of the shorter time available for complete combustion of UTO.

6.3.2.4 Combustion duration

Figure 6.16 illustrates the variation of the combustion duration for the UTO at different injection timings and diesel with engine brake power.

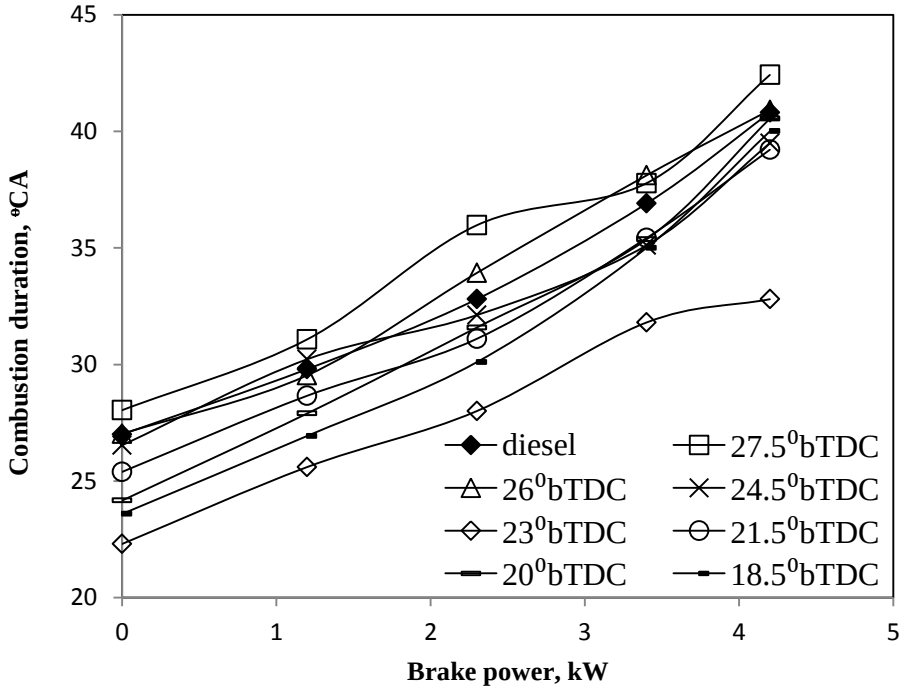

Figure 6.16 Variation of combustion duration with brake power for engine fueled with UTO at different injection timings

The combustion duration of all the fuels increases, with increasing brake power condition due to the accumulation of more fuel inside the cylinder. It can be noticed that the values of

combustion duration as 43.4, 40.5, 39.2, 32.8, 39.4, 40.9 and 42.4 ^{o}CA for 18.5, 20, 21.5, 23, 24.5, 26 and 27.5^{o}bTDC with the UTO respectively and 40.8 ^{o}CA for diesel at maximum brake power. Advanced injection timing of UTO exhibits a longer combustion duration. At retarded injection timing, the combustion duration gets reduced due to shorter ignition delay. These shorter ignition delays, decrease the fraction of burning, resulting in relatively later burning rate of premixed combustion phase, and thus an overall decrease in the combustion duration is noticed. Similar results have been reported by Kannan and Anand [118]

6.3.2.5 Maximum cylinder pressure

Figure 6.17 shows the variation of the maximum cylinder pressure with brake power for the UTO at different injection timing and diesel with engine brake power.

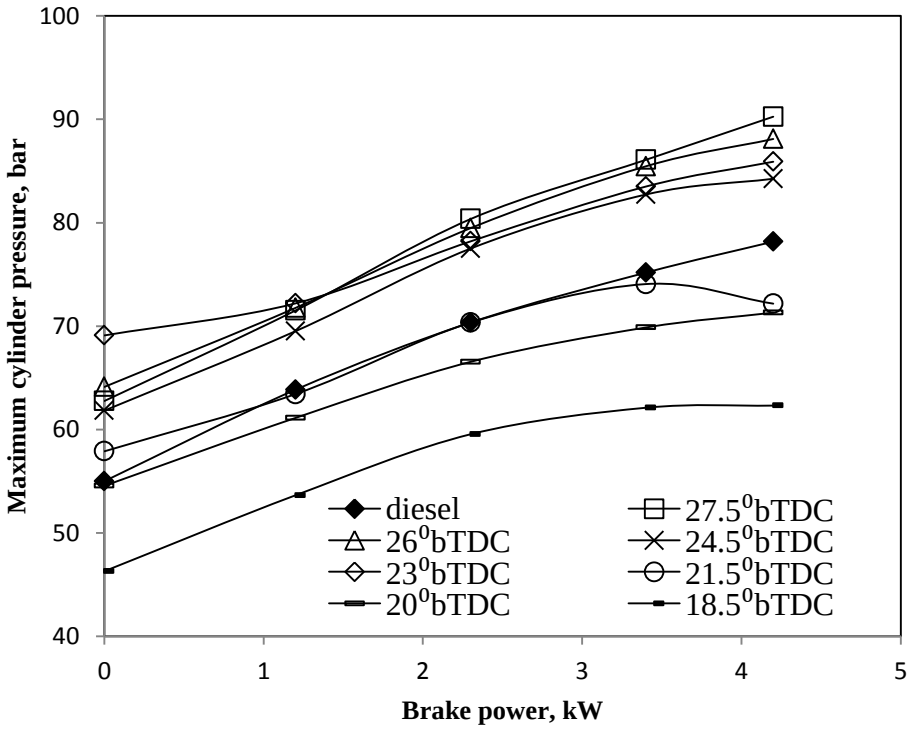

Figure 6.17 Variation of maximum cylinder pressure with brake power for engine fueled with UTO at different injection timings

The maximum cylinder pressure for diesel and UTO at maximum brake power is 78.1 and 85.9 bar, whereas for the UTO at 18.5, 20, 21.5, 24.5, 26 and 27.5^{o}bTDC injection timing, the

maximum cylinder pressure is noticed as 62.31, 71.3, 72.17, 84.25, 88.1 and 90.25 bar at maximum brake power. When compared to diesel, the values of maximum cylinder pressure for the 27.5 and 26^{o}bTDC with UTO found to be higher than that of diesel. At retarded injection timing of 18.5, 20, 21.5 bTDC with UTO shows lower maximum cylinder pressure than diesel at maximum brake power.

6.3.2.6 Maximum Rate of Pressure Rise

It is apparent from the figure that the rate maximum rate of pressure rise increases with an increase in brake power except 100%, which may be due drop in 0.3 bar/^{o}CA. The variation of the maximum rate of pressure rise for the UTO at different injection timings and diesel with engine brake power is presented in Fig. 6.18.

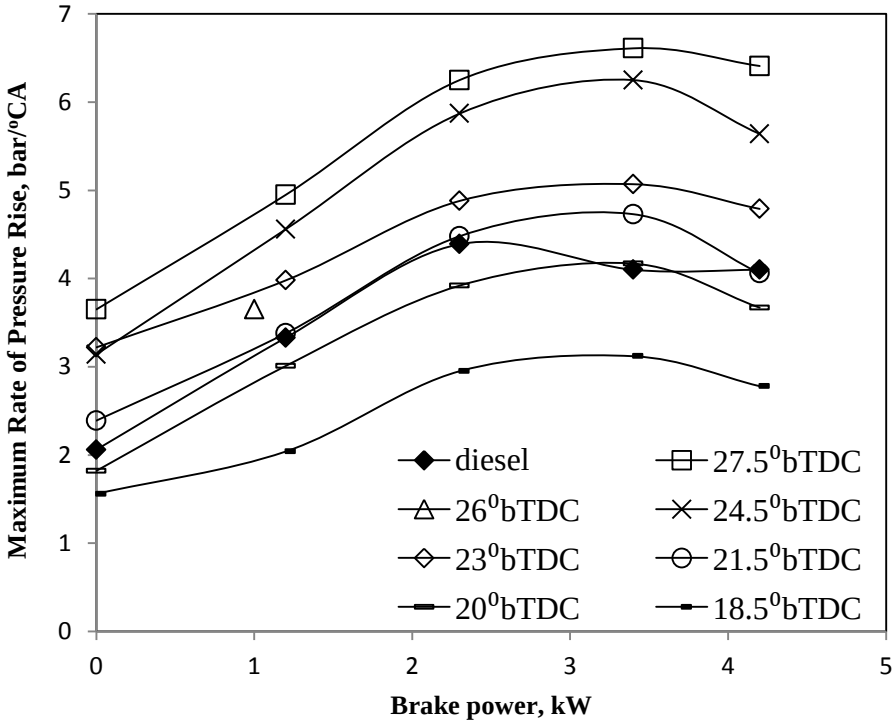

Figure 6.18 Variation of rate of pressure rise with brake power for engine fueled with UTO at different injection timings

The value of the maximum rate of pressure rise are found to be 6.4, 5.9, 5.6, 4.7, 5.6, 5.9 and 6.4 bar/^{o}CA for the injection timing of 18.5, 20, 21.5, 23, 24.5, 26 and 27.5^{o}bTDC with UTO

respectively and 4.1 bar/^{o}C for diesel. At advanced injection timing, the maximum rate of pressure rise is found to be higher due to, larger amount of fuel injected, thus higher pressure occurred before TDC. Retarded injection timing exhibits a lower rate of pressure rise due to increase in ignition delay compared to that of original injection timing of UTO.

6.3 3. Performance parameters

6.3.3.1 Brake specific energy consumption

The BSEC is the input energy required to develop unit power output [12]. The variation of the BSEC for the UTO at different injection timing and diesel with engine brake power is presented in Fig. 6.19. The figure shows the values of brake specific energy consumption as 11.8, 11.5, 11.4, 11.3, 11.2, 11.1 and 11 MJ/kWh for 18.5, 20, 21.5, 23, 24.5, 26 and 27.5^{o}bTDC with UTO respectively and 11.8 MJ/kWh for diesel.

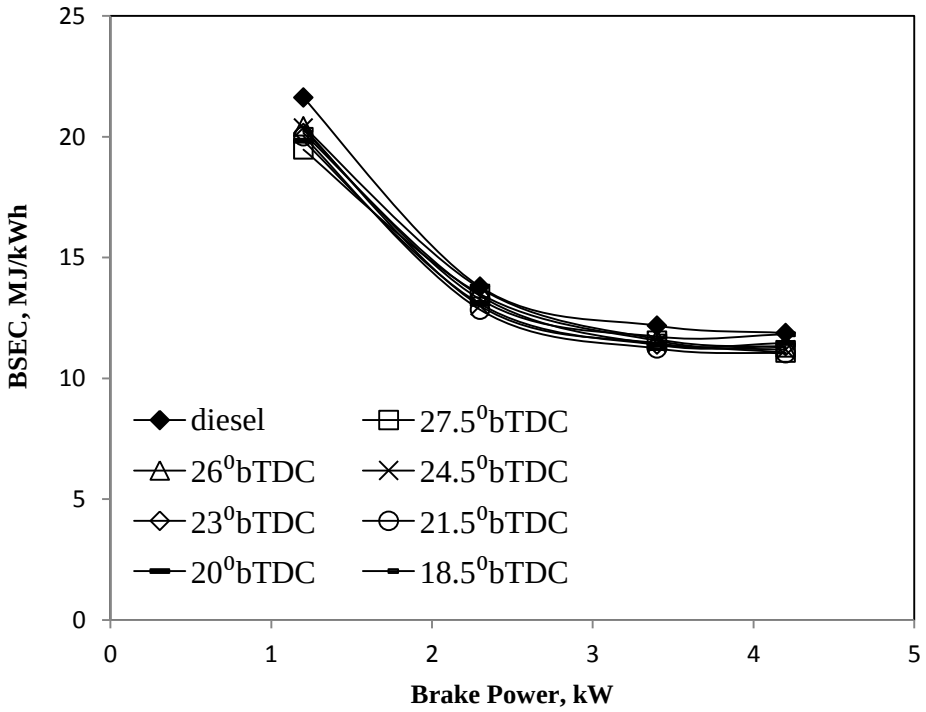

Figure 6.19 Variation of BSEC with brake power for engine fueled with UTO at different injection timings

The BSEC decreases with increase in brake power for diesel and the UTO at different injection timings. Advance injection produces peak pressure closer to TDC and offers sufficient

time to release heat, hence offers a lower BSEC, followed by retarded injection timing shows higher BSEC. The results are agreed by Venkatraman and Devaradjane [119] .

6.3.3.2 Exhaust gas temperature

The variation of the exhaust gas temperature for the UTO at different injection timings and diesel with engine brake power is presented in Fig. 6.20. The values of exhaust gas temperature are found to be 329, 300, 299, 287.32, 285, 282 and 280^{o}C for 18.5, 20, 21.5, 23, 24.5, 26 and 27.5 ^{o}bTDC with UTO respectively and 269.5^{o}C for diesel at maximum brake power. The exhaust gas temperature is found to be lower at advancing injection timing which is due to the occurrence of combustion earlier, and the burnt gas had more time to interact with cooling medium before exit through thorough exhaust valve exit the exhaust valve. With retarding the injection timing of UTO, the exhaust gas temperature is found to increase as a result of partial burning of fuel mixture during the exhaust stroke [31].

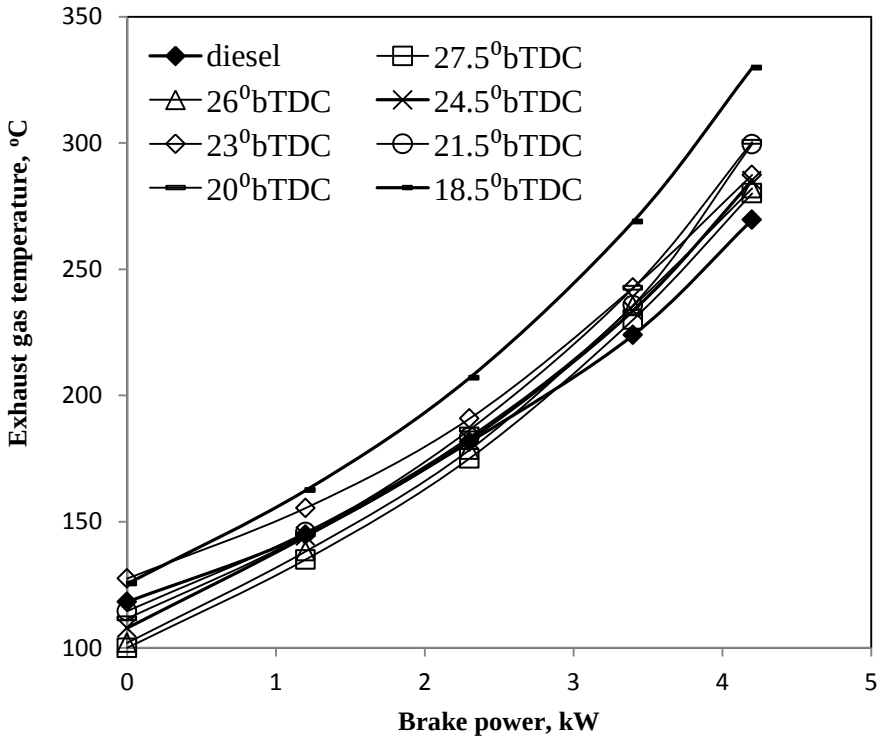

Figure 6.20 Variation of exhaust gas temperature with brake power for engine fueled with UTO at different injection timings

6.3.4. Emission parameters

6.3.4.1 Nitric oxide emission

CI engines are always run with lean mixture and emit high amounts of NO emission. Figure 6.21 shows the comparison of the NO emission for the UTO at different injection timings with diesel at different brake power.

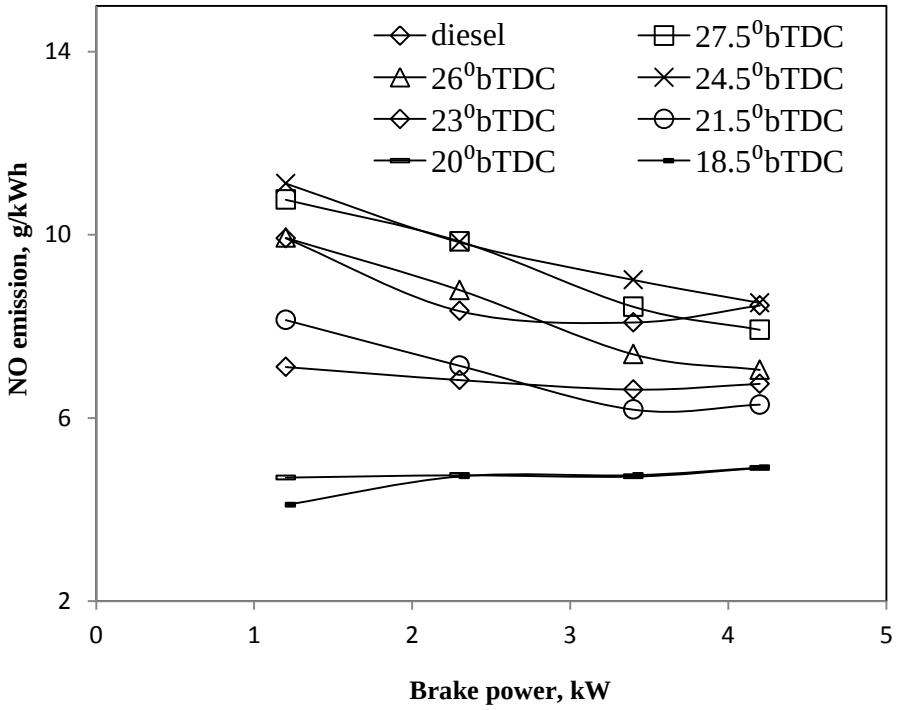

Figure 6.21 Variation of NO emission with brake power for engine fueled with UTO at different injection timings

The values of the NO emission are noticed as 4.1, 4.12, 5.2, 7.1, 7.15, 5.9 and 6.6 g/kWh for 18.5, 20, 21.5, 23, 24.5, 26 and 27.5^{o}bTDC with UTO respectively and 5.6 g/kWh for diesel at standard injection timing for maximum brake power. At the advanced injection timing, there is an increase in the NO emissions compared to that of UTO at standard injection timing at maximum brake power due to the bulk modulus characteristics of the fuel. Another possible reason is stated by Sequera et al., [120] in his work that higher combustion temperature results in higher NO emission. This reason can be matched in the case of UTO also.

6.3.4.2 Carbon monoxide emission

The comparison of CO emission for the UTO at different injection timings with diesel at various brake power is portrayed in Fig. 6.22. The CO emissions are found to be 0.001955 and 0.003893 g/kWh for diesel and UTO respectively at maximum brake power, at standard injection timing. The CO emission decreases for advanced injection timing with the UTO. The CO emission is reduced by about 0.002432 , 0.003127 and 0.003167 g/kWh at and 27.5, 26, 24.5 ^{o}bTDC respectively.This is because of more time available for the oxidation process to occur, leaving less CO in the exhaust. The CO emission is found to increase with retarded injection timing at maximum brake power. The CO emission is increased by about 0.004217, 0.004434 and 0.005191 g/kWh at 21.5, 20, 18.5 ^{o}bTDC respectively at maximum brake power. These may be due to poor mixing of fuel air as a shorter ignition delay.

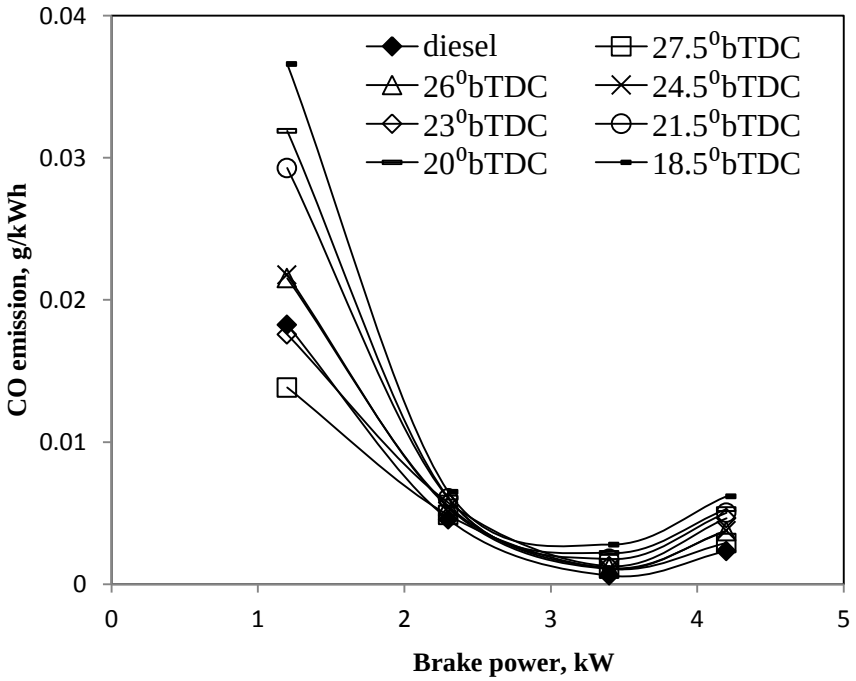

Figure 6.22 Variation of CO emission with brake power for engine fueled with UTO at different injection timings

6.3.4.3 Hydrocarbon emission

Figure 6.23 illustrates the comparison of the HC emission for the UTO at different injection timings with diesel at various brake powers. The values of HC emission are recorded as 0.15,

0.13, 0.0102, 0.0101, 0.0095, 0.0096 and 0.008 g/kWh for 18.5, 20, 21.5, 23, 24.5, 26 and 27.5 ^{o}bTDC with the UTO respectively and 0.005 g/kWh for diesel at maximum brake power. At the advanced injection timings, there is a considerable reduction in the HC emissions compared to that of UTO at standard injection timing at maximum brake power. Retarded injection timing of UTO exhibits higher HC emission due to the combustion process yielding less time for complete combustion.

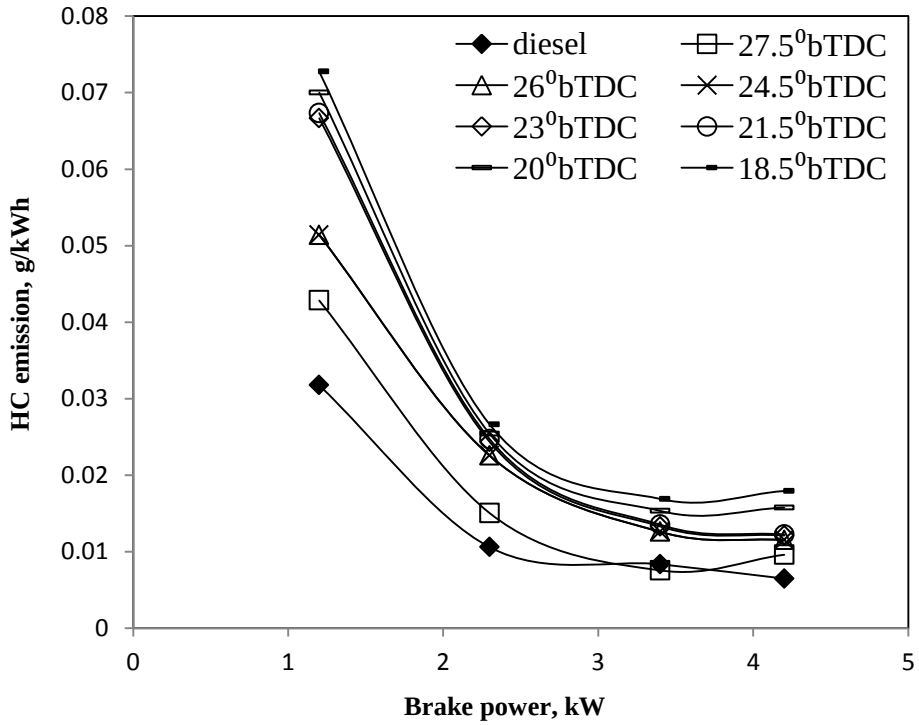

Figure 6.23 Variation of HC emission with brake power for engine fueled with UTO at different injection timings

6.3.4.4 Smoke density

Figure 6.24 depicts the comparison of smoke emission for the UTO at different injection timing with diesel at various brake powers. The values of smoke emission are 21.2, 20.5, 19.5, 19.2, 19.1, 19 and 18.8% for 18.5, 20, 21.5, 23, 24.5, 26 and 27.5 ^{o}bTDC with UTO respectively and 24% for diesel at standard injection timing for maximum brake power. Smoke value decreases with advanced injection timings of UTO due to higher combustion temperature compared to standard injection timings. It can also be observed that the retarded timing of UTO

shows higher values of smoke emission due to incomplete combustion and poor mixture formation.

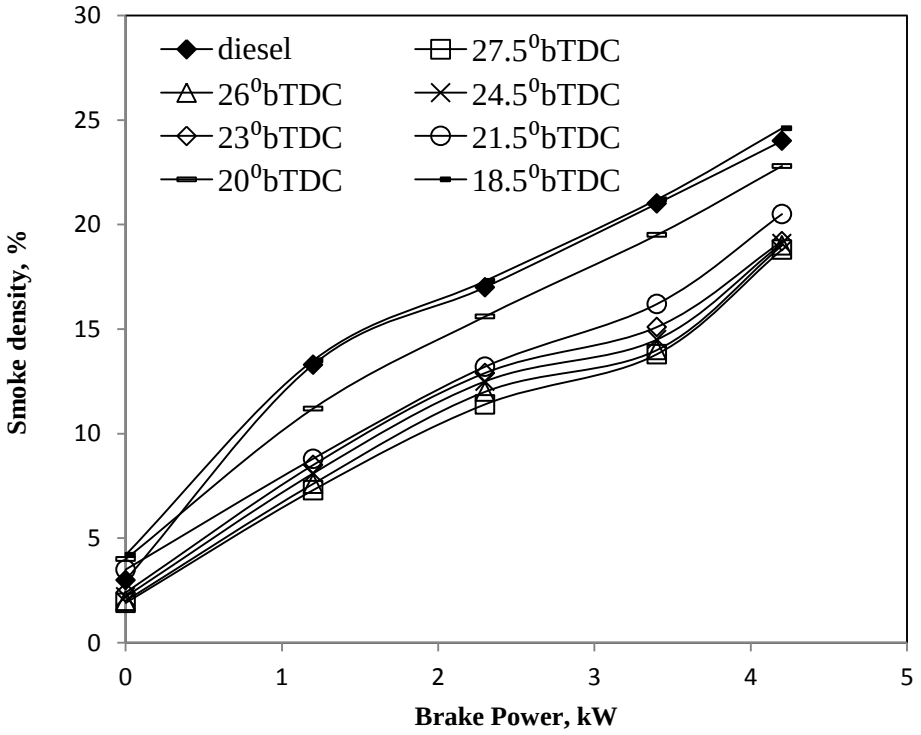

Figure 6.24 Variation of smoke density with brake power for engine fueled with UTO at different injection timings

6.3.5 Closure

It is summarized that the engine was able to run with 100% UTO when the injection timing was advanced and retarded. At the 20^{o}bTDC injection timing, the UTO exhibited NO emissions lower by about 27% compared to that of diesel at maximum brake power. The smoke emission was found to be higher by about 2.5% for the UTO at 20^{o}bTDC than that of diesel at maximum power output.

Table 6.2 Percentage variation of UTO with different injection timing in comparison with diesel at maximum power output

Si. No.	**Parameter**	**27.5^{o}bTDC**	**26^{o}bTDC**	**24.5^{o}bTDC**	**23^{o}bTDC**	**21.5^{o}bTDC**	**20^{o}bTDC**	**18^{o}bTDC**
A Combustion parameters								
1.	Occurrence of ignition	-1.43	-0.87	-1.12	-0.41	-0.20	-0.03	0.81
2.	Ignition delay	11.66	3.23	3.052	0.53	-7.54	-12.02	-16.69
4.	Combustion duration	3.96	0.28	-3.20	-19.60	-3.89	-0.63	-1.96
5.	Maximum heat release	0.78	-0.38	-0.67	-2.34	-2.69	2.26	16.53
6.	Maximum cylinder pressure	15.45	12.70	7.77	9.88	-7.67	-8.78	-20.28
B Performance parameters								
1.	Brake specific energy consumption	-6.82	-5.05	-5.89	-4.63	-7.07	-3.53	-0.50548
2.	Exhaust gas temperature	3.88	4.62	5.73	6.59	11.11	11.41	22.31
C Emission parameters								
1.	HC emission	48.04	77.65	75.45	83.58	83.58	138.66	175.38
2.	CO emission	24.39	59.94	61.99	99.13	115.70	126.80	165.52
3.	NO emission	17.49	4.51	26.21	25.34	-6.72	-27.23	-27.11
4.	Smoke emission	-21.66	-20.83	-20.41	-20	-14.58	-5	2.5

"+" indicates increasing percentage; "-"indicates decreasing percentage.

6.4 UTO at different nozzle opening pressure

6.4.1 General

The change of injection pressure, in other words, operating with higher fuel injection nozzle opening pressures require the engine modification, but yields a good result in terms of the performance and emission parameter of the engine [121]. This section discusses the analysis of the combustion, performance and emission parameters of the diesel engine fueled with the UTO at higher nozzle opening pressures in comparison with diesel. The fuel nozzle opening pressure was varied from 210 to 250 bar in steps of 10 bar in addition to original fuel nozzle opening pressure of the engine. The nozzle opening pressure is UTO in the discussion.

6.4.2 Combustion analysis

6.4.2.1 Pressure crank angle diagram

The variation of the cylinder pressure for the UTO at different nozzle opening pressures and diesel with crank angle at maximum brake power is presented in Fig. 6.25.

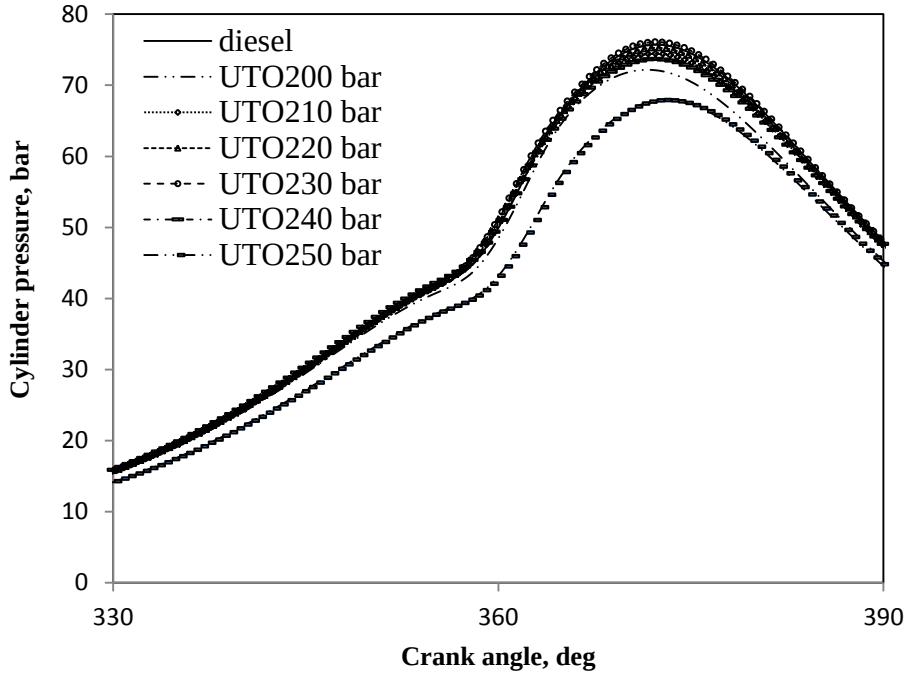

Figure 6.25 Variation of the cylinder pressure with crank angle at maximum brake power for engine fueled with UTO at higher nozzle opening pressures

It can be observed from the figure that the UTO with 230 bar starts to ignite earlier at 372 ^{o}CA followed by diesel at 200, UTO with 220, 210, 240, 200 and 250 bar nozzle opening pressures at 372.4, 372.5, 372.2, 372.2, 371.6 and 372.9 ^{o}CA respectively. The early occurrence of ignition is attributed to better atomisation of UTO in comparison with original nozzle opening pressure.

6.4. 2.2 Ignition delay

The variation of the ignition delay for the UTO at different nozzle opening pressures and diesel with crank angle at maximum brake power is presented in Fig. 6.26. The ignition delay of UTO at different nozzle opening pressures and diesel decreases with increase in the brake power as expected.

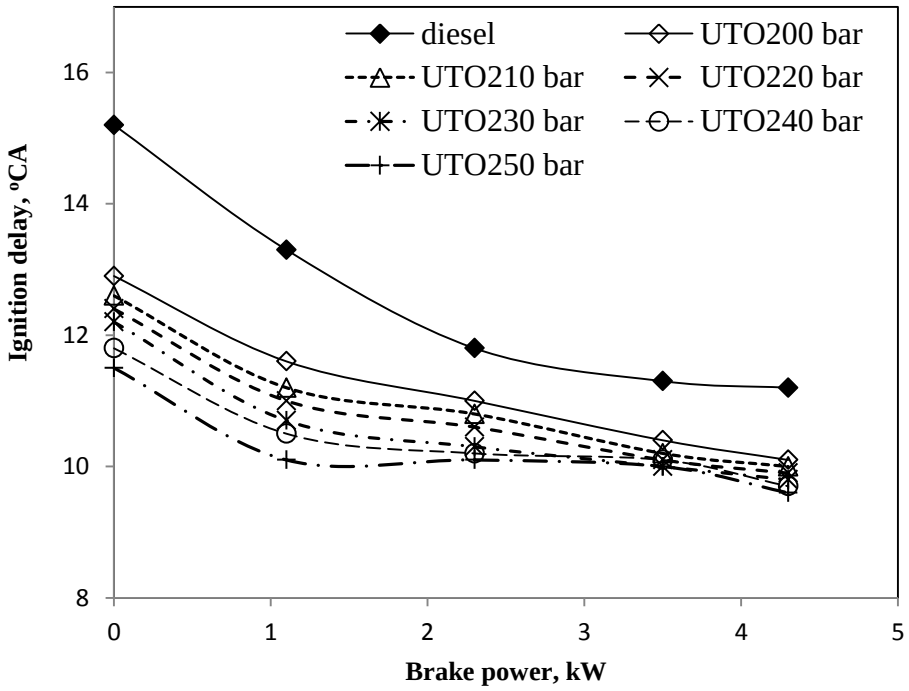

Figure 6.26 Variation of the ignition delay with brake power for engine fueled with UTO at higher nozzle opening pressures

The ignition delay for the UTO reduces as the nozzle opening pressures increases from 210 bar to 250 bar. The droplet size of fuel reduces to smaller at a higher nozzle opening pressure. As a result the initial injection rate and the maximum injection rate

increases, consequently shorter injection period with improved atomization occurs at higher nozzle opening pressures. The fuel droplet size reduces and results in exposer of the outer periphery of the fuel droplet to hot air increases. As a result the heat transfer from outer layer to adjacent layer of the core increases. Therefore the evaporation of the fuel is faster and hence mixing of the fuel vapor with air is also faster. This reduces the ignition delay of UTO at higher nozzle opening pressure marginally. The values of ignition delay for diesel and UTO at 200 bar are 11.2 ^{o}CA and 10.1 ^{o}CA respectively. In the case of the other nozzle opening pressures 210, 220, 230, 240 and 250 bar the values are 10, 9.9, 9.7, 9.8 and 9.6 ^{o}CA respectively at maximum brake power. The difference in the ignition delay between the diesel operation and the UTO with 250 bar at no brake power and maximum brake power are 3.7 ^{o}CA and 1.6 ^{o}CA respectively.

6.4.2.3 Heat release rate

The variation of heat release rate with crank angle at maximum brake power with diesel and UTO at different nozzle opening pressure is given in Fig. 6.27.

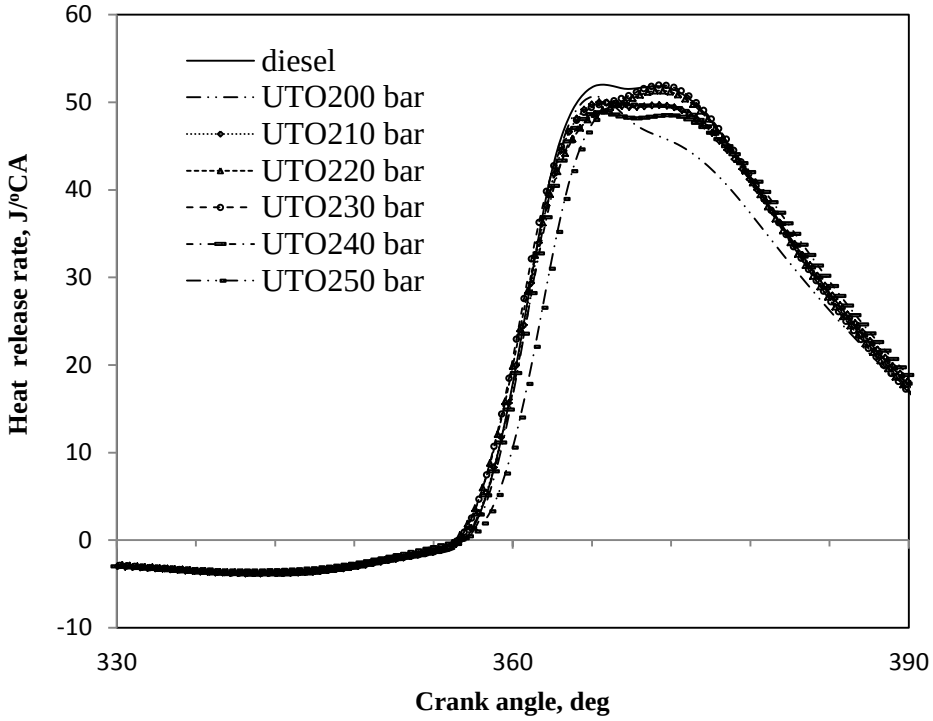

Figure 6.27 Variation of heat release rate with crank angle at maximum brake power for engine fueled with UTO at higher nozzle opening pressures

It can be observed from the figure that the occurrence of maximum heat release rate is found to be little earlier for the UTO than that of diesel, as a result of the bulk modulus characteristics of UTO. The maximum heat release for the UTO and diesel occurred at 371 and 364.78 ^{o}CA at maximum brake power. In case of the occurrence of maximum heat release rate for the UTO at 210, 220, 230, 240 and 250 bar are found to be approximately 366.55, 371.37, 371.06, 366.56 and 368.45 ^{o}CA respectively at maximum brake power.

6.4.2.4 Combustion duration

Figure 6.28 illustrates the variation of the combustion duration for the UTO at different nozzle opening pressure and diesel with engine brake power.

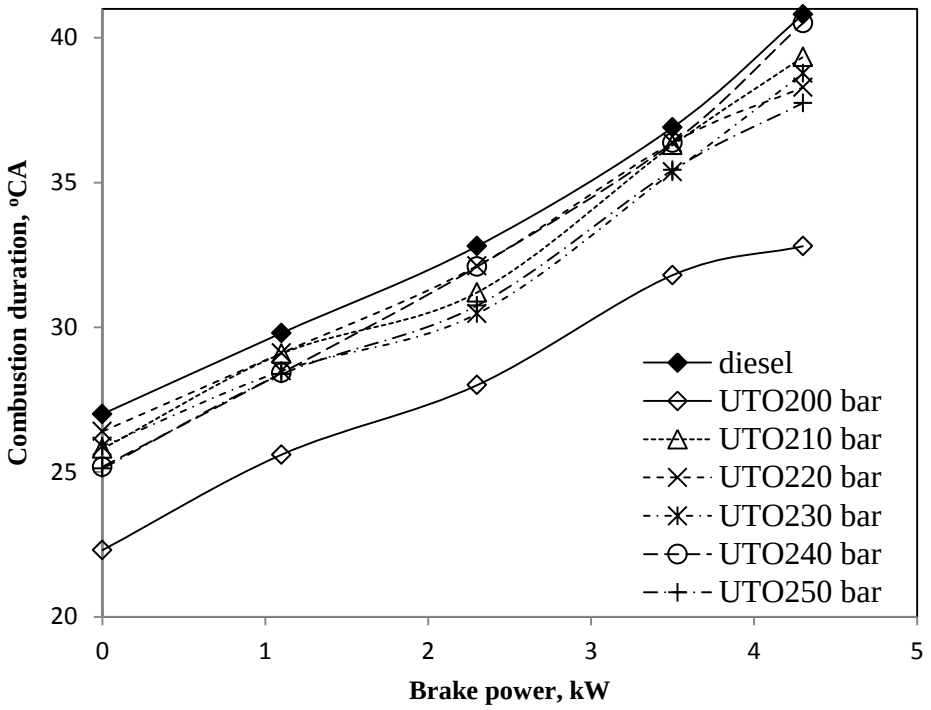

Figure 6.28 Variation of combustion duration with brake power for engine fueled with UTO at higher nozzle opening pressures

The combustion duration of all the fuels increases, with increasing brake power condition due to the accumulation of more fuel inside the cylinder. It can be noticed that the values of combustion duration as 32.8, 39.33, 38.28, 38.76, 40.5 and 37.74 ^{o}CA for

200, 210, 220, 230, 240 and 250 bar with the UTO respectively and 40.8 ^{o}CA for diesel at maximum brake power.

6.4.2.5 Maximum cylinder pressure

Figure 6.29 portrays the variation of maximum cylinder pressure with brake power for the UTO and diesel at different nozzle opening pressures with diesel. The maximum cylinder pressure increases with increase in brake power as the engine gains more heat. The maximum cylinder pressure of diesel, UTO200, UTO210, UTO230, UTO240 and UTO250 bar are 78, 74.42, 75.42, 78.17, 79.2, 74.5 and 75.8 bar respectively at maximum brake power. The maximum cylinder pressure for 230 bar is the highest through the brake power spectrum. It can also be observed that UTO at nozzle opening pressures exhibit higher cylinder pressures than that of diesel at 200 bar nozzle opening pressures at maximum brake power.

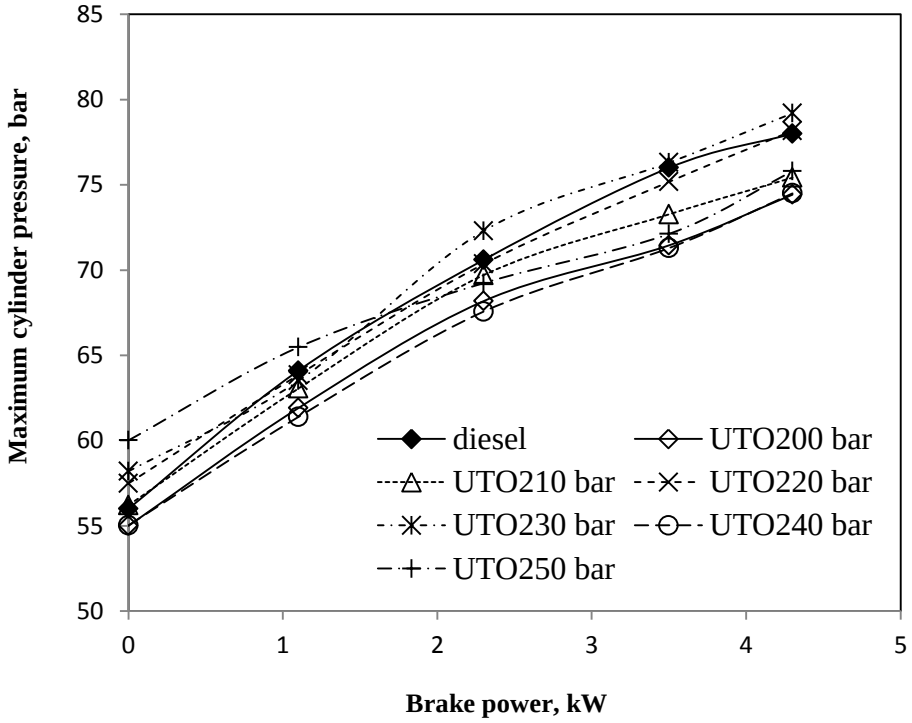

Figure 6.29 Variation of the maximum cylinder pressure with brake power for engine fueled with UTO at higher nozzle opening pressures

This may be due to the smaller droplet, shorter breakup length, higher dispersion and better atomization which results in higher combustion temperatures in the premixed combustion phase. The nozzle opening pressures of 220, 210, 240, 200 and 250 bar are lower than nozzle opening pressure of 230 bar with UTO at maximum brake power. The maximum cylinder pressure for diesel at 200 bar is the lowest among the UTO at different nozzle opening pressures at maximum brake power. In the case of the nozzle opening pressure 250 bar, even with the reduction of ignition delay due to faster evaporation of fuel droplets, the fuel spray cannot sprayed through the cylinder. The initial combustion must occur to a small region near the injector. The flame might sprayed around the chamber at a slower rate and hence resulting in a drop in pressure.

6.4.2.6 Maximum Rate of pressure rise

Figure 6.30 depicts the variation of rate of pressure rise for different nozzle opening pressures for the UTO and diesel, with brake power. The rate of pressure rise increases with increase in brake power for all the nozzle opening pressures with UTO.

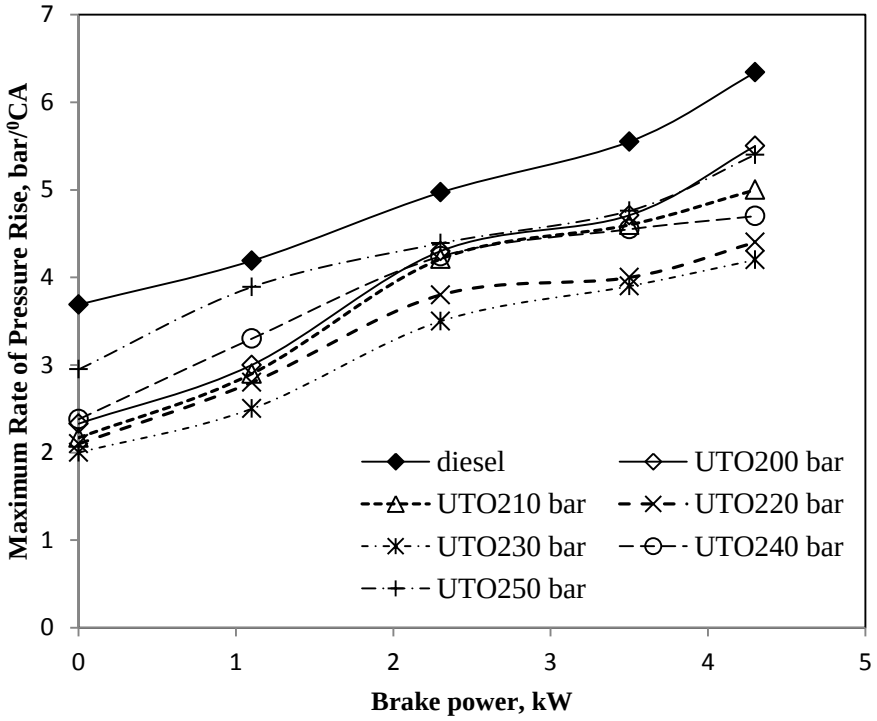

Figure 6.30 Variation of maximum rate of pressure rise with brake power for engine fueled with UTO at higher nozzle opening pressures

The rate of pressure rise for the UTO at 230 bar nozzle opening pressure is the lowest, among all the injection pressures of UTO and diesel. The rate of pressure rise for the UTO at 200, 210 and 230 bar lie between 5.5 bar/^{o}CA to 4.2 bar/^{o}CA at maximum brake power. At 200 bar original nozzle opening pressure, the UTO may generate coarse spray because of higher viscosity, resulting in lower heat release rate and peak cylinder pressure results in lower rate of pressure rise. As the nozzle opening pressure is increased from 210 bar up to 230 bar, the atomization of the fuel might be better and finer spray formation of the fuel droplets might occur resulting in better combustion. This leads to high rate of pressure rise for 210, 220, 230 bar injection pressures, of 5, 4.4 and 4.2 bar/^{o}CA respectively at maximum brake power.

However, further increase in the injection pressures at 240 and 250 bar of 4.7 and 5.4 bar/^{o}CA, results in too small size of fuel droplets that might have low depth of penetration due to the less momentum of droplet and less velocity relative to air from where the fuel has to find oxygen after evaporation. Because of this, the air utilization factor will also reduce due to shorter spray path. Also, with the smallest size droplet, the area of inflammation would increase after ignition. These result in a high rate of pressure rise during the second stage of combustion compared to the first stage of combustion.

6.4.3 Performance parameters

6.4.3.1 Brake specific energy consumption

The variation of BSEC with brake power for diesel and UTO at different nozzle opening pressures is illustrated in Fig. 6.31.

The highest BSEC is found with diesel at 200 bar followed by UTO at 230, 200, 210, 220, 240 and 250 bar nozzle opening pressure. The BSEC of diesel, UTO 200, UTO 210, UTO 220, UTO 230, UTO 240 and UTO 250 bar are 12.5, 11.2, 10.9, 10.7, 11.8, 10.5 and 10.17 MJ/kWh respectively at maximum brake power. The quantity of the fuel injected increases with increase of power and due to the higher injection pressure better atomization of fuels take place which leads to better combustion & decreases BSEC.

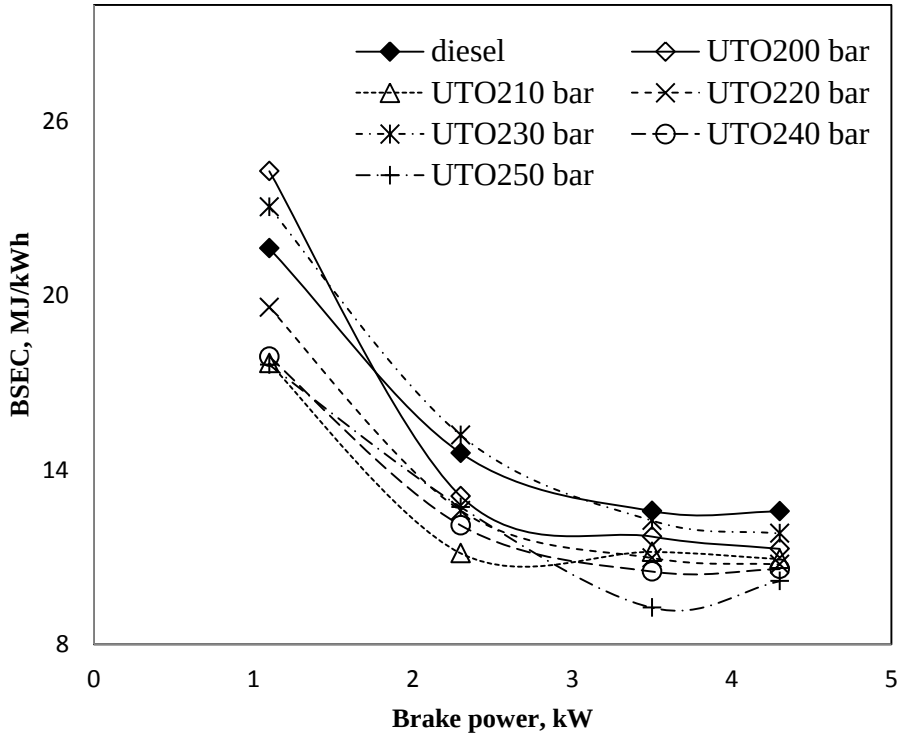

Figure 6.31 Variation of brake specific energy consumption with brake power for engine fueled with UTO at higher nozzle opening pressures

6.4.3.2 Exhaust gas temperature

The variation of the exhaust gas temperature of UTO and diesel at different nozzle opening pressures is shown in Fig. 6.32.

UTO at 200 bar shows the highest exhaust gas temperature of 354.2^{o}C compared to other nozzle opening pressures of 210, 220, 230, 240 and 250 bar as 303, 322, 342, 292 and 285^{o}C respectively at maximum brake power. Diesel operation shows the lowest exhaust gas temperature in the entire range of operation of 269.54^{o}C. Bosch stated that [122] at higher nozzle opening pressures, leaner air-fuel ratio occurs, due to improved atomization and it results to incomplete combustion. This result to earlier heat release rate, higher combustion duration and lower BSEC, and thus higher exhaust gas temperature compared to diesel at maximum brake power. This reason may be matched for the lower exhaust gas temperatures for the UTO at 210 to 250 bar, compared to that of UTO at 200 bar, however they are higher than that of diesel.

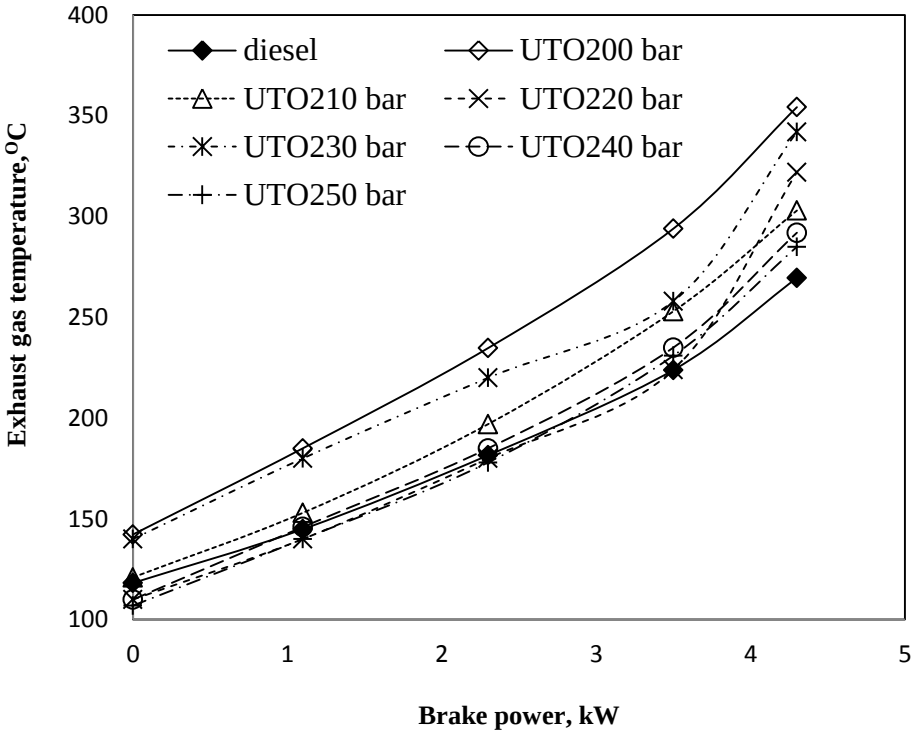

Figure 6.32 Variation of exhaust gas temperature with brake power for engine fueled with UTO at higher nozzle opening pressures

6.4.4 Emission parameters

6.4.4.1 Nitric oxide emission

The NO emission with engine brake power at different injection nozzle opening pressures of UTO and diesel is shown in Fig. 6.33. With the higher viscosity of UTO and shorter ignition delay the fuel accumulated would be very less in the premixed combustion phase. This generates lower heat release rate, therefore low nitric oxide emission is recorded with UTO at 200 bar injection pressure, of 7.3 g/kWh at maximum brake power.

As the fuel injection nozzle opening pressure is increased from 210 bar, the cylinder temperature increases due to better complete combustion that results in higher NO emission, similar reasons are mentioned by Venkatraman and Devaradjane [119].

Another probable reason may be that the oxidized UTO might enhance the premixed combustion, when it is subjected to higher fuel injection nozzle opening pressures.

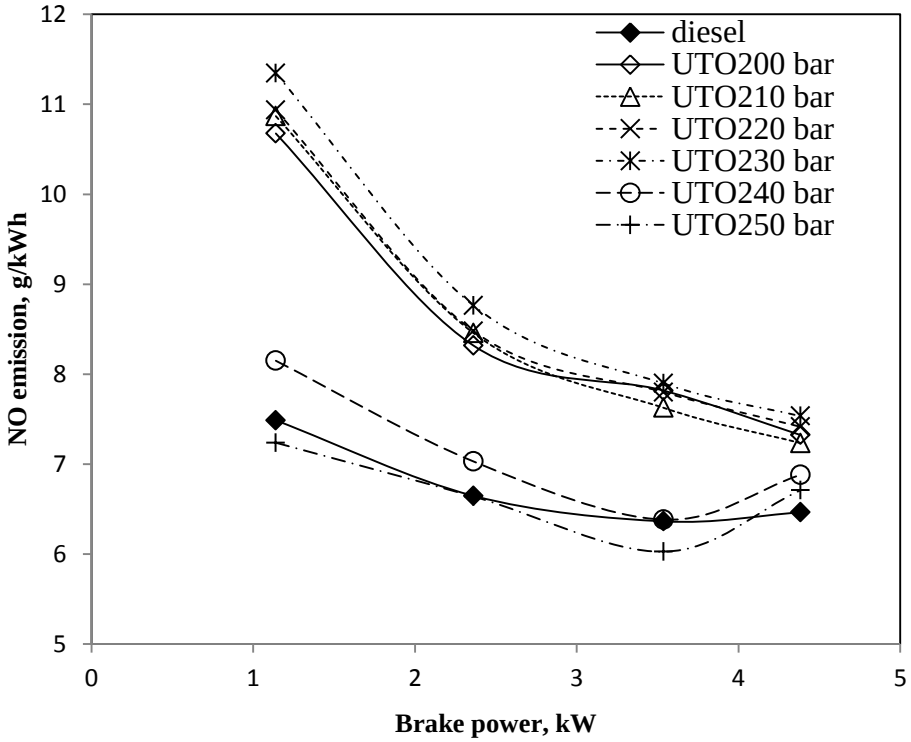

Figure 6.33 Variation of NO emission with brake power for engine fueled with UTO at higher nozzle opening pressures

Therefore, the NO emission is more for the nozzle opening pressure for 210, 220 and 230 bar which are 7.23, 7.4 and 7.5 g/kWh respectively at maximum brake power. However, the NO formation is lower in the case of nozzle opening pressures at 240 and 250 bar as 6.8 and 6.7 g/kWh for the UTO operation as a result of lower heat release rate of in the premixed combustion phase. The NO emission for the UTO at 250 bar is found to be the lowest, at maximum brake power.

6.4.4.2 Carbon monoxide emission

CO emission with brake power is shown in Fig. 6.34. The general trend of CO emission in a CI engine matches for diesel and the UTO at different fuel injection nozzle opening pressures are found to be similar for a given power output.

However, the CO emission for the UTO at different nozzle opening pressures is found to be higher than that of diesel. The CO emission for the UTO at 200 bar is 0.0047 g/kWh as the highest followed by 250, 240, diesel, 220, 210 and 230 bar as 0.00221, 0.0022, 0.005, 0.0014, 0.001 and 0.0007 g/kWh respectively at maximum brake power. The reason for higher CO emissions at 210 and 220 bar compared to that of 230 bar may be due to relatively poor mixture formation because of lesser atomization of fuel droplets. These results are in agreement with the reason stated by Venkanna et al., [123]. CO emission for the UTO at 240 and 250 bar is also higher than diesel at maximum brake power, because some of the higher boiling points compounds may not break up even at higher injection nozzle opening pressures.

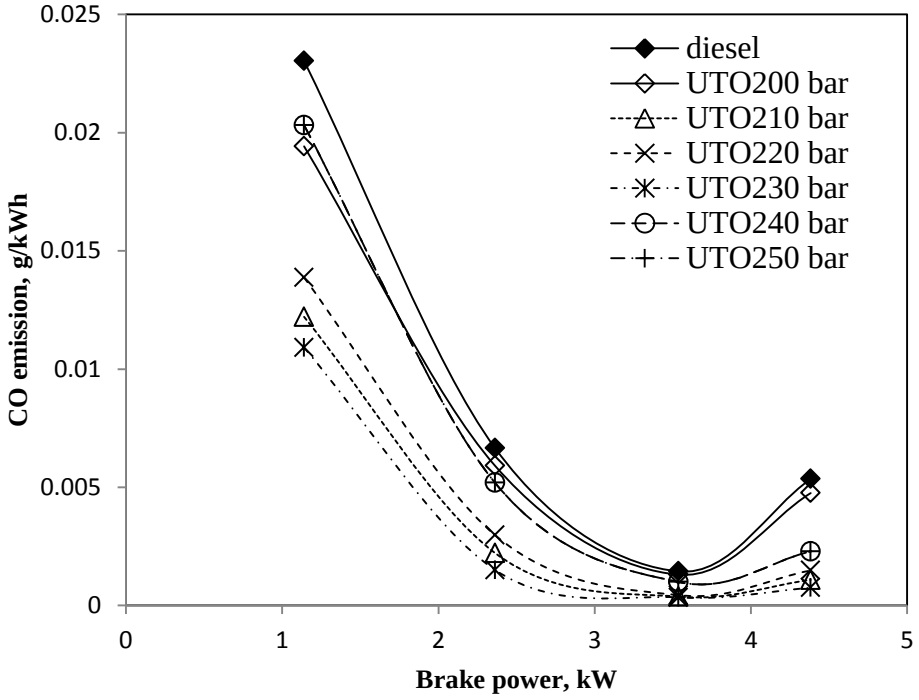

Figure 6.34 Variation of CO emission with brake power for engine fueled with UTO at higher nozzle opening pressures

6.4.4.3 Hydro carbon emission

The unburnt HC emission with brake power at different injection nozzle opening pressures of UTO and diesel is shown in Fig. 6.35. The HC emission for diesel, UTO,

UTO200, UTO230, UTO240 and UTO250 bar are 0.006, 0.012, 0.01, 0.008, 0.007, 0.0114 and 0.0115 g/kWh respectively at maximum brake power.

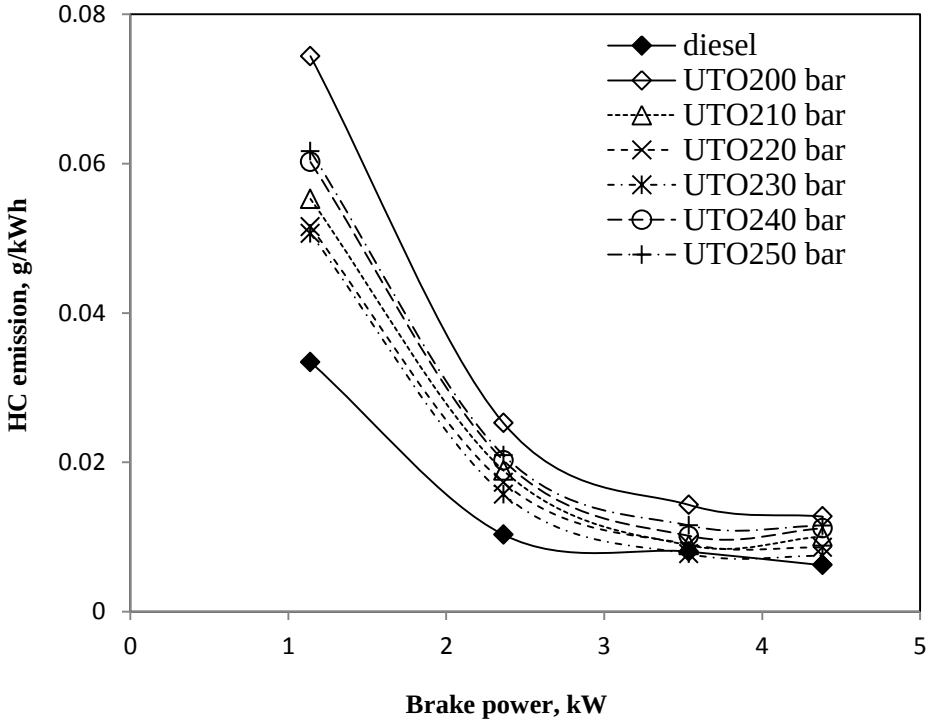

Figure 6.35 Variation of HC emission with brake power for engine fueled with UTO at higher nozzle opening pressures

UTO with the injection nozzle opening pressure of 230 bar shows the lowest hydro carbon emissions among all nozzle opening pressures of UTO tested. This may be due to better mixing of fuel air mixture leading to more complete combustion. UTO at 200 bar injection nozzle opening pressure is the highest among all the injection pressures and diesel. This is because of the higher viscosity and low volatility of UTO that causes coarse spray that result in poor mixture formation.

The HC emission at 250 bar and 240 bar are found to be lower than that of 200 bar injection nozzle opening pressure, but higher than the lower injection nozzle opening pressures of 210, 220 and 230 bar. At higher injection nozzle opening pressures of 240 and 250 bar, local rich regions and some of the fuel droplet may occupy the crevice volume, which may be the reasons for higher unburnt hydro carbon emissions. At higher

injection nozzle opening pressures, some of the high molecular weight compounds present in the UTO may not breakup and undergo complete combustion.

6.4.4.4 Smoke density

Figure 6.36 illustrates the variation of the smoke density with engine brake power at different injection nozzle opening pressures of UTO and diesel. The percentage of smoke density of diesel, UTO, UTO210, UTO220, UTO230, UTO240 and UTO250 bar 24, 25.5, 23, 22.9, 22.3, 23.2 and 24% respectively at maximum brake power.

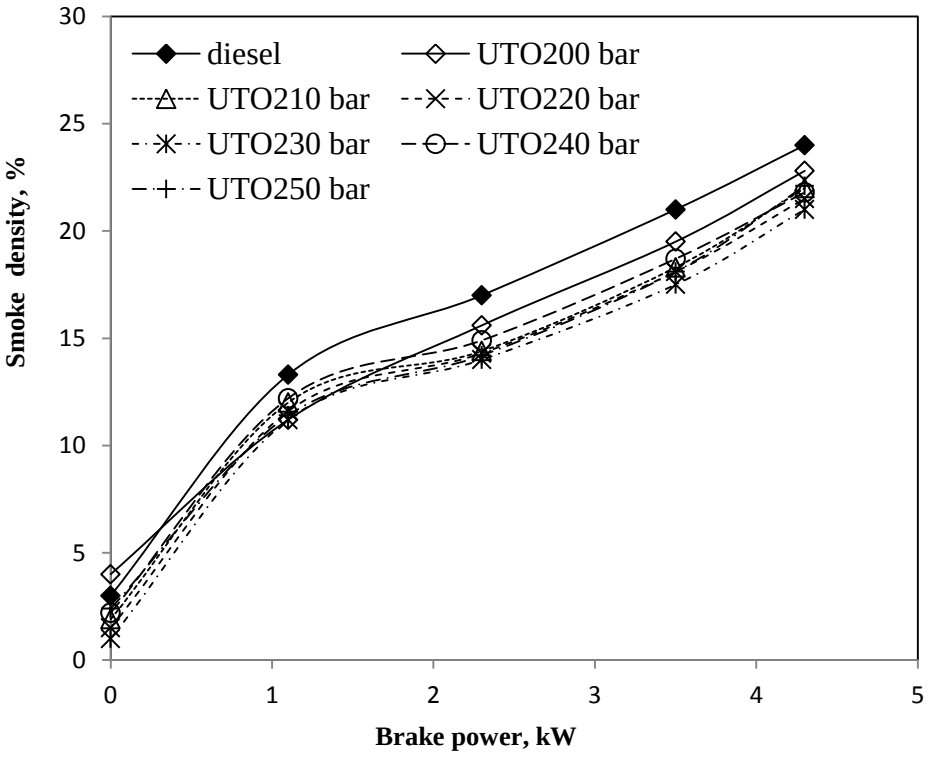

Figure 6.36 Variation of smoke density with brake power for engine fueled with UTO at higher nozzle opening pressures

The UTO at 200 bar exhibits the highest smoke density value at maximum brake power. As the injection nozzle opening pressures increase, the smoke density decreases, as a result of improved combustion. Among the fuel injection nozzle opening pressures, 240 and 250 bar are higher than the lower nozzle opening pressures of 210 bar and 220 bar. In case of UTO at 230 bar, the smoke density is found to be the lowest among all

the nozzle opening pressures. The higher smoke at higher nozzle opening injection pressures may be due to the pyrolysis of some of the higher molecular species. The reason may be considered in the case of UTO also.

The percentage variation of UTO with different nozzle pressure with diesel are illustrated and given in Table 6.3.

6.4.5 Closure

The UTO can be used as a sole fuel in CI engines as it possesses physical properties similar to that of diesel fuel but the engine has to be operated with optimum injection timing and nozzle opening pressure, since it has higher viscosity and density than that of diesel. The NO emission of UTO230 bar is higher by about 1.75% and 29.7% than that of UTO200 bar and diesel respectively at full load, whereas the smoke emission of UTO230 bar is lower by about 7.8% and 8.92% than that of UTO200 bar and diesel respectively at full load. It is suggested that UTO at 230 bar is the optimum injection nozzle opening pressure among the tested nozzle opening pressures.

Table 6.3 Percentage variation of UTO and UTO with different nozzle opening pressure in comparison with diesel at maximum power output

Si.No.	**Parameter**	**UTO 200 bar**	**UTO 210 bar**	**UTO 220 bar**	**UTO 230 bar**	**UTO 240 bar**	**UTO 250 bar**
A Combustion parameters							
1.	Occurrence of ignition	-0.20	-0.04	0.02	-0.05	-0.03	0.14
2.	Ignition delay	-9.82	-10.71	-11.60	-12.5	-13.39	-14.28
4.	Combustion duration	-19.60	-3.59	-6.16	-4.98	-0.71	-7.48
5.	Maximum heat release	-2.34	-1.34	0.53	1.691	-2.26	-4.30
6.	Maximum cylinder pressure	-4.58	-3.30	0.22	1.53	-4.48	-2.82
B Performance parameters							
1.	Brake specific energy consumption	-10.23	-13.05	-14.49	-6.049	-15.77	-19.09
2.	Exhaust gas temperature	31.43	12.41	19.46	26.88	8.33	5.73
C Emission parameters							
1.	HC emission	104.90	61.95	38.26	20.32	79.40	85.08
2.	CO emission	-11.16	-79.75	-72.35	-86.01	-57.28	-57.28
3.	NO emission	13.30	11.92	14.72	16.55	6.45	3.79
4.	Smoke emission	6.25	-4.16	-4.58	-7.08	-3.33	0

“+” indicates increasing percentage; “-“indicates decreasing percentage.

6.5 UTO at different compression ratio

6.5.1 General

Advantage of operating the engine with a variable compression ratio is that, the engine provides increased power output and reduced smoke emission with the conventional diesel fuel and alternative fuels with a higher viscosity [124]. Due to the wide applications of CI engines, engine manufactures are forced to produce the engines with high compression ratio. The engine sole UTO was subjected to different compression ratio that one higher compression ratio that 18.5 and two lower compression ratio as 16 and 17.The numeric proportion before UTO refers to the compression ratio of the engine. The effect of compression ratio on combustion, performance and emission parameters of the engine fueled with UTO are analyzed, compared and presented in this section.

6.5.2 Combustion analysis

6.5.2.1 Pressure crank angle diagram

The variation of combustion pressure with respect to crank angle at maximum brake power is shown in Fig. 6.37.

The commencement of ignition of UTO at compression ratio 16:1, 17:1, 17.5:1 and 18.5:1 occurs at 372.9, 371.6, 370.8 and 369.1 ^{o}CA at maximum brake power, whereas, the ignition of diesel occurs at 351.3 ^{o}CA at maximum brake power which is the latest among all the fuel tested. When the compression ratio of the engine increased, the occurrence of ignition becomes earlier to that of diesel for the UTO, while ignition of UTO commences little later at maximum brake power. The early or later occurrences of the ignition are attributed to the increased or decreased cylinder gas temperature respectively.

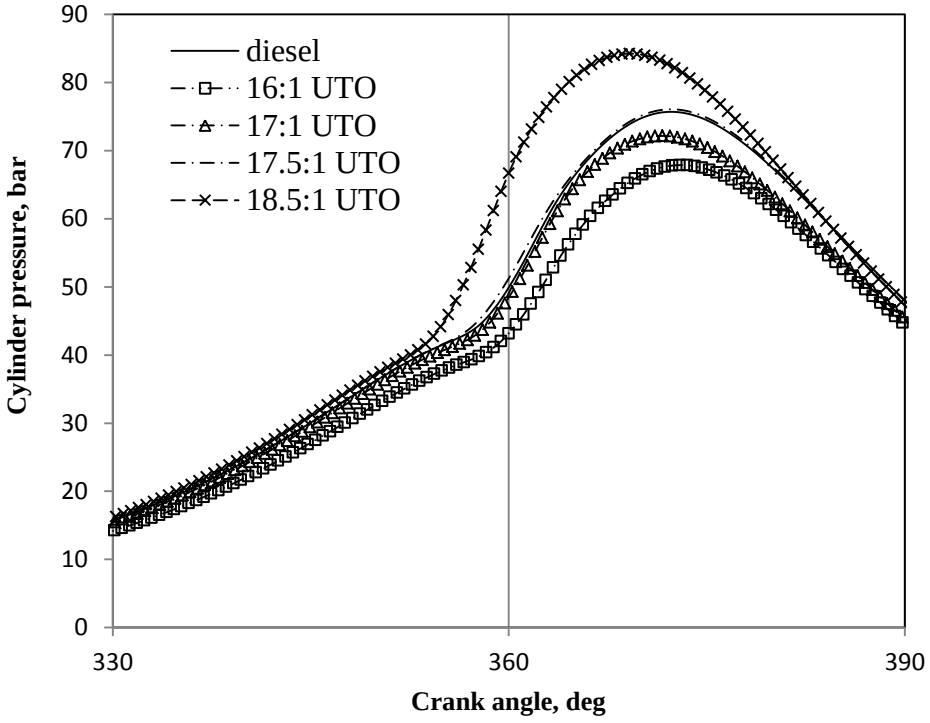

Figure 6.37 Variation of cylinder pressure with crank angle at maximum brake power for engine fueled with UTO at different compression ratio

6.5.2.2 Ignition delay

The variation of the ignition delay for the UTO in different compression ratio and diesel with respect to brake power is presented in the Fig. 6.38. The ignitions of delay of diesel, UTO at standard compression ratio are 11.2 and 10.1^{o}CA whereas for compression ratio 16:1, 17:1 and 18.5:1, with UTO are 11.5, 10.8 and 10 ^{o}CA respectively at maximum brake power.

The ignition delay of the tested compression ratio in this study decreases as the brake power increases. As the brake power increases, the heat prevailing inside the cylinder increases and helps the air fuel mixture to ignite sooner, so that this trend is genuine. It can also be observed from the figure that the ignition delay is found to decrease with increasing compression ratio. Longer mixing of fuel with air gives rise to a larger premixed combustion phases and conversely less diffusion combustion occurs which results in increased ignition delay at 16:1 compression ratio. Increasing the compression

ratio also results in an increased gas temperature. Considering the diesel at standard compression ratio as a reference, it is clear that at maximum brake power compression ratio 16:1 shows 2.68% longer ignition delay while compression ratio 17:1, 17.5:1 and 18.5:1 results in shorter ignition delay of 3.39%, 9.82% and 10.7% respectively.

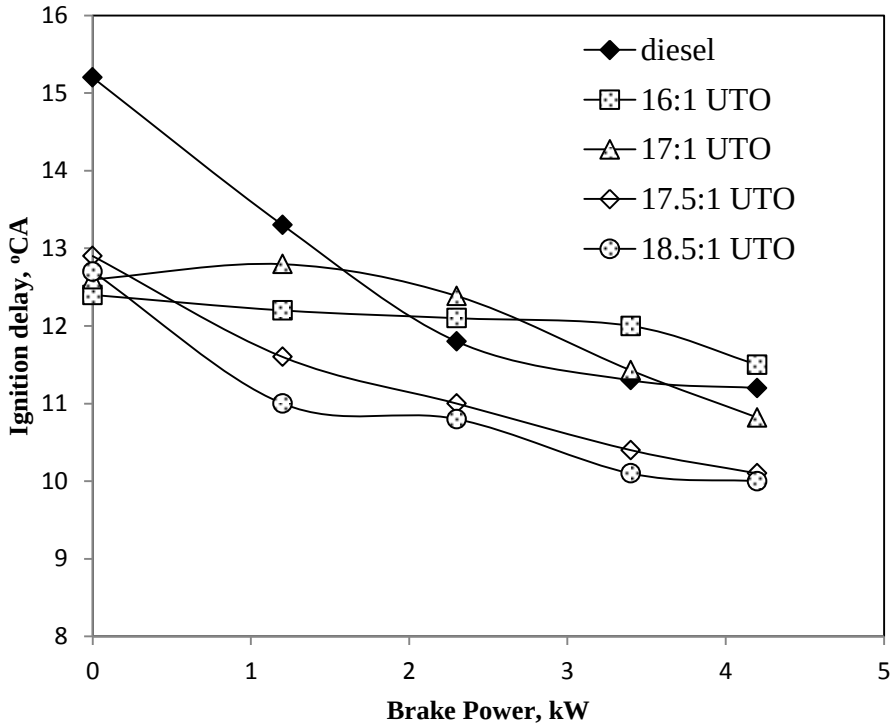

Figure 6.38 Variation of the ignition delay with brake power for engine fueled with UTO at different compression ratio

6.5.2.3 Heat release rate

Heat release rate directly affects rate of pressure rise and accordingly the power produced [125]. The variation in heat release rate with crank angle for the UTO at various compression ratio is shown in Fig. 6.39. The heat release is analyzed based on the crank angle variation of the cylinder. It can be observed from the figure, that the heat release rate increases with lower compression ratios and marginally decrease at higher compression ratios. This may be due to the air entertainment and lower air/fuel mixing rate and effect of viscosity of UTO.

The peak heat release rate at compression ratio 16:1, 17:1, 17.5:1 and 18.5:1 occurs at 368.4, 366.6, 372.2 and 365.7 °CA respectively at maximum brake power. The heat release rate of standard diesel is higher than the UTO due to its reduced viscosity and better spray formation. The heat release rate of UTO increases with higher compression ratio, and good spray formation in the cylinder. The heat release rate values are found to be 49.7, 50.6, 51.9 and 52.9 J/^{o}CA for diesel, UTO with compression ratio 16, 17, 17.5 and 18.5:1 respectively at maximum brake power.

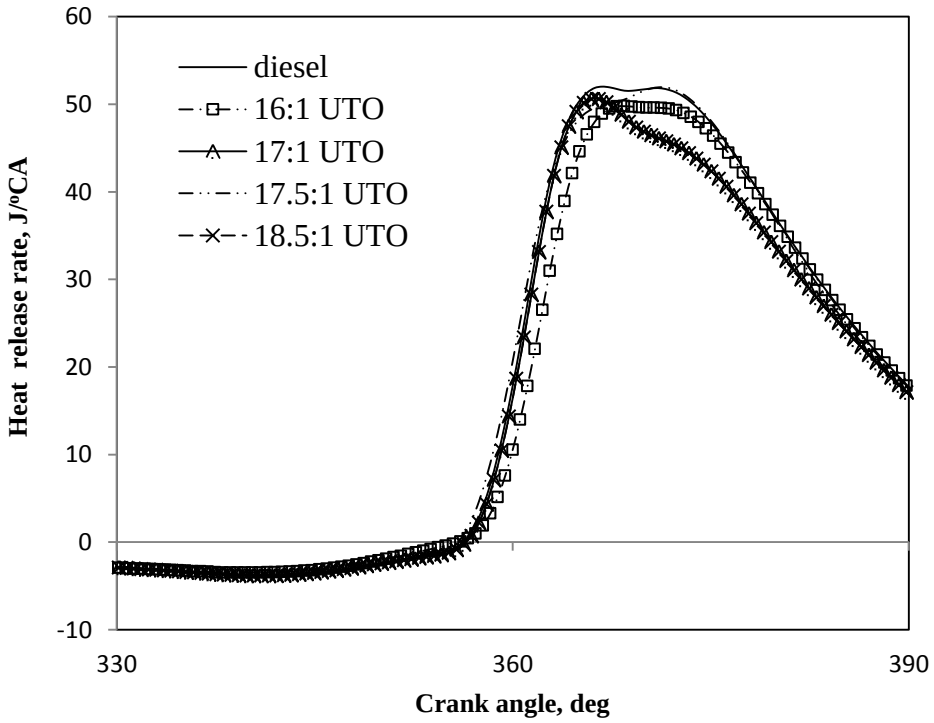

Figure 6.39 Variation of heat release rate with crank angle at maximum brake power for engine fueled with UTO at different compression ratio

6.5.2.4 Combustion duration

Figure 6.40 illustrates the variation of the combustion duration for the UTO at different compression ratio and diesel with engine brake power. The figure shows that the values of combustion duration as 49.2, 46.91874, 32.8 and 43.5 ^{o}CA for 16:1, 17:1, 17.5:1 and 18.5:1 with the UTO respectively and 40.8 ^{o}CA for diesel at maximum brake power. As the compression ratio increases, the combustion duration decreases at maximum brake power.

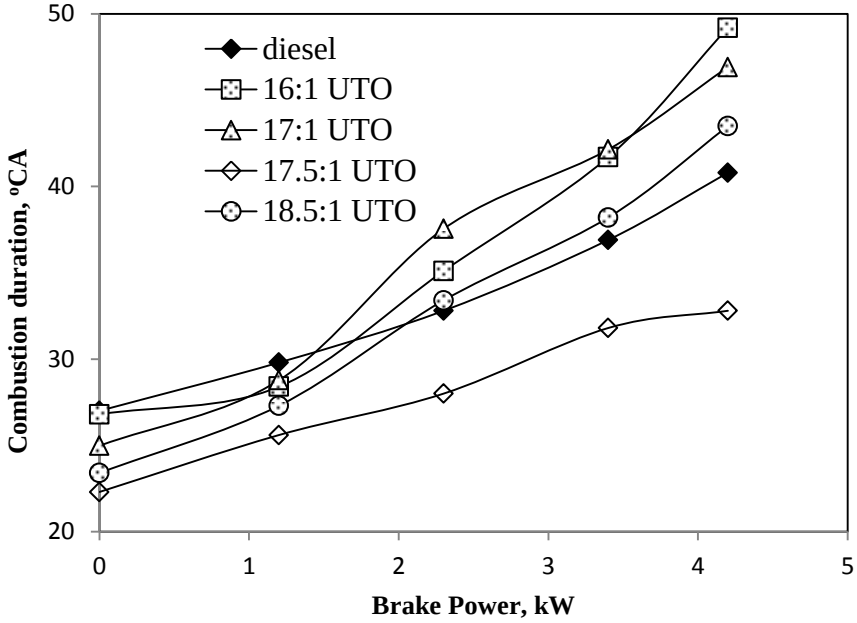

Figure 6.40 Variation of the combustion duration with brake power for engine fueled with UTO at different compression ratio

6.5.2.5 Maximum cylinder pressure

Figure 6.41 portrays the variation of maximum cylinder pressure with brake power for the UTO and diesel at different compression ratio with brake power.

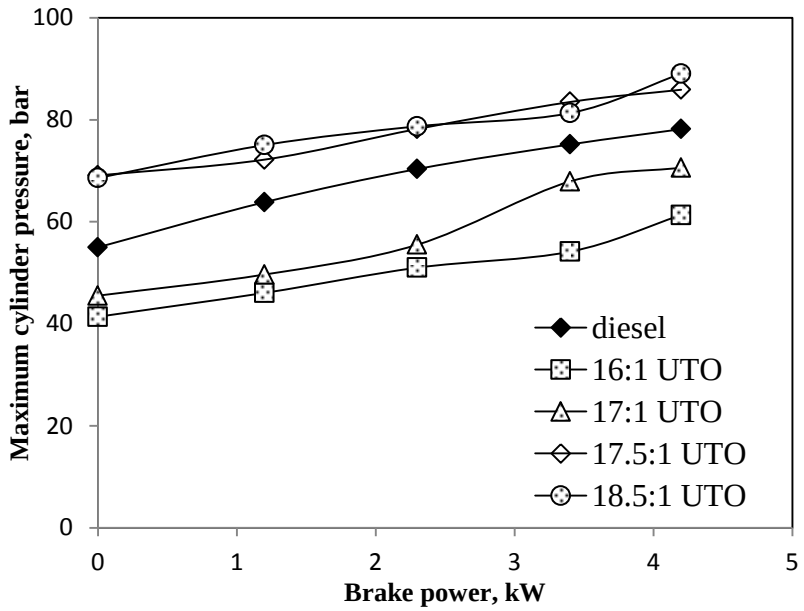

Figure 6.41 Variation of the maximum cylinder pressure with brake power for engine fueled with UTO at different compression ratio

The maximum cylinder pressures of diesel and UTO at compression ratio 16:1, 17:1, 17.5:1 and 18.5:1 are 78, 61.31, 70.62, 85.9 and 89.06 bar respectively at maximum brake power. Higher compression ratio shows higher maximum cylinder pressure due to higher combustion temperature in the premixed combustion phase.

6.5.2.6 Maximum rate of pressure rise

Figure 6.42 portrays the variation of maximum rate of pressure rise with brake power for the UTO and diesel at different compression ratio with brake power. The maximum rate of pressure rise increases with increase in brake power for the entire variable compression ratio with UTO. The maximum rates of pressure rise of diesel and UTO at compression ratio of 16:1, 17:1, 17.5:1 and 18.5:1 are 6.34 3.78 4.78 5.5 and 5.59 bar/^{o}CA respectively at maximum brake power.

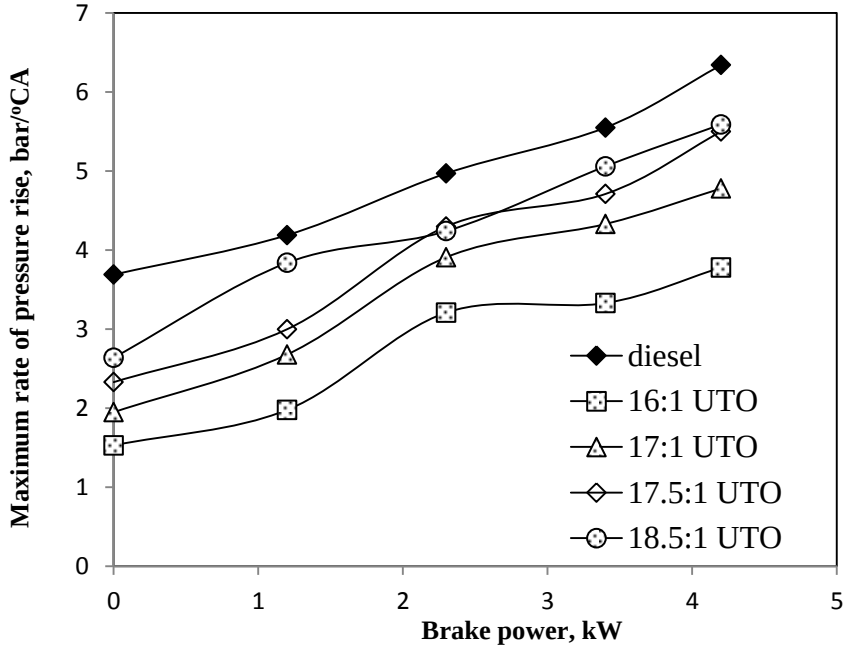

Figure 6.42 Variation of the maximum rate of pressure rise with brake power for engine fueled with UTO at different compression ratio

6.5.3 Performance parameters

6.5.3.1 Brake specific energy consumption

Figure 6.43 shows the variation between brake specific energy consumption at different brake power. As the fact, the BSEC decreases with increase in engine brake

power. BSEC for diesel and UTO at 17.5:1 compression ratio are 11.2 and 11.35 MJ/kWh respectively at maximum brake power. The BSEC for compression ratio 16:1, 17:1 and 18.5:1 with UTO at maximum brake power are 13.3, 12,5 and 13.2 MJ/kWh respectively. In comparison with diesel, the UTO shows 18.5%, 11.9% and 0.5% higher consumption at compression ratio 16:1, 17:1 and 18.5:1 while compression ratio of 18.5:1 consumes 6.7% lower than that of diesel at maximum power output. The increase in energy consumption is due to lower cylinder gas temperature as a result of high density and viscosity of UTO, but with higher compression ratio lesser value of BSEC is apparently desirable.

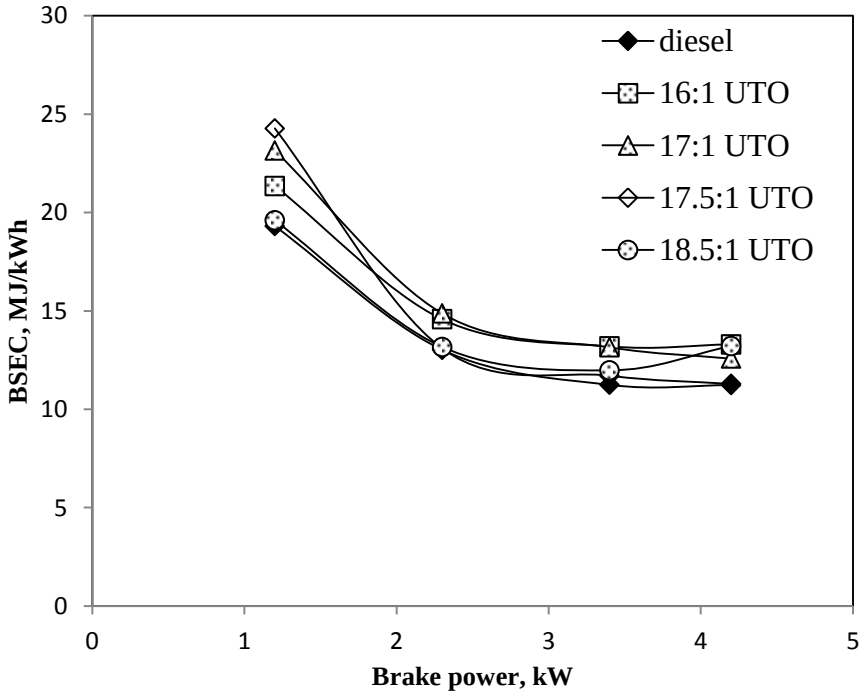

Figure 6.43 Variation in brake specific energy consumption with brake power for engine fueled with UTO at different compression ratio

6.5.3.2 Exhaust gas temperature

During the combustion, the temperature inside the cylinder is very high, but with expansion there is a great reduction in the exhaust gas temperature. The exhaust gas temperature is strongly dependent on in-cylinder temperature and expansion process. Figure 6.44 portrays the variation of the exhaust gas temperature with brake power for diesel and the UTO.

The exhaust gas temperature increases with an increase in the engine brake power for the UTO and diesel. It is higher for the UTO than that of diesel in the entire operation as a result of higher viscosity and density of UTO. The exhaust gas temperature of UTO at compression ratio of 16:1, 17:1, 17.5:1 and 18.5:1 are 385, 392, 354 and 350 ^{o}C respectively whereas in diesel 269 ^{o}C. The reason for the reduction in the exhaust gas temperature at increased compression ratio is due to improved energy conversion of UTO as compared to that of diesel.

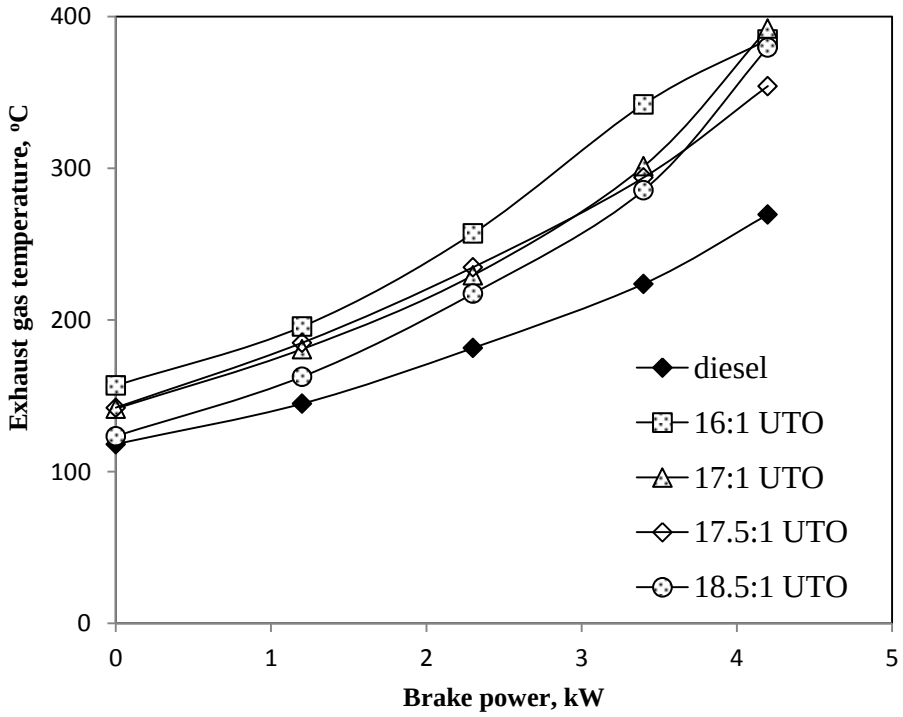

Figure 6.44 Variation in exhaust gas temperature with the brake power for engine fueled with UTO at different compression ratio

6.5.4 Emission parameters

6.5.4.1 Nitric oxide emission

Figure 6.45 portrays the variation of the NO emission with brake power for the UTO compared to diesel at different compression ratio. The NO emission for diesel and UTO at 17.5:1 compression ratio are 6.7 and 7.6 g/kWh, whereas the NO emission for the UTO at 16:1, 17:1 and 18.5:1 shows 7.1, 7.6 and 8.8 g/kWh respectively at maximum brake power. The NO emissions for the UTO with compression ratio of 16:1 shows lower by

6.2% whereas 17:1, 17.5:1 and 18.5:1 are found to be higher by about 12.3%, 27.5% and 30.6% respectively to that of diesel at maximum brake power. In comparison with standard compression ratio of UTO, when lower the compression ratio to 16:1 and 17:1 NO emission reduced by 33.7%. and 15.2% and with higher compression ratio of 18.5:1 increased by 3.1% at maximum brake power. With the higher compression ratio, the NO emission for the UTO is increased due maximum cylinder temperature, which is agreed by Raheman and Ghadge, [126].

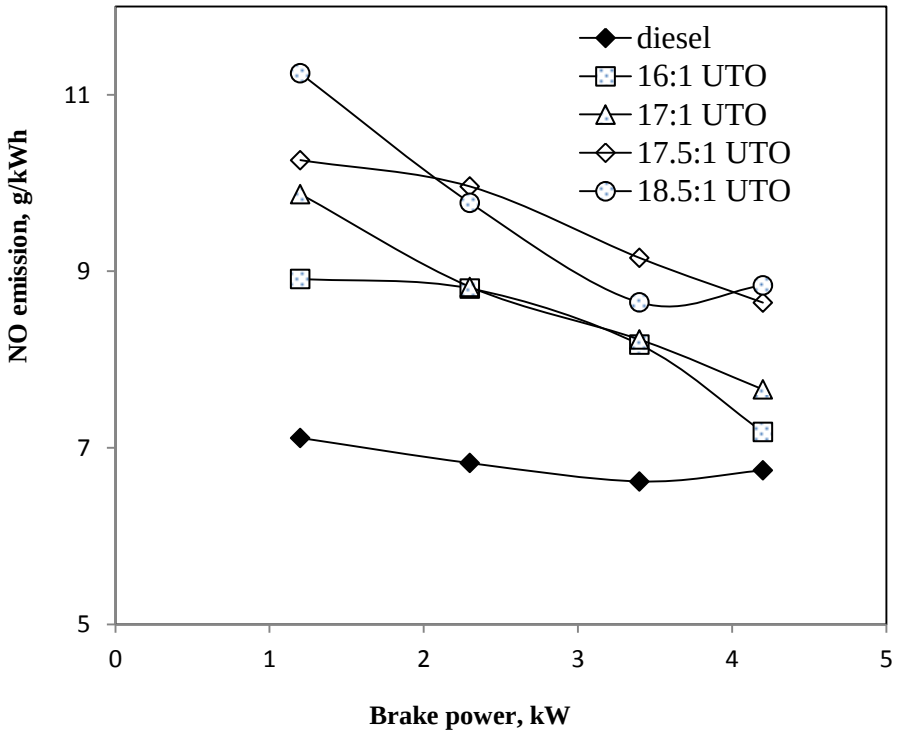

Figure 6.45 Variation in NO emission with the brake power for engine fueled with UTO at different compression ratio

6.5.4.2 Carbon monoxide emission

Figure 6.46 portrays the percentage variation of the CO emission with brake power for the UTO compared to diesel at different compression ratio. CO emission for diesel and UTO, at standard compression ratio are found to be 0.0023 and 0.00075 g/kWh respectively at maximum brake power. It can be observed from the figure that the CO emission is higher for the UTO compared to that of diesel at maximum brake power for

all compression ratios. Lower compression ratio of 16:1, 17:1 shows 0.0053 and 0.0049 g/kWh CO emission, whereas 18.5:1 compression ratio shows 0.0039 g/kWh CO emission at maximum brake power. The decrease in the CO emission at higher compression ratio may be due to better mixing of fuel with air. Thus, the CO emission is found increase with decreasing the compression ratio.

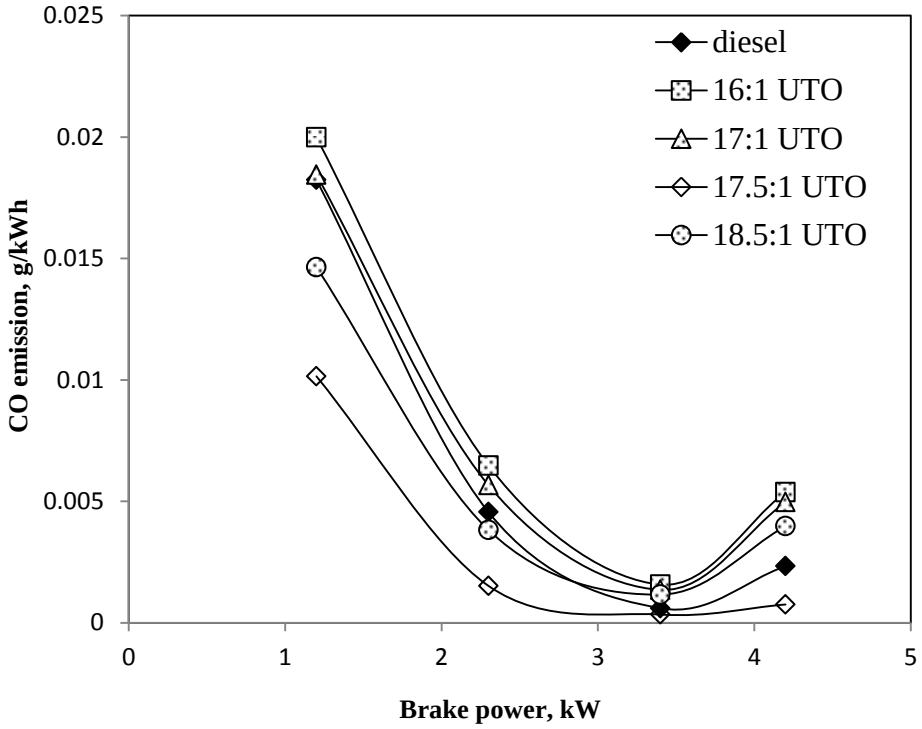

Figure 6.46 Variation in the CO emission with brake power for engine fueled with UTO at different compression ratio

6.5.4.3 Hydrocarbon emission

Figure 6.47 portrays the percentage variation of the HC emission with brake power for the UTO compared to diesel at different compression ratio. The HC emission for diesel, UTO at compression ratio 16:1, 17:1, 17.5:1, and 18.5:1 are 1.5, 1.1, 0.75, 0.71 g/kWh respectively at maximum brake power. The HC emission in the UTO is much higher than that of diesel for all compression ratios. It can be observed from the figure that the HC emission found to be higher by about 36.6% and 12.7% for compression ratio of 16:1 and 17:1 compared to standard compression ratio of UTO while the compression

ratio of 18.5:1 shows 30.6% lower at maximum brake power due to delay in ignition. Fuel viscosity and spray quality is also responsible for increase in the HC with the UTO. More fuel is accumulated in the delay period and as a result, higher HC emission is formed with lower compression ratio than standard compression ratio.

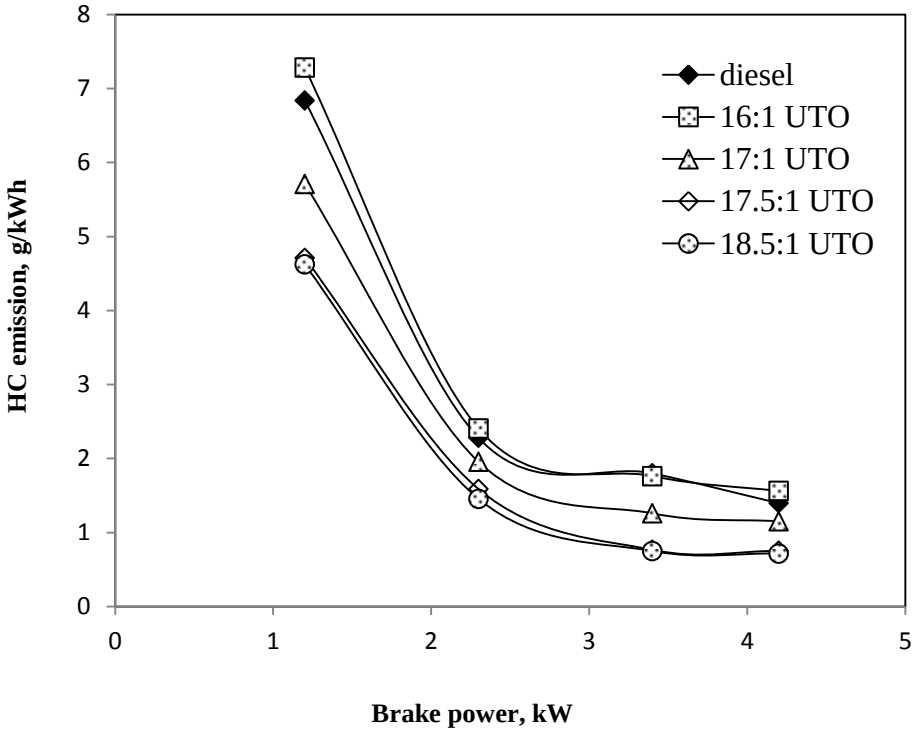

Figure 6.47 Variation in HC emission with brake power for engine fueled with UTO at different compression ratio

6.5.4.4 Smoke density

Figure 6.48 portrays the percentage variation of the smoke density with brake power for the UTO compared to diesel at different compression ratio. Smoke density for diesel, UTO at 17.5:1, 16:1, 17:1 and18.5:1 are 24, 22.3, 25.2, 23 and 21.5% respectively at maximum brake power. It can be observed that the smoke density increases with an increase in the brake power as expected, the hydrogen to carbon ratio of UTO is lower by about 49% than that of diesel. Among all the compression ratios, UTO with compression ratio 18.5 exhibits the lowest smoke density by 4.1% compared to diesel at maximum power. With the compression ratio of 16:1 and 17.1, the UTO shows 14.1% and 9.2%

increase while higher compression ratio 18.5:1 shows 8.6% less smoke density compared to that of UTO at standard compression ratio. This may be due to the maximum temperature during the combustion increases and this, in turn, decreases smoke density.

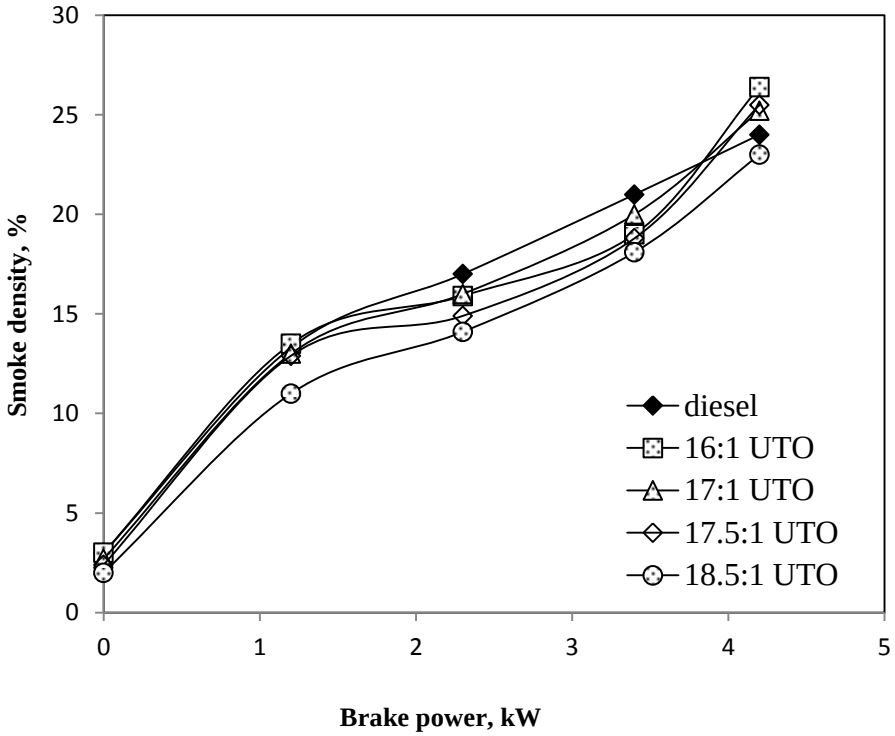

Figure 6.48 Variation of smoke density with brake power for engine fueled with UTO at different compression ratio

The percentage variation of the results for the UTO at different compression ratio with diesel is given in Table 6.4

6.5.5 Closure

The results of combustion, performance and emission characteristics of the diesel engine fueled with the UTO at different compression ratio in comparison with diesel indicated that the fuel can be used in variable compression ratio engines also. The analysis implies that the engine operated with 18.5:1 compression ratio gives a better performance and lower emissions in comparison with UTO at standard compression ratio . At the 18.5:1 compression ratio, the NO emission is found to be 31% higher compared to that of diesel.

Table 6.4 Percentage variation of results of UTO at different compression ratio with diesel

Si.No.	**Parameter**	**UTO 16:1**	**UTO 17:1**	**UTO 17.5:1**	**UTO 18.5:1**
A Combustion parameters					
1.	Occurrence of ignition	0.14	-0.20	-0.41	-0.87
2.	Ignition delay	2.67	-3.39	-9.821	-10.71
4.	Combustion duration	20.58	14.99	-19.60	6.61
5.	Maximum heat release	-21.60	-31.46	-2.34	-18.74
6.	Maximum cylinder pressure	-21.55	-9.65	9.88	13.93
B Performance parameters					
1.	Brake specific energy consumption	18.45	11.95	0.50	17.68
2.	Exhaust gas temperature	42.83	45.49	31.43	40.86
C Emission parameters					
1.	HC emission	11.76	-17.51	-46.10	-48.64
2.	CO emission	130.99	113.24	-67.62	70.89
3.	NO emission	6.42	13.59	28.17	31.06
4.	Smoke density	10	5	6.25	-4.16

"+" indicates increasing percentage; "-"indicates decreasing percentage.

6.6 UTO at different preheating temperatures

6.6.1 General

Pugazhvadivu and Sankaranarayanan [127] stated that preheating of fuel offers reduction of viscosity and smooth flow of fuel in fuel lines and injection systems. In this section, the effect of preheating of UTO on combustion, performance and emission parameters, with UTO is discussed and compared with diesel. As described in the chapter "Methodology", the maximum preheating temperature was fixed at 110^{o}C. The numeric value of temperature after UTO indicates the preheating temperature. Four preheating temperature were adapted from 80^{o}C to 110^{o}C in steps of 10^{o}C, in this study.

6.6.2 Combustion analysis

6.6.2.1 Pressure crank angle diagram

Figure 6.49 shows the variation of the cylinder pressure with crank angle for diesel, UTO and UTO at different preheating temperatures with maximum power output.

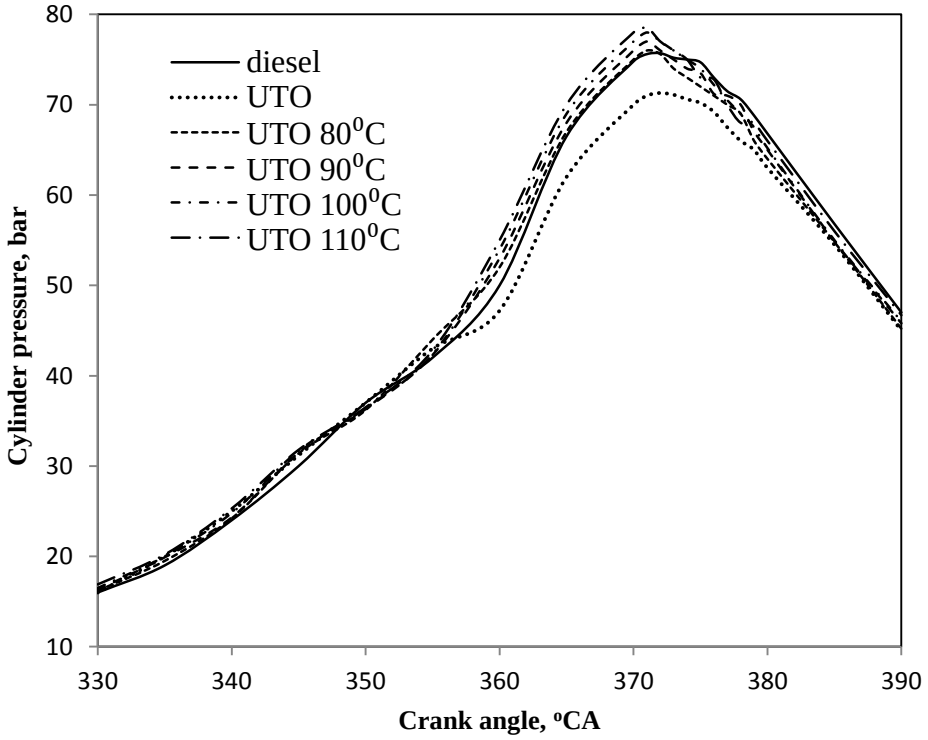

Figure 6.49 Variation of cylinder pressure with crank angle at maximum brake power for engine fueled with UTO at different preheating temperatures

The occurrence of the ignition timing of UTO is found to be approximately 1 ^{o}CA, earlier than that of UTO at 80 and 90^{o}C. The UTO at 100 and 110 ^{o}C indicate the occurrence of ignition 1 and 1.5 ^{o}CA respectively, earlier than that of UTO operation. The ignition of UTO occurs approximately by about 1 ^{o}CA earlier than that of diesel at maximum power output. At higher preheating temperatures, the fuel atomises and vaporises better, and mixes with air to form a combustible mixture, which might auto-ignite earlier than that of UTO. As a result, the UTO at preheated temperatures exhibits early ignition compared to that of UTO.

6.6.2.2 Ignition delay

The variation of ignition delay of diesel, UTO and the UTO at different preheating temperatures with brake power is shown in Fig. 6.50. The UTO shows a shorter ignition delay as compared to diesel.

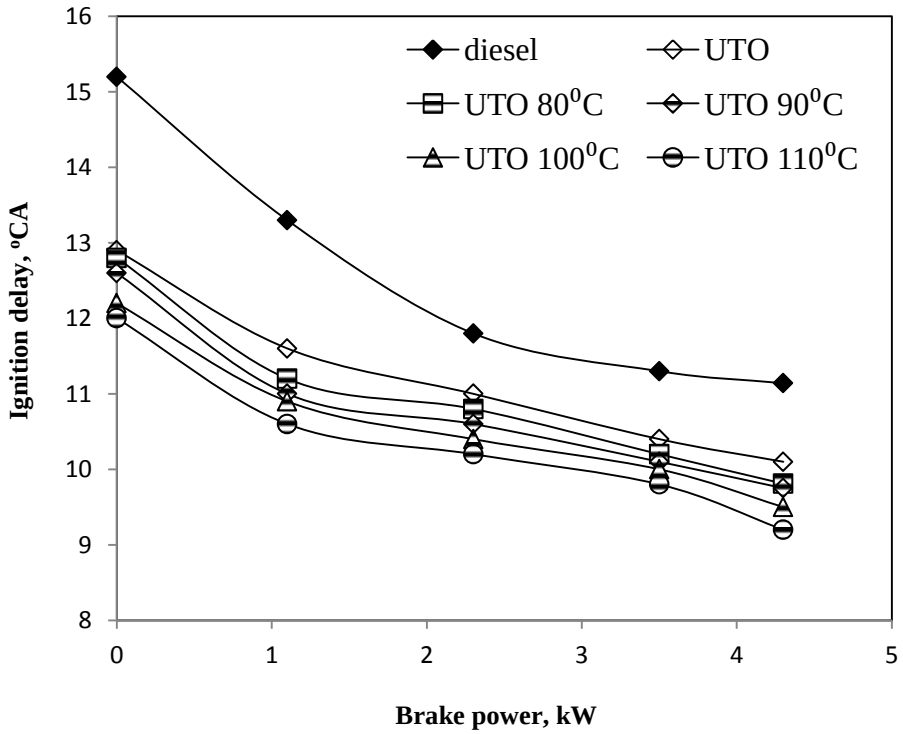

Figure 6.50. Variation of the ignition delay with brake power for engine fueled with UTO at different preheating temperatures

The ignition delay of diesel at maximum brake power is found to be about 11 ^{o}CA for the UTO it is found 10 ^{o}CA with the UTO operation. As mentioned in earlier chapter the UTO has a low and high boiling point in it. The injection of UTO at high temperature might result in the breakdown of higher molecular weight compounds to products of lower molecular weight. These complex chemical reactions led to the formation of gases of lower molecular weight on the peripheral region with a very dense inner core of liquids of higher molecular weight. The rapid vaporization of this lighter oil in the fringe of the spray spread out the jet, and thus volatile combustible compounds ignited earlier and reduced the delay period.

Rao [128] stated that a high viscous fuel, would exhibit shorter ignition delay when it has a higher cetane number. It can be observed from the figure that the UTO exhibits a shorter ignition delay than that of diesel due to faster evaporation of fuel. It can also be observed from Fig. 6.46 that the reduction in ignition delay is noticed with increasing power outputs for all the tested fuels in this study. The ignition delay decreases with increase in the preheating temperatures of UTO at maximum brake power. The ignition delay for the UTO at 80, 90, 100, 110 ^{o}C is 9.81, 9.75, 9.5 and 9.2 ^{o}CA respectively at maximum brake power.

6.6.2.3. Heat release rate

Figure 6.51 portrays the heat release rate with crank angle for diesel, UTO and the UTO at different preheating temperatures. It can be observed that the premixed burning and diffusion burning phase is found to be lower with the UTO than that of diesel at maximum brake power. However, at preheated temperatures of UTO, there is an improvement in the heat release rate with the UTO. By increasing the temperature, the intensity of the heat release rate in the premixed phase increases. Preheating improves atomisation and vaporisation of UTO. The low viscosity of the preheated fuel leads to form more flammable fuel air mixture during the delay period and enhances the combustion, which results in high heat release rates. Similar reasons are explained by Senthil et al., [129].The maximum heat release rate for diesel and the UTO at maximum power output is found to be about 51.3 and 50.2 J/^{o}CA respectively. The maximum heat

release for the UTO 80, 90, 100 and 110^{o}C is 50.3, 50.6, 50.8 and 51 J/^{o}CA respectively at maximum brake power.

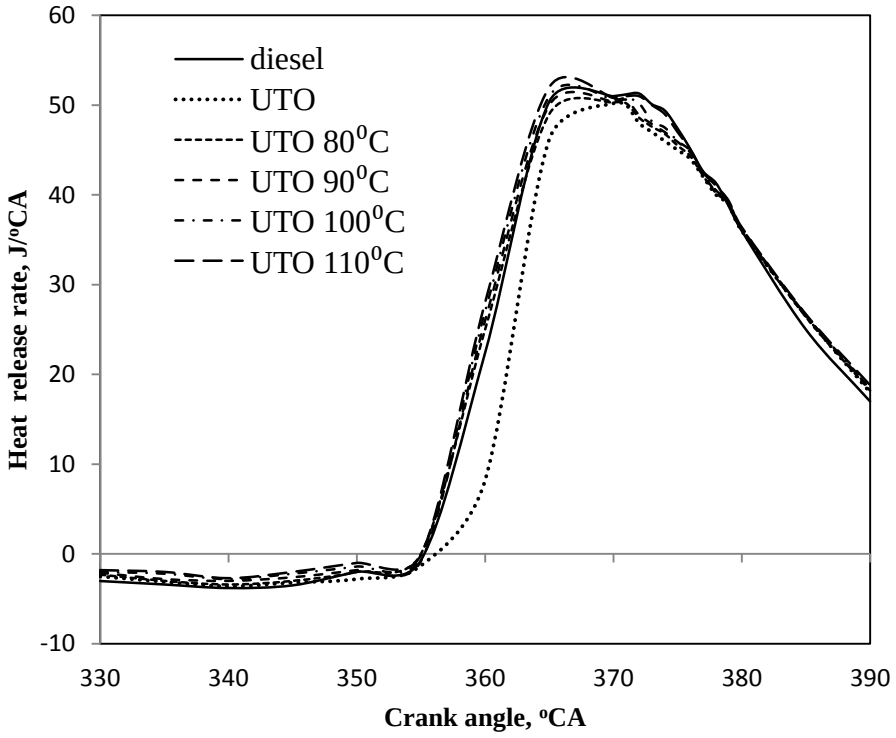

Figure 6.51 Variation of the heat release rate with crank angle at maximum brake for engine fueled with UTO at different preheating temperatures

6.6.2.4 Combustion duration

The combustion duration for diesel, UTO and the UTO at preheated temperatures is depicted in Fig. 6.52. The combustion duration with diesel, UTO, UTO at 80, 90, 100 and 110^{o}C are 40.8, 32.8, 40, 39.6, 39 and 38.2 ^{o}CA respectively at maximum brake power. The combustion duration decreases with the UTO and UTO at different preheating temperatures as compared to that of diesel at maximum brake power. It can be observed from the figure that the whole combustion phase is advanced, leading to significant higher combustion pressures and temperatures, and hence, shorter ignition delay, and thus, lower combustion duration. Similar reasons are explained by Martin M

and Prithviraj [130]. The preheated UTO shows a significant reduction in the combustion duration at high temperatures, mainly at maximum brake power.

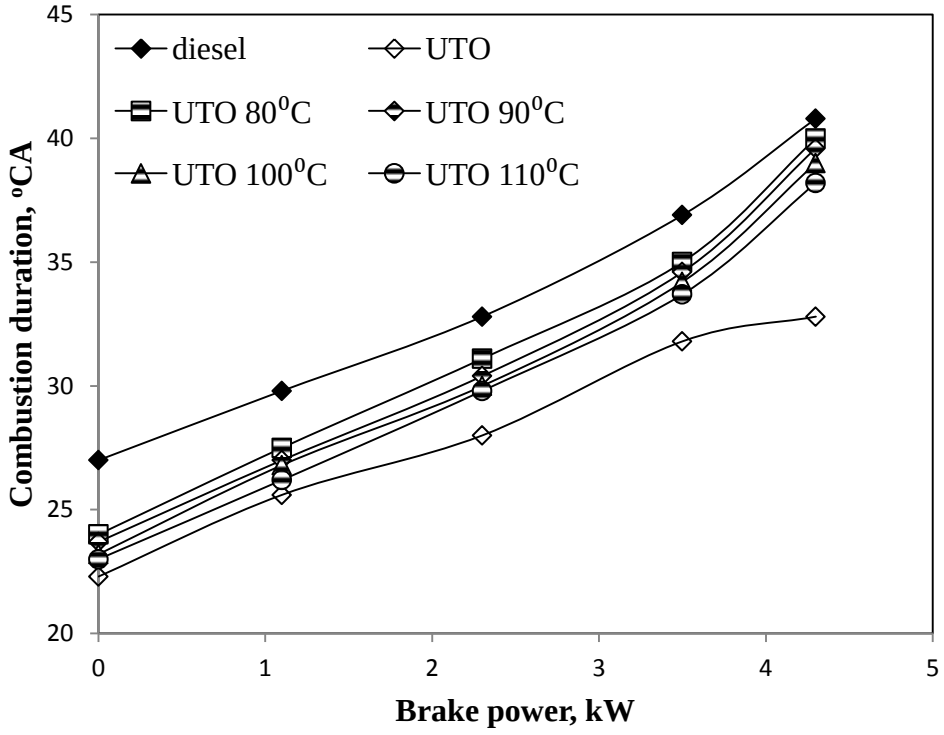

Figure 6.52 Variation of the combustion duration with brake power for engine fueled with UTO at different preheating temperatures

6.6.2.5 Maximum cylinder pressure

Figure 6.53 portrays the variation of maximum cylinder pressure with brake power for the UTO at different preheating temperatures and diesel with brake power. The maximum cylinder pressures of diesel, UTO and UTO at preheating temperatures of 80, 90, 100 and 110^{o}C are 78, 61.31, 72, 73, 74 and 75 bar respectively at maximum brake power.

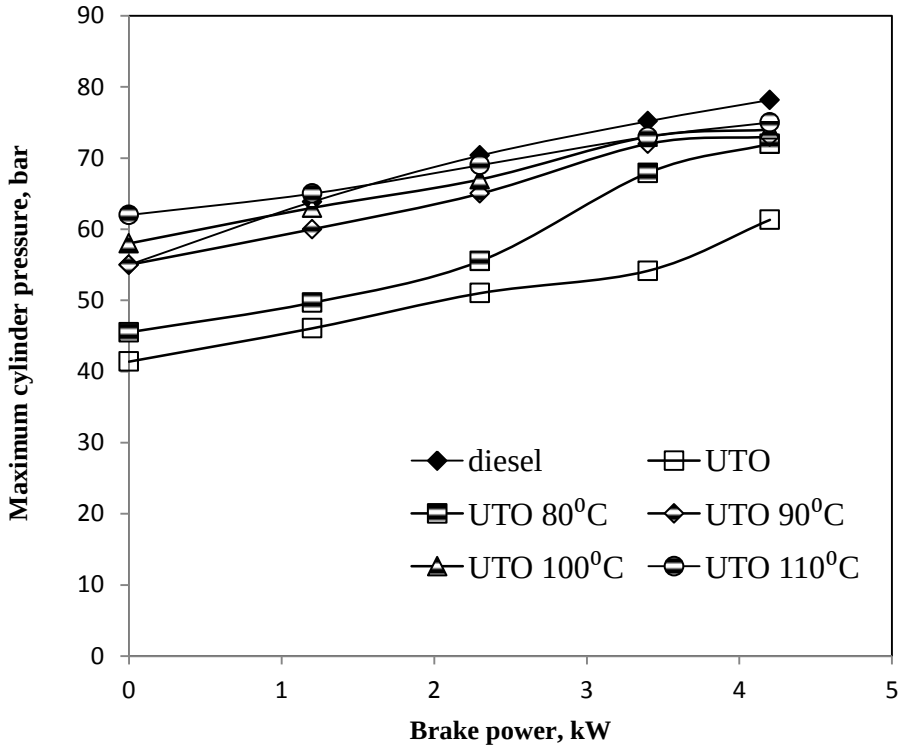

Figure 6.53 Variation of the maximum cylinder pressure with brake power for engine fueled with UTO at different preheating temperatures

6.6.2.6 Maximum Rate of Pressure Rise

Figure 6.54 portrays the maximum rate of pressure rise with brake power for diesel, UTO and UTO at different preheating temperatures with respect to brake power. The rate of pressure rise is an indication of how far can the engines components sustain with high forces. The value for maximum rate of pressure rise is found to be 4.1 bar/^{o}CA for diesel and 5.5 bar/^{o}CA for the UTO.

Low heat release is the reason for lower maximum rate of pressure rise for the UTO than that of diesel at maximum power output. With an increase in the temperature of the fuel, the maximum rate of pressure rise is increased, due to lower viscosity and better mixing of injected fuel. The maximum rate of pressure rise of 4.9 bar/^{o}CA is noticed with the UTO at the preheating temperature of 110^{o}C. However, there is no much deviation of the value of maximum rate of pressure rise with UTO at different preheating temperature at maximum bake power.

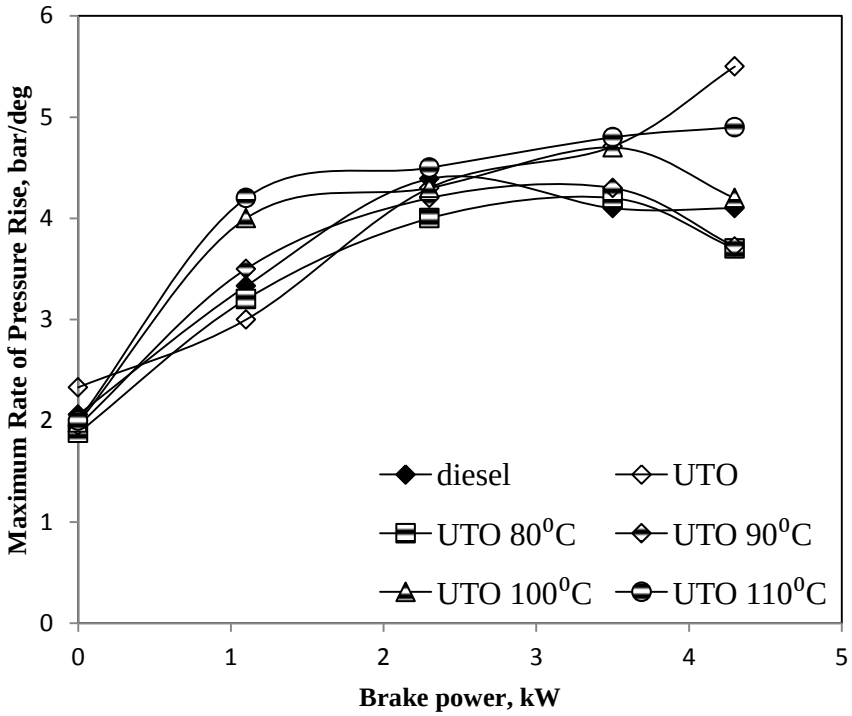

Figure 6.54 Variation of the maximum rate of pressure rise with brake power for engine fueled with UTO at different preheating temperatures

6.6.3 Performance parameters

6.6.3.1 Brake specific energy consumption

Figure 6.55 depicts the BSEC of diesel, the UTO and the UTO at different preheating temperatures**.** The UTO has a lower calorific value than that of diesel. Hence, the specific fuel consumption is marginally found to be higher than that of diesel for the UTO at maximum brake power. The fuel consumption decreases as the UTO temperature increases. The reduction in viscosity of fuel results in better mixture formation with air and hence lower BSEC is noticed. The values of BSEC at maximum brake power are about 11.2, 9.78, 8.6, 7.8 and 7 MJ/kWh with UTO at 27, 80, 90, 100 and 110^{o}C, respectively, whereas it is about 11.8 MJ/kWh with diesel.

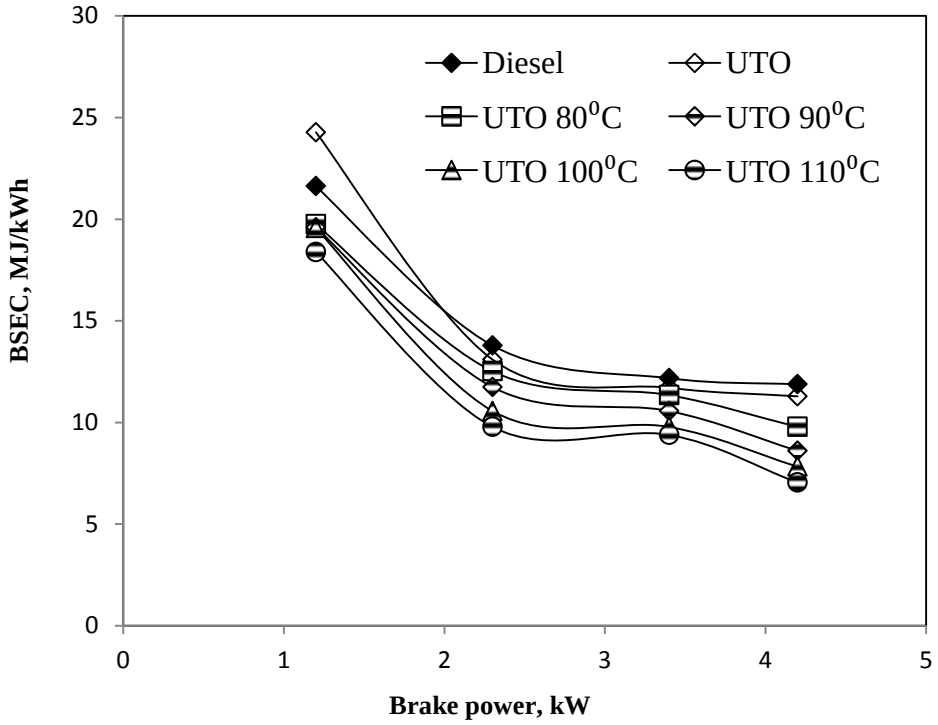

Figure 6. 55 Variation of the BSEC with brake power for engine fueled with UTO at different preheating temperatures

6.6.3.2 Exhaust gas temperature

Exhaust gas temperature is found to be higher with the UTO as compared to that of diesel, as seen in Fig. 6.56. Higher viscosity and poor volatility are the reasons for higher exhaust gas temperature for the UTO than that of diesel at maximum power output. When the UTO is admitted at preheated temperatures, the viscosity reduces. As a result of better atomisation and combustion, the exhaust gas temperature reduces, as suggested by Martin et al., [131], but is little higher than that of diesel. Some of the higher boiling point compounds present in the UTO may enter the combustion. This may be the reason for higher exhaust gas temperature even after preheating the UTO. The maximum temperature of the exhaust gas at maximum brake power is about 321, 312, 299 and 285^{o}C with UTO at 80, 90, 100 and 110^{o}C, respectively.

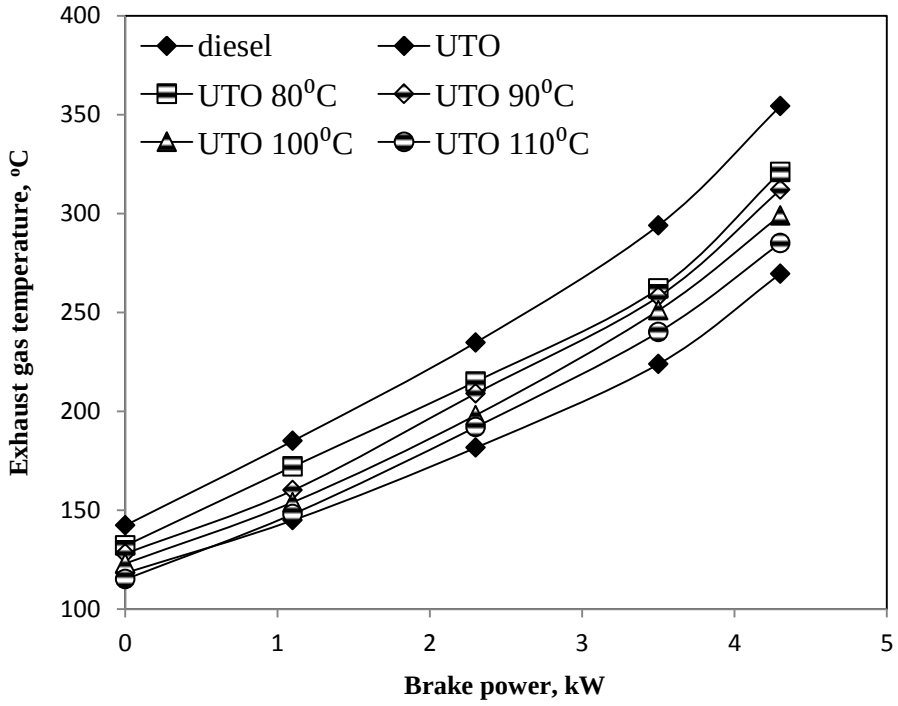

Figure 6.56 Variation of the exhaust gas temperature with brake power for engine fueled with UTO at different preheating temperatures

6.6.4 Emission parameters

6.6.4.1 Nitric oxide emission

The variation of the NO emission with brake power is shown in Fig. 6.57. The NO emission for diesel, UTO, UTO at 80, 90, 100 and 110^{o}C are 6.4, 5.1, 6.11, 6.8, 6.6 and 6.2 g/kWh respectively at maximum brake power. As the engine power increases the combustion gas temperature increases, which in turn, decrease the formation of NO emission. It can be observed that UTO emits lower NO emission compared to that of diesel in the entire power range. It can also be observed that the NO emission increases with an increase in the preheating temperatures, but decreases with the given power output. The increase in the NO emission for the preheated UTO may be attributed to the increase in the combustion gas temperature.

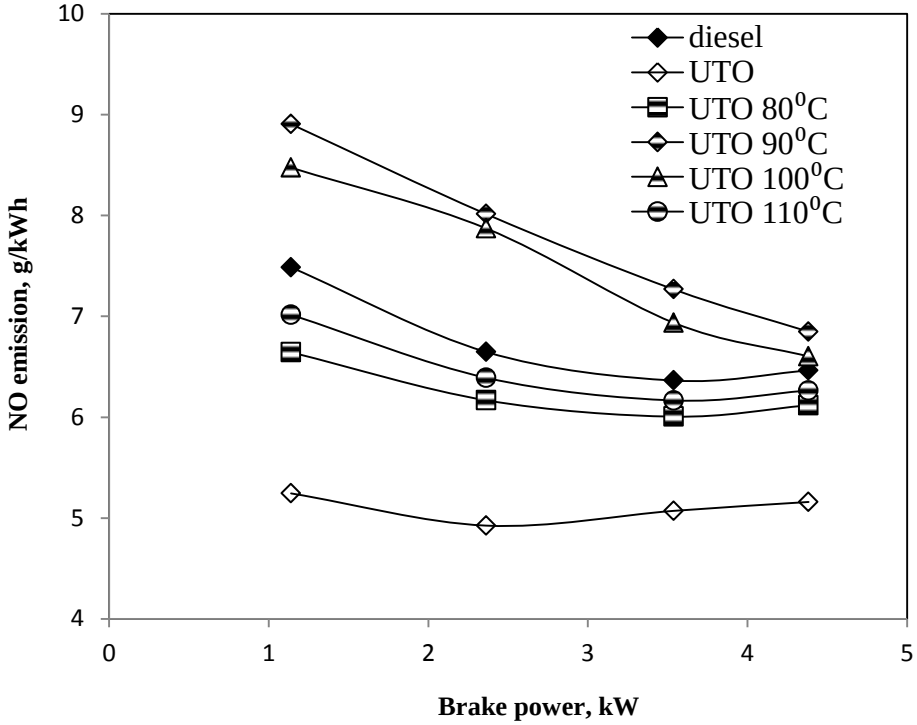

Figure 6.57 Variation of the NO emission with brake power for engine fueled with UTO at different preheating temperatures

6.6.4.2 Carbon monoxide emission

The CO emission for diesel, UTO, UTO at 80, 90, 100 and 110^{o}C are 0.0022, 0.0047 0.00469, 0.00444, 0.0037 and 0.00381g/kWh respectively at maximum brake power. The UTO forms higher CO emissions than that of diesel throughout the engine operation, as seen in Fig. 6.58. The CO emission is found to be higher with the UTO among all the fuels tested in this study, while it is found to be the lowest with UTO at 100^{o}C. This trend may be due to the high viscosity of UTO, resulting in poor mixture formation. It can be noticed that the high brake specific fuel consumption with the UTO leads to the injection of higher quantities of fuel as compared to that of diesel, for the same power outputs. Less oxygen may also be the reason for the UTO due to rich pockets. It may be noted that the high brake specific fuel consumption with UTO leads to the injection of higher quantities of fuel as compared to that of diesel, for the same brake power conditions. However, fuel preheating results in better complete combustion and reduces the CO emission.

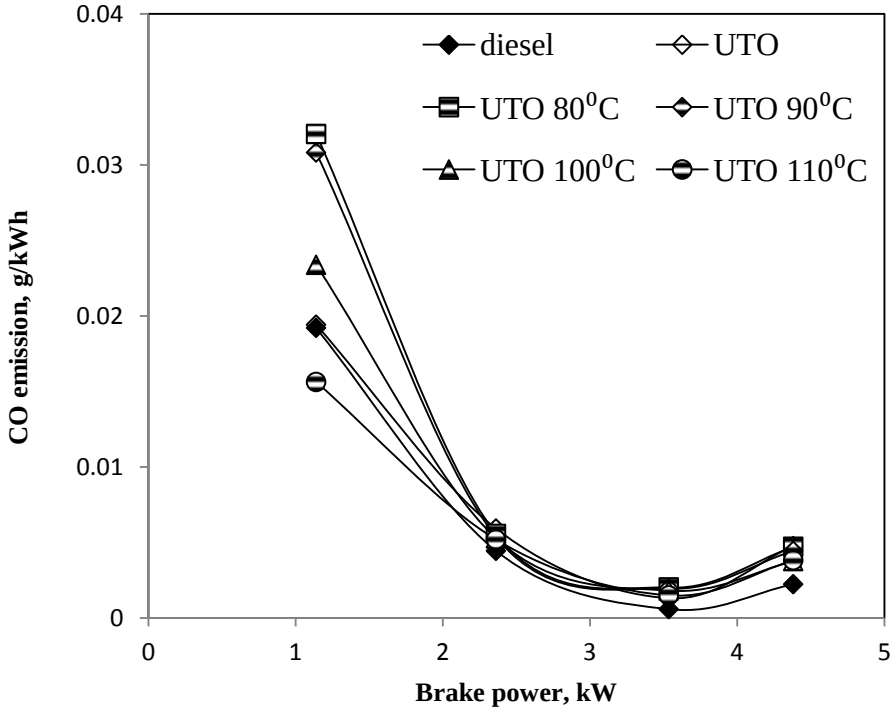

Figure 6.58 Variation of the CO emission with brake power for engine fueled with UTO at different preheating temperatures

6.6.4.3 Hydrocarbon emission

The variation of the HC emissions with diesel, UTO and UTO at different preheating temperatures is shown in Fig. 6.59. It can be observed that UTO leads to higher unburnt fuel emission than diesel operation. The HC emission is recorded higher with the UTO, as 0.012 g/kWh than with diesel as 0.006 g/kWh, at maximum brake power. The HC emission of UTO at 80, 90, 100 and 110^{o}C are 0.013, 0.012, 0.01 and 0.0088 g/kWh respectively at maximum brake power. Some of the species in the UTO might form lean mixture while some other may contribute to the rich mixture. As a result, the combustion may expenses the supply of lean and rich mixtures. However, with the preheated UTO, a reduction in the HC emission noticed. Due to the improved vaporization and fuel air mixing rates, combustion becomes complete and results in lower unburnt HC emissions with the preheated UTO. The HC emissions for all the tested fuels decrease with the increase in the brake power.

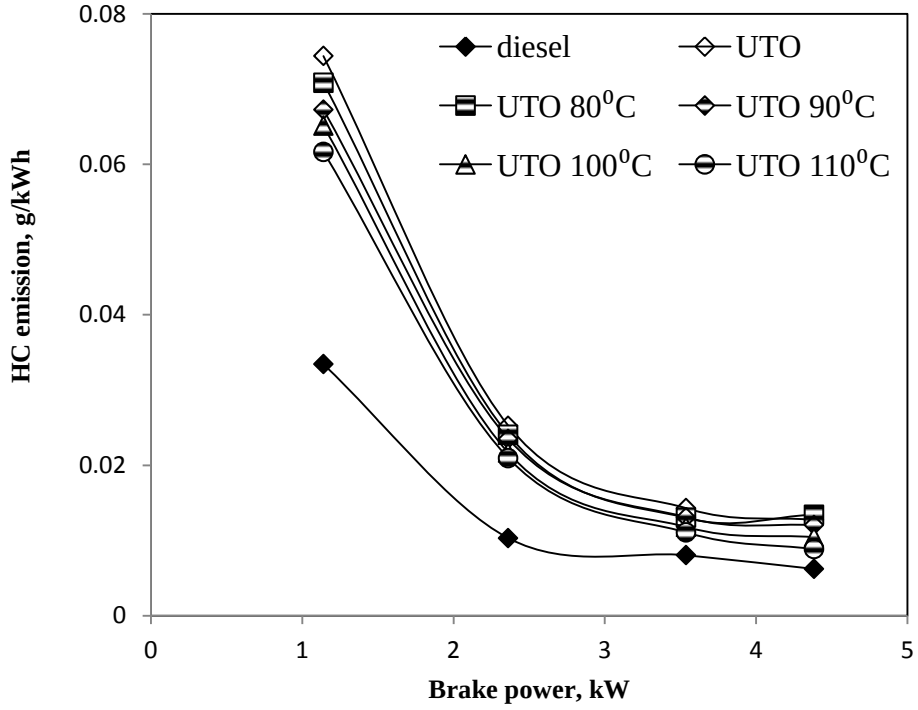

Figure 6.59 Variation of the HC emission with brake power for engine fueled with UTO at different preheating temperatures

6.6.4.4 Smoke density

Figure 6.60 depicts the variation of smoke emission with diesel, UTO and the UTO at different preheating temperatures with brake power. The smoke density for diesel, UTO, UTO at 80, 90, 100 and 110 ^{o}C are found to be 24, 25.5, 25.4, 25.2, 25 and 24.7% respectively at maximum brake power. It can be observed that the smoke emission for the UTO is significantly higher than that of diesel at maximum brake power. This may be due to the higher viscosity and poor volatility of UTO compared to that of diesel. The UTO at different preheating temperatures shows a lower smoke density compared with the UTO at maximum brake power. This may be due to the reduction in viscosity and subsequent improvement in spray, fuel-air mixing and combustion characteristics by preheating.

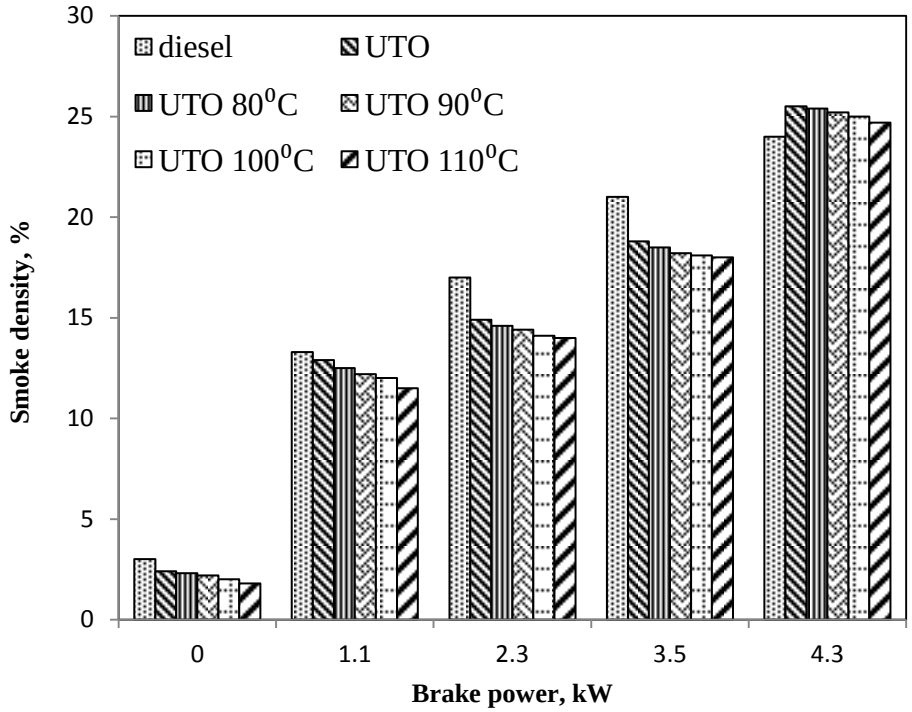

Figure 6.60 Variation of the smoke density with brake power for engine fueled with UTO at different preheating temperatures

The percentage variation of different parameters for the UTO at different preheating temperatures with diesel is given in Table 6.5.

6.6.5 Closure

The UTO can be used as a preheated fuel in a CI engine with reduced smoke, HC and CO emissions, without any deterioration in the engine performance. UTO at 110^{o}C gives lower HC and NO emissions. The brake specific energy consumption of UTO at 110^{o}C is lower by about 40.6% at maximum brake power.

Table 6.5 Percentage variation of results of UTO at different preheating temperatures with diesel

Si.No.	Parameter	UTO	UTO 80^{o}C	UTO 90^{o}C	UTO 100^{o}C	UTO 110^{o}C
A Combustion parameters						
1.	Occurrence of ignition	0	0	0	-0.26	-0.26
2.	Ignition delay	-9.33	-11.94	-12.48	-14.72	-17.41
4.	Combustion duration	-19.60	-1.96	-2.94	-4.41	-6.37
5.	Maximum heat release	-2.14	-1.94	-1.36	-0.97	-0.58
6.	Maximum cylinder pressure	9.88	10.01	10.26	11.16	11.54
B Performance parameters						
1.	Brake specific energy consumption	-4.95	-17.63	-27.51	-34.10	-40.69
2.	Exhaust gas temperature	31.43	19.09	15.75	10.92	5.73
C Emission parameters						
1.	HC emission	104.90	115.95	93.56	67.89	42.37
2.	CO emission	113.17	110.52	99.05	67.86	70.82
3.	NO emission	-20.18	-5.34	5.95	2.14	-3.07
4.	Smoke emission	6.25	5.83	5	4.16	2.91

“+” indicates increasing percentage; “-” indicates decreasing percentage.

6.7 UTO on dual fuel mode

6.7.1 General

Dual fuel operation in a diesel engine offers a potential of reduction in smoke emission with improved performance at maximum brake power for high viscous fuels [107]. In this section, the results of combustion, performance and emission parameters are discussed for the UTO operated in a dual fuel mode. Different flow rates of acetylene were inducted with air in the suction. Four different flow rates of acetylene 132, 198, 264 and 330 g/h were used in this study. The flow rates are indicated after UTO in the dual operation.

6.7.2 Combustion analysis

6.7.2.1 Pressure crank angle diagram

Figure 6.61 (a) shows the variation of cylinder pressure with crank angle for diesel, and diesel with acetylene, at different flow rates. The occurrence of the ignition timing of diesel with acetylene of 132 g/h, 198 g/h, 264 g/h and 330 g/h is at 1, 1.5, 2, 3 ^{o}CA earlier than that of diesel operation at maximum brake power.

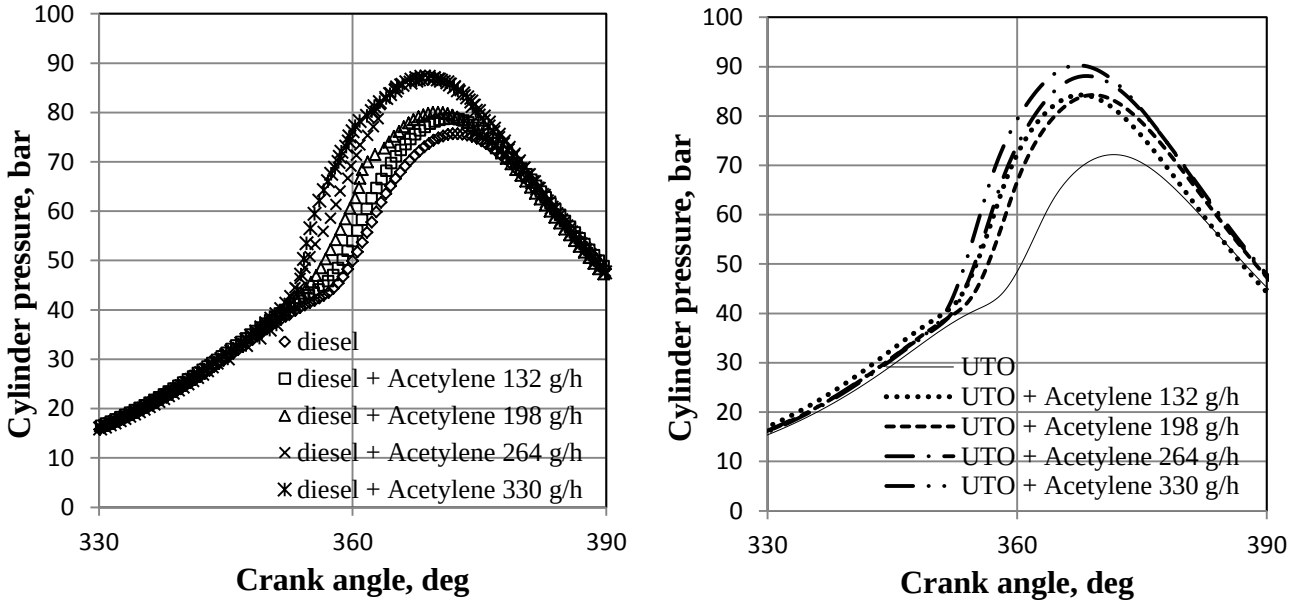

Figure 6.61 (a), 6.61 (b) Variation of cylinder pressure with crank angle at maximum brake power for engine fueled with diesel and UTO on dual fuel mode

The advancement in occurrence of ignition while inducting the acetylene is because of the instantaneous combustion, i.e., in the first stage of combustion the acetylene gets ignited and is burnt very quickly, while diesel burnt progressively in the second stage, Figure 6.61 (b) shows the variation of the cylinder pressure with crank angle for the UTO and UTO with acetylene, at different flow rates. The occurrence of the ignition of UTO with acetylene of 132 g/h, 198 g/h, 264 g/h and 330 g/h is approximately 0.5, 1, 1.5 and 2 ^{o}CA earlier than that of UTO operation, at maximum brake power. As the acetylene quantity increases, the maximum cylinder pressure increases, and combustion also occurs earlier. This is due to higher pressure and temperature attained during the expansion process, and more chemical energy being converted into mechanical energy.

6.7.2.2 Ignition delay

Figure 6.62 illustrates the variation of the ignition delay with brake power for diesel and the UTO with acetylene, at different flow rates.

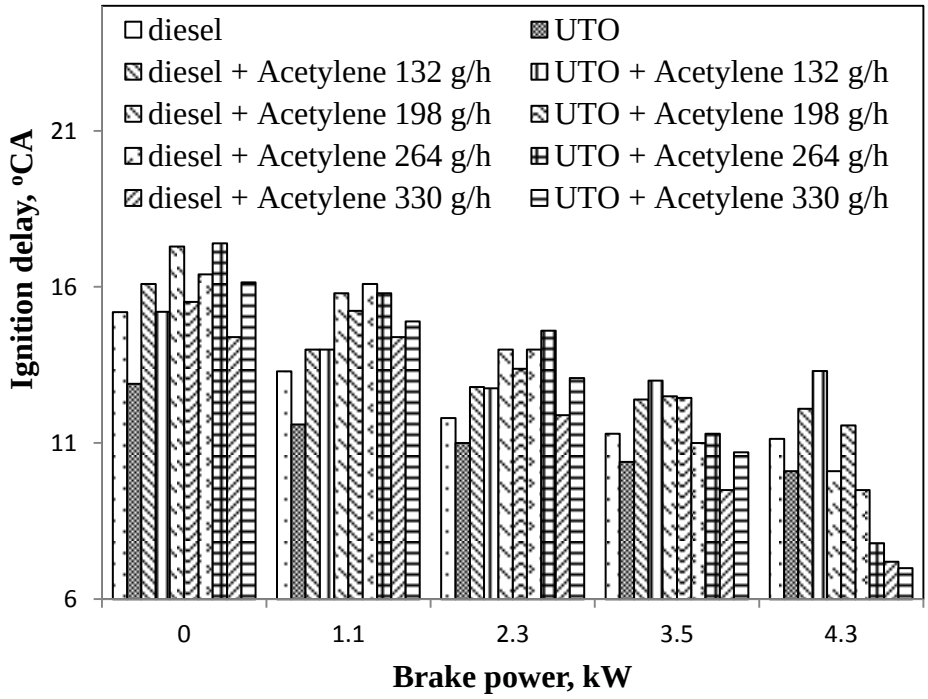

Figure 6.62 Variation of the ignition delay with brake power for engine fueled with diesel and UTO on dual fuel mode

The ignition delay for diesel is 11.2 ^{o}CA. In the case of diesel at different flow rates of 132 g/h, 198 g/h, 264 g/h and 330 g/h the ignition delay is 12.1 ^{o}CA, 10.1^{o}CA, 9.5^{o}CA and 7.2 ^{o}CA respectively, at maximum brake power, whereas the ignition delay for the sole UTO is approximately 10.1 ^{o}CA, and for the UTO with different acetylene flow rates of 132 g/h, 198 g/h, 264 g/h and 330 g/h flow rates, the ignition delay is 13.3 ^{o}CA, 11.5 ^{o}CA, 7.8 ^{o}CA and 7 ^{o}CA respectively, at maximum brake power. The ignition delay reduces with increase of acetylene flow rates, at maximum brake power due to overlapping of valve openings and high diffusion rate of acetylene.

6.7.2.3 Heat release rate

Figure 6.63 portrays the heat release rate with crank angle for diesel and the UTO with acetylene at different flow rates. The maximum heat release rate for diesel and the UTO at maximum brake power is 51.3 and 50.2 J/^{o}CA respectively at maximum brake power.

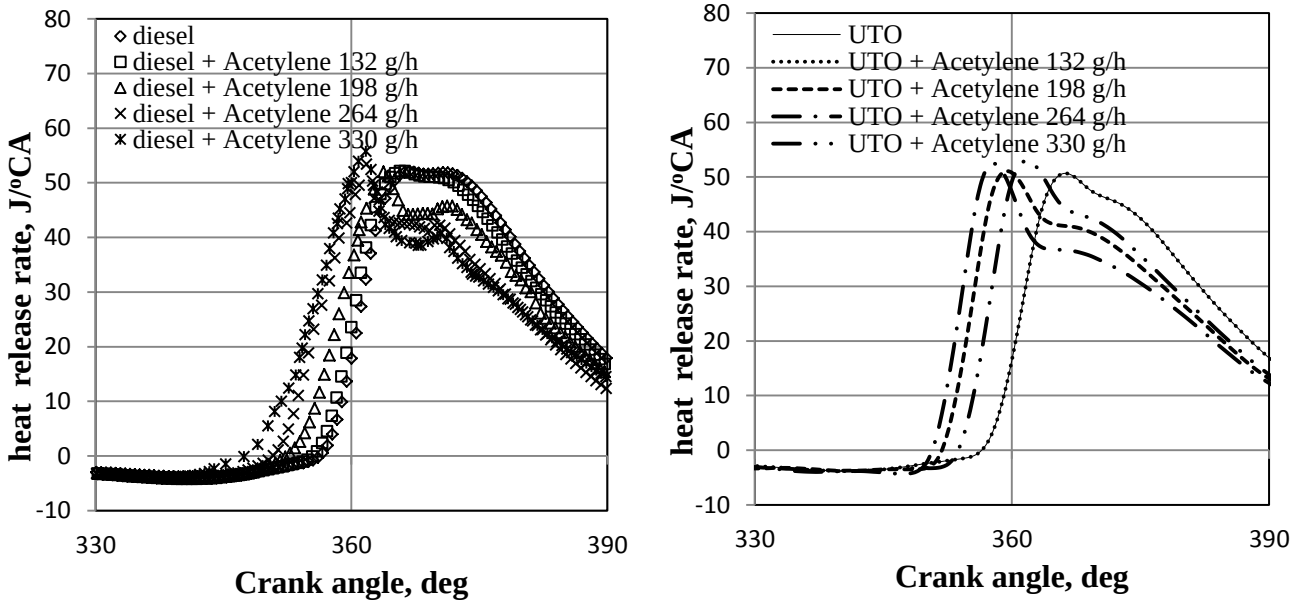

Figure 6.63 (a), 6.63 (b) Variation of the heat release rate with crank angle at maximum brake power for engine fueled with diesel and UTO on dual fuel mode

Higher viscosity of UTO leads to a less flammable fuel air mixture during the delay period, which results in lower heat release rate of UTO than that of diesel at maximum brake power. The maximum heat release for diesel with acetylene at the flow rates of 132, 198, 264 and 330 g/h is 51.8, 52, 53.4 and 55.7 J/^{o}CA respectively, at maximum brake power, whereas for the UTO with acetylene at different flow rates of 132, 198, 264 and 330 g/h, the maximum heat release rate is found to be 50.6, 51, 52.4 and 52.9 J/^{o}CA respectively, at maximum brake power. In dual fuel mode, the premixed phase which consists of the combustion of a portion of the fuel (diesel or UTO) and the inducted acetylene dominates, as the inducted acetylene quantity is higher.

6.7.2.4 Combustion duration

The variation of the combustion duration for diesel and the UTO with acetylene at different flow rates is depicted in Fig. 6.64. The combustion duration of diesel and UTO is found to be approximately 41 and 33 ^{o}CA respectively at maximum brake power.

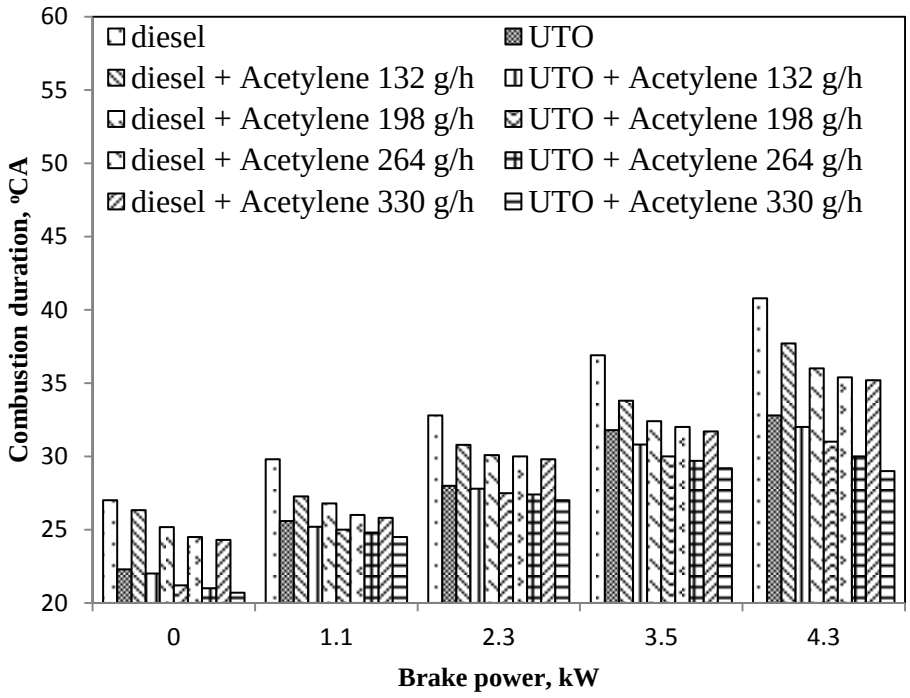

Figure 6.64 Variation of the combustion duration with brake power for engine fueled with diesel and UTO on dual fuel mode

The decrease in the combustion duration is due to shorter ignition delay. The combustion duration in the dual fuel mode at maximum brake power with diesel, is found to be 38 ^{o}CA at 132 g/h, 36 ^{o}CA at 198 g/h, 35.4 ^{o}CA at 264 g/h and 35.2 ^{o}CA at 330 g/h of gas flow rates respectively, whereas for the UTO, the combustion duration is 32 ^{o}CA at 132 g/h, 31 ^{o}CA at 198 g/h, 30 ^{o}CA at 264 g/h and 29 ^{o}CA at 330 g/h of gas flow rates respectively. The combustion duration decreases with the UTO as compared to that of diesel at maximum brake power. This may be due to the advancement of the combustion phase (ignition delay, premixed combustion, diffusion and late diffusion combustion), leading to higher combustion pressures and temperatures, and hence, shorter ignition delay and lower combustion duration. With the acetylene admission, there is a reduction in combustion duration due to the higher flame speed of acetylene.

6.7.2.5 Maximum cylinder pressure

From Fig. 6.65, it is seen that the maximum cylinder pressure at lower brake power are higher for acetylene induction than that of diesel operation.

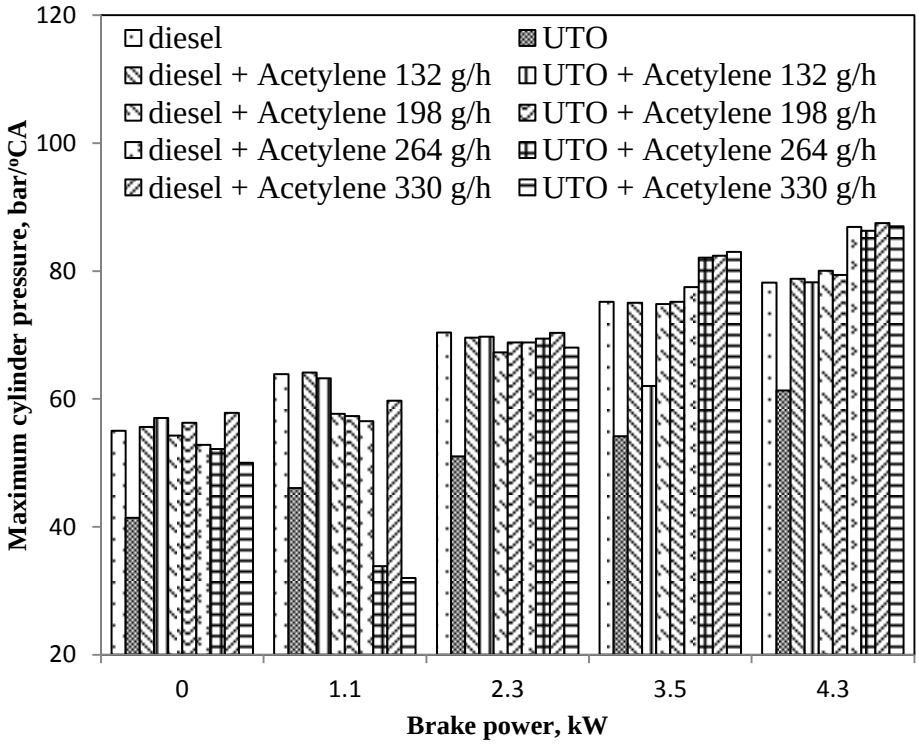

Figure 6.65 Variation of the maximum cylinder pressure with brake power for engine fueled with diesel and UTO on dual fuel mode

This is due to less heat release rate and at maximum brake power the maximum cylinder pressure is higher for acetylene induction than that of diesel operation. The maximum cylinder pressure for diesel operation at maximum brake power is 75.7 bar while for acetylene induction with flow rates of 132, 198, 264 and 330 g/h are 78.77bar, 80 bar, 86.9 bar and 87.51 bar respectively, whereas for the UTO and UTO with acetylene flow rates of 132, 198, 264 and 330 g/h are 61.31, 78.22, 79.39, 86.28 and 87 bar respectively at maximum brake power.

6.7.2.6 Maximum rate of pressure rise

Figure 6.66 illustrates the maximum rate of pressure rise of diesel and UTO and with different acetylene flow rates. The maximum rate of pressure rise for diesel operation at maximum brake power is 4.1 bar while for acetylene induction with flow rates of 132, 198, 264 and 330 g/h are 4.39bar, 4.4 bar, 4.8 bar and 5.41 bar/^{o}CA respectively, whereas for the UTO and UTO with the acetylene flow rates of 132, 198, 264 and 330 g/h are 5.5, 4.11, 4.25, 5.55 and 6.21 bar/^{o}CA respectively at maximum brake power.

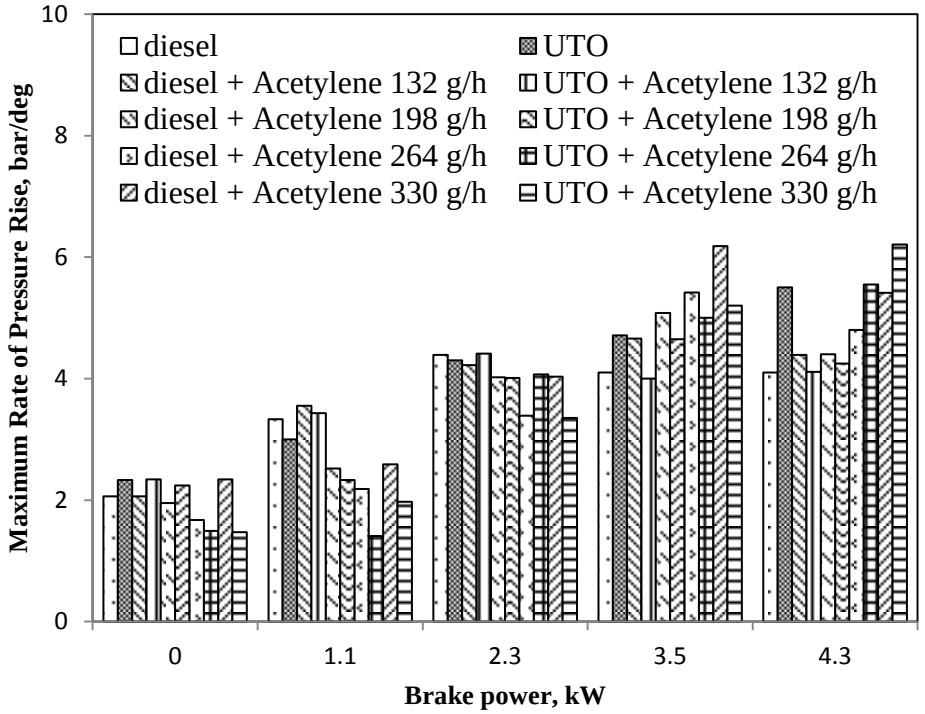

Figure 6.66 Variation of the maximum rate of pressure rise with brake power for engine fueled with diesel and UTO on dual fuel mode

6.7.3 Performance parameters

6.7.3.1 Brake specific energy consumption

Figure 6.67 shows the BSEC for diesel and the UTO with acetylene, at different flow rates. The brake specific energy consumption for diesel and the UTO is 11.8 and 11.2 MJ/kWh respectively at maximum brake power. The efficiency in the dual fuel mode at maximum brake power of diesel is found to be 11, 9.4, 8.4 and 8.3 at 132, 198, 264 and 330 g/h of gas flow rates respectively. For the UTO at different acetylene flow rates of 132, 198, 264 and 330 g/h the brake specific energy consumption is 9.8, 8.4, 7.5 and 7.4 MJ/kWh respectively, at maximum brake power. By the induction of acetylene, specific energy consumption decreases compared to that of diesel and the UTO operation. This may be due to the high heat release rate, which leads to high cylinder pressure and better utilization of the heat input.

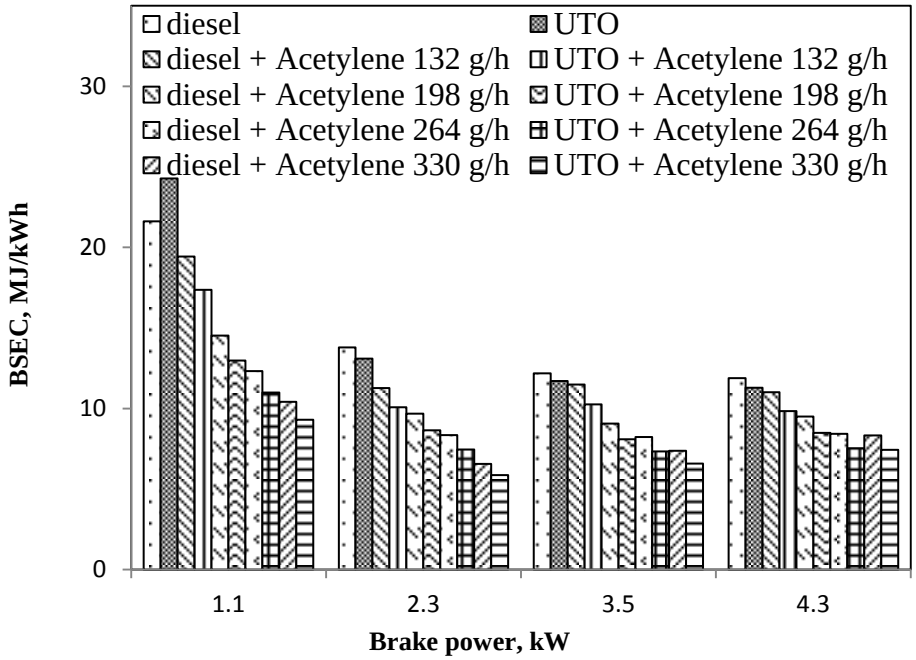

Figure 6.67 Variation of the BSEC with brake power for engine fueled with diesel and UTO on dual fuel mode

6.7.3.2 Exhaust gas temperature

Figure 6.68 illustrates the variation of the exhaust gas temperature with brake power for diesel and the UTO at different acetylene flow rates. diesel exhaust gas temperature is 270^{o}C,

whereas for the UTO, it is 354^{o}C at the maximum brake power. The exhaust gas temperature is 384^{o}C at 132 g/h, 362 ^{o}C at 198 g/h, 333 ^{o}C at 264 g/h and 299^{o}C at 330 g/h of acetylene flow rates, for diesel operation with acetylene, and for the UTO at different acetylene flow rates of 132, 198, 264 and 330 g/h it is 322, 315, 301 and 270^{o}C respectively The decrease in the exhaust gas temperature with increase of acetylene flow rate may be due to the earlier of energy release in the cycle.

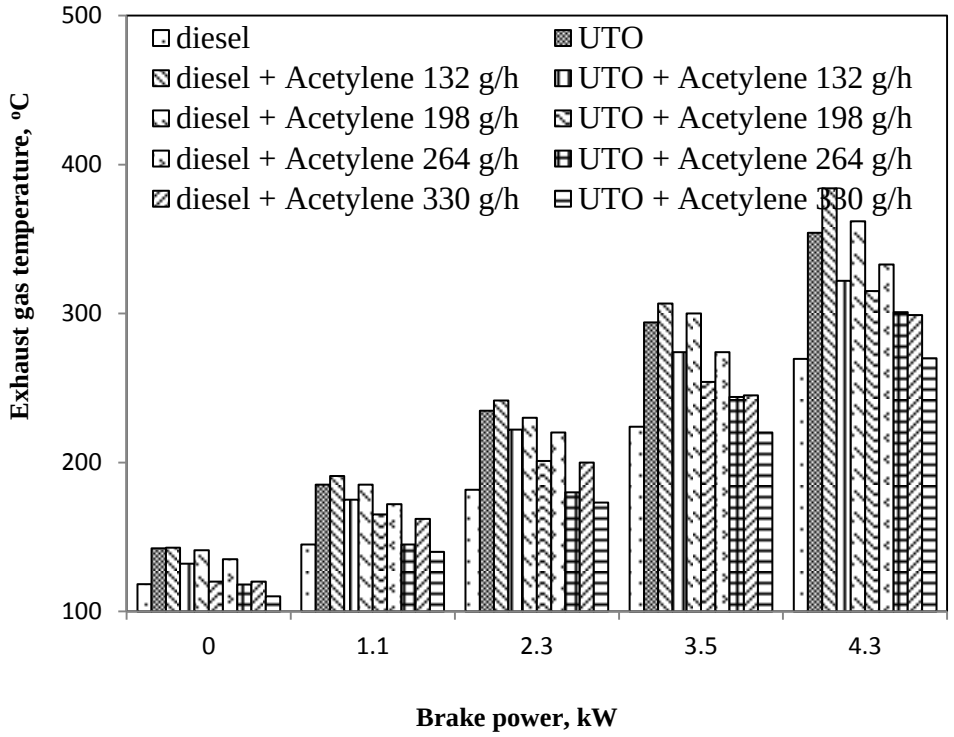

Figure 6.68 Variation of the exhaust gas temperature with brake power for engine fueled with diesel and UTO on dual fuel mode

6.7.4 Emission parameters

6.7.4.1 Nitric oxide

The variation of the NO emission with brake power is depicted in Fig. 6.69. It can be observed that the UTO emits lower NO emission levels as compared to that of diesel. As the brake power increases the combustion gas temperature increases, which in turn, increase the formation of NO emission. In dual fuel operation, with the acetylene induction, the NO emission increases maximum brake power for both diesel and the UTO. The NO emission for diesel and UTO are 6.6 and 5.3 g/kWh respectively at maximum brake power. NO emission for diesel with

132, 198, 264 and 330 g/h acetylene flow rates are 5, 5.8, 6 and 6.1 g/kWh respectively at maximum brake power, whereas for the UTO with 132, 198, 264 and 330 g/h acetylene flow rates shows 5.9, 6.1, 6.2 and 6.5 g/kWh respectively at maximum brake power. This is due to the enhancement of combustion rate, which increases the temperature, and thus increases the NO emission.

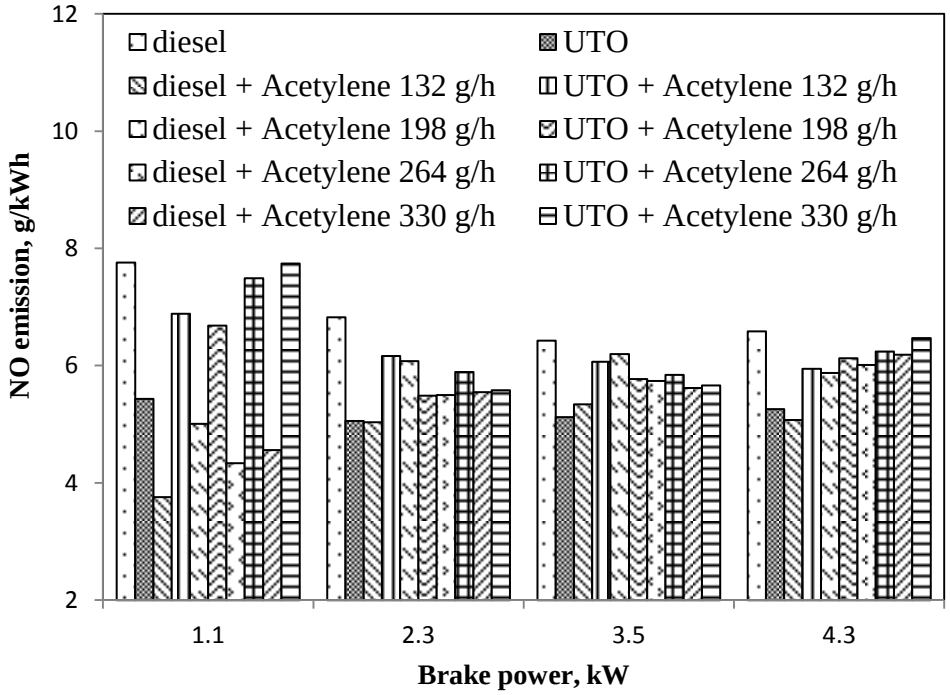

Figure 6.69 Variation of NO emission with brake power for engine fueled with diesel and UTO on dual fuel mode

6.7.4.2 Carbon monoxide emission

CO is present in the exhaust gas is due to unavailability of oxygen for complete combustion process. Higher concentration of the CO emission in the exhaust is a clear indication of incomplete combustion of the pre-mixed mixture. Figure 6.70 shows the CO emission with brake power for diesel and UTO for different acetylene flow rates. CO emission for diesel and diesel with 132, 198, 264 and 330 g/h acetylene flow rates are 0.0022, 0.0021, 0.00215, 0.0021 and 0.002 g/kWh respectively, whereas for the UTO and UTO with 132, 198, 264 and 330 g/h acetylene flow rates gives 0.004, 0.003, 0.0026 and 0.0023 g/kWh respectively at maximum brake power. An observation of the figure shows that CO emissions are lower in dual fuel

operation when compared with sole diesel and the UTO operation. The decrease in the CO emission may be due to operation of dual fuel engine in lean range than the UTO.

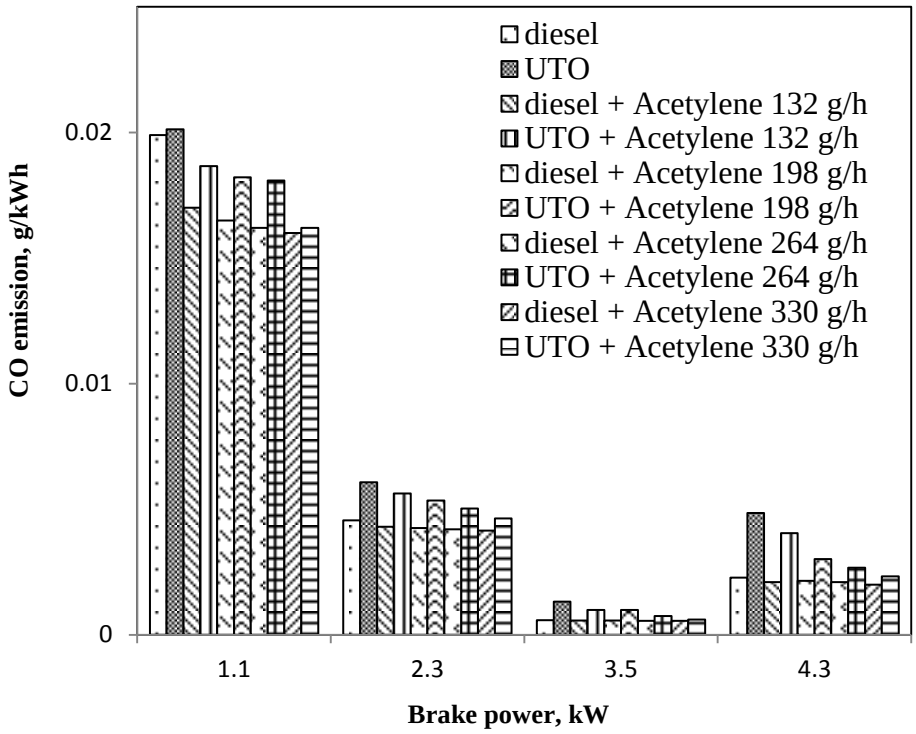

Figure 6.70 Variation of CO emission with brake power for engine fueled with diesel and UTO on dual fuel mode

6.7.4.3 Hydrocarbon emission

Figure 6.71 depicts the variation of HC emissions with brake power with for diesel and UTO for different acetylene flow rates. The HC emission was 0.006 and 0.013 g/kWh with sole diesel and UTO operation at maximum brake power. Since, the viscosity of UTO is found to be higher than diesel the SMD of UTO may be larger than diesel, hence the spray of UTO becomes much coarse than the diesel spray. Due to the poor mixing of UTO with air as a result of this higher viscosity and density the HC emission is high. It is observed from the figure that HC emission in dual fuel mode is always lower than diesel and the UTO operation. The HC emission of diesel with 132, 198, 264 and 330 g/h acetylene flow rates shows 0.005, 0.0049, 0.0046 and 0.0045 g/kWh whereas for UTO with 132, 198, 264 and 330 g/h acetylene flow rates shows the HC emission as 0.011, 0.01, 0.0097 and 0.009 g/kWh respectively at maximum brake power.

The reduction in HC emission in the case of dual fuel mode is due to the higher burning velocity of acetylene and due to the lean operation of the engine.

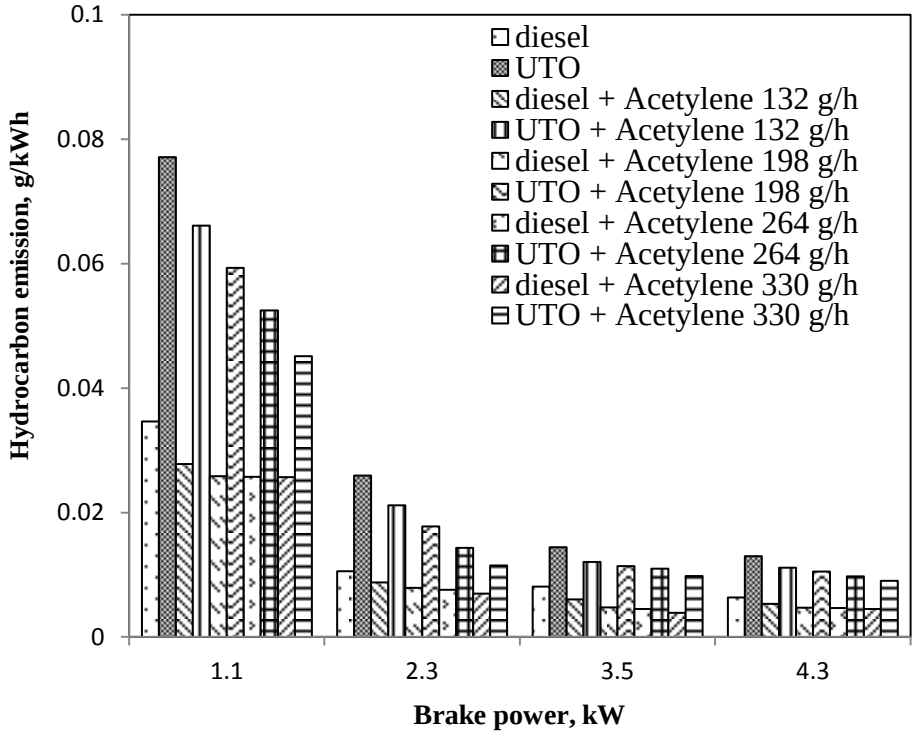

Figure 6.71 Variation of HC emission with brake power for engine fueled with diesel and UTO on dual fuel mode

6.7.4.4 Smoke density

Figure 6.72 depicts the variation of smoke emission with diesel and the UTO for different acetylene flow rates. It can be observed that the smoke emission for the UTO is significantly higher than that of diesel at maximum power. Smoke density of diesel and UTO are 24 and 25.5% respectively at maximum brake power. Smoke density of diesel and UTO with 132, 198, 264 and 330 g/h acetylene flow rates shows 23, 22, 21, 20, 25, 24.3, 24 and 22% respectively at maximum brake power. The UTO with acetylene at different flow rates produces higher smoke, than that of diesel with acetylene at different flow rates. But, as the acetylene gas flow rate increases, the smoke density decreases, for both the primary fuels at maximum brake power. In the dual fuel mode, mixing of acetylene with the primary fuels leads to better combustion, resulting in lower smoke emission.

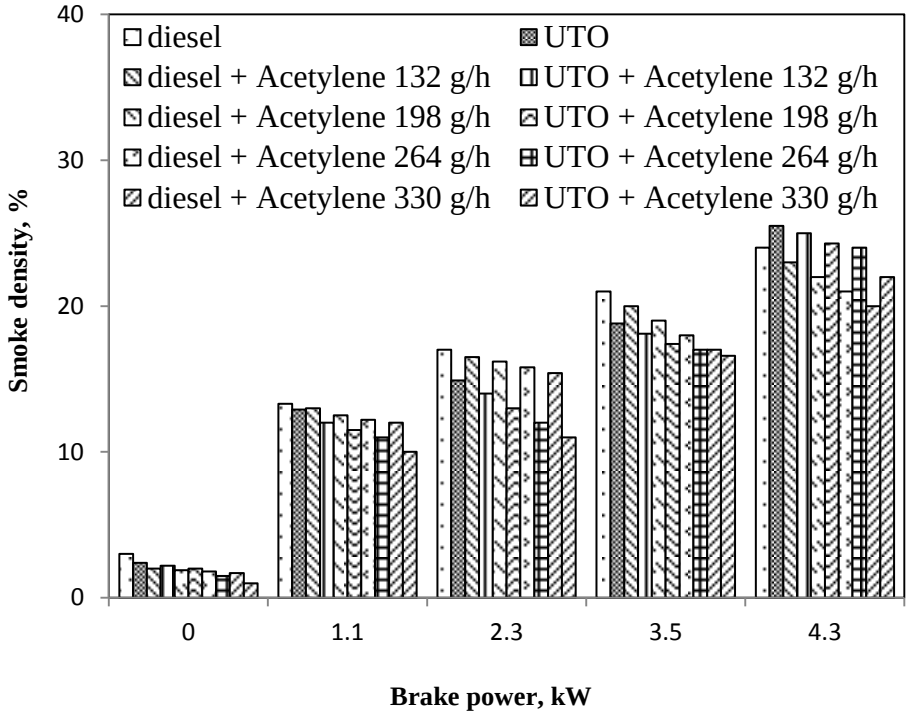

Figure 6.72 Variation of smoke density with brake power for engine fueled with diesel and UTO on dual fuel mode

Table 6.6 and 6.7 give the percentage variation of different parameters for diesel and UTO with acetylene in dual fuel mode with that of diesel.

6.7.5 Closure

The UTO can be as dual fuel mode with acetylene in a CI engine. Reduced smoke, HC and CO emissions, without any deterioration in the engine performance were obtained in a CI engine. It is apparent that acetylene at 330 g/h flow rate with UTO gave a better performance and lower emission then that of UTO, and UTO with other acetylene flow rate in dual fuel operation.

Table 6.6 Percentage variation of different parameters for diesel in dual fuel mode with diesel

Si.No.	**Parameter**	**Diesel + Acetylene 132 g/h**	**Diesel + Acetylene 198 g/h**	**Diesel + Acetylene 264 g/h**	**Diesel + Acetylene 330 g/h**
A Combustion parameters					
1.	Occurrence of ignition	-0.26	-0.62	-1.03	-0.91
2.	Ignition delay	8.61	-9.33	-14.72	-35.36
4.	Combustion duration	-7.57	-11.76	-13.23	-13.72
5.	Maximum heat release	-7.02	-8.60	-4.67	-0.57
6.	Maximum cylinder pressure	0.76	2.39	11.16	11.94
B Performance parameters					
1.	Brake specific energy consumption	-7.22	-20.08	-28.97	-29.84
2.	Exhaust gas temperature	42.49	34.30	23.54	10.92
C Emission parameters					
1.	HC emission	-14.12	-24.41	-25.34	-27.24
2.	CO emission	-6.83	-4.614	-6.83	-11.26
3.	NO emission,	-10.46	3.72	6.11	9.24
4.	Smoke density	-4.16	-8.33	-12.5	-16.66

Table 6.7 Percentage variation of different parameters for the UTO in dual fuel mode with diesel

Si.No.	**Parameter**	**UTO + Acetylene 132 g/h**	**UTO + Acetylene 198 g/h**	**UTO + Acetylene 264 g/h**	**UTO + Acetylene 330 g/h**
A Combustion parameters					
1.	Occurrence of ignition	-0.20	-1.12	-1.43	-0.87
2.	Ignition delay	19.45	3.88	-29.98	-37.16
4.	Combustion duration	-21.56	-24.01	-26.47	-28.92
5.	Maximum heat release	-9.63	-8.95	-6.40	-5.43
6.	Maximum cylinder pressure	0.06	1.56	10.38	11.29
B Performance parameters					
1.	Brake specific energy consumption	-17.21	-28.66	-36.58	-37.42
2.	Exhaust gas temperature	19.46	16.86	11.67	0.17
C Emission parameters					
1.	HC emission	80.67	70.84	58.46	46.60
2.	CO emission	81.54	35.27	19.74	4.48
3.	NO emission	6.09	9.25	11.28	15.42
4.	Smoke density	4.16	1.25	0	-8.33

Table 6.8 (gives in the next page) gives the overall comparison of optimum results obtained in terms of combustion, performance and emission in each technique adopted for the UTO in a single cylinder, four stroke, air cooled DI diesel engine. From the table it is understood that UTO230 bar gives better performance than other techniques adopted for the UTO.

Table 6.8 Overall comparison of UTO at optimum results with diesel obtained in terms of combustion, performance and emission

Si. No.	**Parameter**	**UTO40**	**UTO20 bTDC**	**UTO230 bar**	**18.5:1 CR**	**UTO 110^{o}C**	**UTO + Acetylene 330 g/h**
A Combustion parameters							
1.	Occurrence of ignition	0.46	-0.03	-0.05	-0.87	-0.26	-0.87
2.	Ignition delay	-4.4	-12.02	-12.5	-10.71	-17.41	-37.16
4.	Combustion duration	-14.21	-0.63	-4.98	6.61	-6.37	-28.92
5.	Maximum heat release	-12.35	2.26	1.691	-18.74	-0.58	-5.43
6.	Maximum cylinder pressure	6.17	-8.78	1.53	13.93	11.54	11.29
B Performance parameters							
1.	Brake specific energy consumption	-2.44	-3.53	-6.049	17.68	-40.69	-37.42
2.	Exhaust gas temperature	6.59	11.41	26.88	40.86	5.73	0.17
C Emission parameters							
1.	HC emission	79.7	138.66	20.32	-48.64	42.37	46.60
2.	CO emission	49.31	126.80	-86.01	70.89	70.82	4.48
3.	NO emission	22.41	-27.23	16.55	31.06	-3.07	15.42
4.	Smoke density	-16.25	-5	-7.08	-4.16	2.91	-8.33

CHAPTER 7
CONCLUSIONS

7.1 Conclusions

The combustion, performance and emission characteristics of a single cylinder, four stroke, air-cooled, direct injection diesel engine having a power output of 4.4 kW at a constant speed of 1500 rpm, fueled with UTO using different engine and fuel techniques, were analysed and compared with diesel operation of the same engine. The conclusions of each technique are given below.

7.1.1 UTO and its diesel blend

- The UTO can be used as a fuel in the CI engines as it possesses a heating value. Considering the specific energy consumption, UTO40 can be the optimum blend among the UTO diesel blends tested.
- The ignition delay for the UTO and its diesel blends is shorter by about 1-3^{o}CA compared to that of diesel in the entire range of operation.
- The HC and CO emissions for the UTO and its diesel blends are marginally higher than those of diesel operation at maximum brake power.
- The NO emission is higher by about 25.9% for the UTO and its diesel blends than diesel at maximum brake power.
- Smoke is lower for the UTO and its diesel blends than diesel at maximum brake power. The smoke value of UTO40 is lower by about 5.9% than that of diesel at maximum brake power.

7.1.2 UTO at different injection timings

- The engine was able to run with 100% UTO when the injection timing was advanced and retarded.
- A maximum cylinder pressure is found to occur earlier for advanced injection timing and later for retarded injection timing at maximum brake power.
- The ignition delay increases with advanced injection timing and decreases with retarded injection timing at maximum brake power.

- A retarded injection timing UTO gives a maximum reduction in the NO emission with 18.5 ^{o}CA at maximum brake power by about 2% compared to that of original injection timing for UTO.
- An increased level of smoke by about 10.4% was noticed with 18.5 ^{o}CA while retarding the injection timing with UTO compared to that of original injection timing for UTO.
- Based on the combustion, performance and emission the optimum injection timing is found to be at 20 ^{o}bTDC.

7.1.3 UTO at different nozzle opening pressures

- The UTO can be used as a sole fuel in CI engines as UTO possesses physical properties similar to that of diesel fuel, but the engine has to be operated with optimum injection timing and nozzle opening pressure, since it has higher viscosity and density than that of diesel.
- The ignition delays of UTO230 bar is lower by about 3% than that of UTO200 bar and lower by about 14.2% than that of diesel at maximum brake power.
- The maximum cylinder pressure of UTO230 bar is higher by about 6% than that of UTO200 bar and lower by about 1.5% than that of diesel at maximum brake power.
- The maximum heat release rate of UTO230 bar is higher by about 3.9% than that of UTO200 bar and lower by about 1.6% than that of diesel at maximum brake power.
- The brake specific energy consumption of UTO230 bar is lower by about 4.4% than that of UTO200 bar and lower by about 6.4% than that of diesel at maximum brake power.
- The exhaust gas temperature of UTO230 bar is lower by about 3.4% than that of UTO200 bar and higher by about 26.8% than that of diesel at maximum brake power.

- The NO emission of UTO230 bar is higher by about 1.75% and 29.7% than that of UTO200 bar and diesel respectively at maximum brake power.
- The smoke emission of UTO230 bar is lower by about 7.8% and 8.92% than that of UTO200 bar and diesel respectively at maximum brake power.
- It is suggested that UTO at 230 bar is the optimum injection nozzle opening pressure among the tested nozzle opening pressures.

7.1.4 UTO at different compression ratios

- UTO can be used in variable compression ratio engines.
- The ignition delay is found to be lower with higher compression ratio.
- The increase in heat release rate and the peak pressure increase in the compression ratio.
- The HC and CO emissions for the all compression ratio of the UTO are marginally lower than those of diesel operation at maximum brake power.
- The NO emission is optimum at compression ratio 18.5 for the UTO fuel than that of diesel at maximum brake power.
- The smoke value of UTO is lower at compression ratio 18.5 than that of diesel at maximum brake power.

7.1.5 UTO at different preheating temperatures

- The ignition delay is shorter with the UTO as compared to diesel at maximum brake power. With fuel preheating there is further decrease in the ignition delay in comparison to the UTO.
- UTO results in increased exhaust temperature compared to that of diesel at maximum power output. It increases further with fuel preheating. Lowest exhaust gas temperature is found with the UTO at 110^{o}C.
- The smoke density is higher with the UTO as compared to diesel at maximum brake power. It decreases with fuel preheating.

- The hydrocarbon emissions and carbon monoxide emissions are higher with the UTO as compared to diesel. However, fuel preheating reduces these emissions.
- Higher levels of NO emissions are found with the UTO at 80 and 90^{o}C preheating temperature.

7.1.6 UTO on dual fuel mode

- The ignition delay is found to be shorter with the UTO operation as compared to that of diesel at maximum brake power, whereas for dual fuel, there is a decrease in the ignition delay in comparison to sole diesel and the UTO.
- The UTO results in a higher exhaust temperature compared to that of diesel at maximum brake power. It is reduced in the dual fuel mode by about 23.7% for the UTO at maximum brake power.
- The NO emissions are found to increase by about 9 % and 23 % with sole diesel and the UTO operation with acetylene at different flow rates.
- The smoke density is higher with the UTO as compared to diesel at maximum brake power. Smoke density decreases by 20.8 and 13.7% for diesel and UTO respectively at maximum brake power.

7.2 Scope for future work

The following are suggested as future work for the investigations on the use of UTO.

- Durability test is to be done for checking the longevity of the engine fueled with UTO
- A detailed CFD analysis for reactive conditions needs to be undertaken for greater understanding and explanation of the results.
- Mathematical modeling is suggested for supporting the results theoretically.
- The UTO can be tested in an automotive engine and in gensets.
- Adopting emission control techniques to bring the emission results closer to that of diesel operation.

Appendix A1

Specification of the test engine

Description	Unit	Data
Name of the engine manufacturer	-	Kirolaskar oil engines Ltd.
Type of engine	-	Vertical, 4-stroke cycle, single acting, totally enclosed, high speed compression ignition diesel engine
Number of cylinders	-	1
Power output rating at 1500 rpm	kW	4.41
Bore	mm	87.5
Stroke	mm	110
Cubic capacity	litres	0.662
Compression ratio		17.5:1
Injection timing	^{o}CA	23
Inlet valve opens bTDC	^{o}CA	4.5
Inlet valve closes aTDC	^{o}CA	35.5
Exhaust valve opens bBDC	^{o}CA	35.5
Exhaust valve opens aTDC	^{o}CA	4.5
Weight	kg	163
Method of cooling		Air cooled with radial fan
Type of fuel injection		Pump-line-nozzle injection system
Nozzle type		Multi hole
No. of holes		3
Connecting rod length	mm	220

Appendix A2

Specifications of the AVL five gas analyzer

Measured quality	**Measuring range**	**Accuracy**
CO	0-10%	<0.6% vol: ±0.03% vol ≥0.6% vol: ±5% of ind. Val.
CO_2	0-20%	<10% vol: ±0.05% vol ≥10% vol: ±5% vol
HC	0-20000ppm vol	<200 ppm vol: ±10 ppm vol ≥200 ppm vol: ±5% of ind. Val.
O_2	0-22% vol	<2% vol: ±0.01% vol ≥2% vol: ±5% vol
NO	0-5000 ppm vol	<500 ppm vol: ±50 ppm vol ≥500 ppm vol: ±10% of ind. Val.
Voltage	11-22 V DC	
Power concumption	≈25W	
Warm up time	≈7 min	
Operating temperature	5-45^{o}C	
Dimension(W*D*H)	270x320x85	
Weight	4.5 Kg net weight without accessories.	

Appendix A3

Specifications of theAVL 437 diesel smoke meter

Description	Data
Measuring chamber	0-100% opacity
Accuracy and repeatability	±1% of full scale
Alarming signal temperature	Lights up when temperature of measuring chamber is below 70^{o}C.
Linearity check	48.4%-53.1%/1.54m^{-1}-1.76m^{-1} of measurement range
Measuring chamber length	430±5 mm
Measuring chamber heating	Thermostatically cotrolled
Light source	Halogen lamp, 12V
Sensor	Selenium Photocell
Weight	24 kg

Appendix A4

Specification of the pressure transducer

Description	Type	Data
Kistler		
Pressure range		0-100 bar
transducer	Piezoelectric	
Cooling	Air Cooled	
Sensitivity (±0,5%)		25 mV/bar

Appendix A5

Heat release analysis

The details about combustion stages and events can be determined by analyzing heat release rates as determined from cylinder pressure measurements. Analysis of heat release can help to study the combustion behaviour of the engine. The analysis for the heat release rate is based on the application of first law of thermodynamics for an open system. It is assumed that cylinder contents are homogeneous mixture of air and combustion products and are at uniform temperature and pressure during the combustion process. The first law for such system can be written as

$$\frac{dU}{dt} = \dot{Q} - \dot{W} \qquad \text{(A5.1)}$$

Where,

U=Change in internal energy of the system

$\dot{Q}$= the combination of the heat release rate and the heat transfer rate across the cylinder wall,

$\dot{W}$ = the rate of work done by the system due to system boundary displacement.

Change in internal energy can be written as,

$$mC_v \frac{dT}{dt} = \dot{Q} - P\frac{dv}{dt} \qquad \text{(A5.2)}$$

To simplify the equation (A5.2) the ideal gas assumption can be used.

$$PV = mRT \qquad \text{(A5.3)}$$

Where; P=Pressure

V=Volume

T=Temperature

R=Gas constant

Equation (A5.3) can be differentiated (assuming constant mass)

$$\frac{dT}{dt} = \frac{1}{mR}\left[P\frac{dV}{dt} + V\frac{dP}{dt}\right] \qquad \text{(A5.4)}$$

After combining these the equations A5.2 and A5.3, the heat release equation becomes

$$\dot{Q} = \left[\frac{Cv}{R} + 1\right] P\frac{dV}{dt} + \frac{Cv}{R} V\frac{dP}{dt} \qquad \text{(A5.5)}$$

Where; Cv=Specific heat at constant volume

M=Mass

After replacing time (t) with the crank angle (h), the equation becomes

$$\dot{Q} = \frac{\lambda}{\lambda-1} P \frac{dV}{d\theta} + \frac{1}{\lambda-1} V \frac{dP}{d\theta} \qquad \text{(A5.6)}$$

where θ=Crank angle in degrees; λ=Ratio of specific heats of the fuel and air. For diesel heat release analysis λ is 1.35 [107].

This relation makes it possible to calculate the heat release rate. All the quantities on the right hand side are known or can be easily derived once the pressure time history is recorded.

Appendix A6

The calculated cetane index is determined from the following equation:

Cetane index =-420.34 + 0.016 G_2 + 0.192 G log M
+ 65.01 $(\log M)_2$- 0.0001809 M_2. (1) (A6.1)

G = API Degrees @ 60 ^oF
M = D86 Temperature @ 50% volume, in ^oF

Energy share of acetylene

Acetylene mass share =$m_{A2}/(m_{A2} + m_f)$; (A6.2)

where m_{A2} is the mass flow rate of Acetylene that is inducted along with air, $m_f$the mass flow rate of liquid fuel, i.e. UTO or petroleum diesel that is injected as the pilotfuel.

BSEC= (Brake specific fuel consumption x calorific value)/1000 (A6.3)

Percentage to g/kWh

HC emissions in g/kWh

HC (g/kWh) =[$(m_f+m_a)/(29*1000)$ * HC (in ppm)*13/BP] (A6.4)

CO emissions in g/kWh

CO (g/kWh) =[$((m_f+m_a)/29)*10$ * CO (in %vol)*28/BP] (A6.5)

NO emissions in g/kWh

NO (g/kWh) =[$(m_f+m_a)/(29*1000)$ * NO (in ppm)*32.4/BP] (A6.6)

Annexure A7

Range, accuracy and percentage of each instrument

Instrument	**Measurement**	**Range**	**Accuracy**	**Uncertainty, %**
Load cell	Loading device	250-6000W	± 1W	0.2
Temperature indicator	Exhaust gas measurement	0–900	±1 ^{o}C	0.15
Burette	Fuel consumption	1–30cc	±0.2 cc	1.5
Speed sensor	Speed	0–10000 rpm	± 10rpm	± 1
Exhaust gas analyser	NO emission	NO 0–5000 ppm	±50ppm	1
	HC	HC 0–20000ppm	±10ppm	0.5
	CO	CO 0–10%	0.03%	1
Smoke meter	Smoke density	0–100 %		
Pressure transducer	Cylinder pressure	0–110bar	±1bar	0.15
Crank angle encoder	Crank angle		±1	1

Appendix A8

Uncertainty analysis

The total percentage of the uncertainty of this experiment is calculated as given below:

Total percentage of uncertainty of this experiment = [$[(m_f)^2$ + $(BP)^2$ + $(BSFC)^2$ + $(\text{brake thermal efficiency})^2$ + $(CO)^2$ + $(CO_2)^2$ + $(HC)^2$ + $(NO)^2$ + $(O_2)^2$ + $(\text{smoke number})^2$ + $(EGT)^2$ + $(\text{uncertainty of pressure pick up})^2$ + $(\text{crank angle encoder})^2]^{1/2}$

(A8.1)

Total percentage of uncertainty = $[\{(1.5)^2 + (0.2)^2 + (1.5)^2 + (1)^2 + (0.03)^2 + (0.5)^2 + (1)^2 + (1)^2 + (1)^2 + (1)^2 + (0.15)^2 + (1)^2]^{1/2}$ (A8.2)

Total percentage of uncertainty = ± 3.28 % (A8.3)

Appendix A9

Mechanism of NO formation

The thermal NO is formed at high temperatures under slightly lean conditions with the burned products. The involved nitrogen and oxygen stem from the combustion air. NO is formed during the post flame combustion process in a high temperature region. The most widely accepted mechanism was suggested by Zeldovich[131]. The principal source of NO formation is the oxidation of the nitrogen present in atmospheric air. The nitric oxide formation chain reactions are initiated by atomic oxygen which forms from the dissociation of oxygen molecules at the high temperature reached during the combustion process:

$$O + N_2 = NO + N \quad \text{(A9.1)}$$

$$N + O_2 = NO + O \quad \text{(A9.2)}$$

$$N + OH = NO + H \quad \text{(A9.3)}$$

The initial NO formation rate (KmoL m^{-3} sec) is given as:

$$\frac{d[NO]}{dt} = \frac{6\times10^{16}}{10^{0.5}} \exp\left(\frac{-69090}{T}\right)[O_2]_{0.5}^{e}[N_2]_e \quad \text{(A9.4)}$$

NO formation is strong dependent on temperature and oxygen concentration during the combustion phase. Chemical equilibrium consideration indicates that for burnt gases at typical flame temperatures, NO_2/NO ratios should be negligible small.
Maximum amount of nitrogen is generated in the temperature range of 2500-3000 K.

REFERENCES

[1] www.Wikipidea.com/wiki/history of the automobiles.

[2] World energy outlook. International Energy Agency. 2012.

[3] BP Stastical review of World Energy. 2012.

[4] www.eia.gov.aer. Annual Energy Review 2011.

[5] Environmental and Energy Sustainability: An approach for India, Executive Summary. 2011.

[6] Dedobert P. Automobiles and pollution, Editions Technip, 1995.

[7] Ganesan V. Internal combustion engines, Tata Mcgraw-hill publishing company limited, 2003.

[8] Basel convention technical guidelines on used oil re-refining or other re-uses of previously used oil CCME, 1995.

[9] CCME. Code of practice for used oil management in Canada. The Canadian council of ministers of the environment. 1989.

[10] John E. Dec. Advanced compression-ignition engines understanding the in-cylinder processes. Proceedings of the combustion institute. 2009; 32: 2727-2742.

[11] Stuart HA. Engine operated by the explosion of mixtures of Gas or Hydrocarbon Vapor and Air.1893.

[12] Diesel Rodolf, Diesel engine, Patent number: 542846, 1895.

[13] Rao PV, Experimental investigations on the influence of properties of jatropha biodiesel on performance, combustion, and emission characteristics of a DI-CI Engine. World academy of science engineering and technology. 201; 51.

[14] www.epa.gov.in.

[15] Knothe Gerhard. Biodiesel and renewable diesel: A comparison progress in energy and combustion science. 2010; 36: 364-373.

[16] www.eagle.org, Notes on heavy fuel oil, 1984.

[17] Reddy PC. Studies on droplet size measurement and engine performance using non-edible oils as alternate fules. Proceedings of XVII national conference on I.C engines & combustion. December. 2001; 18-20.

[18] Alptekin E, Canakci M. Characterization of the key fuel properties of methyl ester-diesel fuel blends. Fuel. 2009; 88: 75–80.

[19] Scheepers and Bos RP. Combustoin of diesel fuel from a toxicological perspective. Toxicology department, University of Nijmegen. 1992; 64: 149-161.

[20] Akasaka Y and Sakurai Y. Effects of fuel properties on exhaust emission from DI diesel engine. International Conference on Fluid Engineering. 1998; 41: 13-18.

[21] Hossian AK. Plant oils as fuels for compression ignition engines: A technical review and life-cycle analysis. Renewable Energy. 2010; 35: 1–13.

[22] Hiroyasu H. and Kadota T. Fuel droplet size distribution in diesel combustion chamber. SAE Paper. 740715. 1974.

[23] Arai M, Shimizu M and Hiroyasu H. Break-Up Length and Spray Angle of High Speed Jet, ICLASS. 1985; 85.

[24] Tabata M, Fujii H, Arai M. and Hiroyasu H. Mean drop diameter of a diesel spray in a vaporizing process. JSME International Journal. 1991; 34: 369-378.

[25] Geo EV, Nagarajana G. and Nagalingam B. Studies on dual fuel operation of rubber seed oil and its bio-diesel with hydrogen as the inducted fuel. International journal of hydrogen energy. 2008; 33: 6357-6367.

[26] Geo EV, Nagarajana G and Nagalingam B. Experimental investigations to improve the performance of rubber seed oil fueled diesel engine by dual fuelling with hydrogen. International Journal of Green Energy. 2009; 6: 343-358.

[27] Saravanan N and Nagarajan G. Performance and emission study in manifold hydrogen injection with diesel as an ignition source for different start of injection. Renewable Energy. 2009; 34: 328-334.

[28] Saravanan N and Nagarajan G. Performance and emission studies on port injection of hydrogen with varied flow rates with Diesel as an ignition source. Applied Energy. 2010; 87: 2218-2229.

[29] Lakshmanan T and Nagarajan G. Performance and Emission of Acetylene-Aspirated Diesel Engine, Jordan Journal of Mechanical and Industrial Engineering. 2009; 3: 125-130.

[30] Lakshmanan T and Nagarajan G. Experimental investigation on dual fuel operation of acetylene in a DI diesel engine. Fuel processing technology 2010; 91: 496-503.

[31] Lakshmanan T and Nagarajan G. Experimental investigation of timed manifold injection of acetylene in direct injection diesel engine in dual fuel mode, Energy. 2010; 35: 3172-3178.

[32] Lakshmanan T and Nagarajan G. Experimental investigation of port injection of acetylene in DI diesel engine in dual fuel mode. Fuel. 2011; 90: 2571-2577.

[33] Sharma PK, Harihar K, Praveen S and Suman P. Use of acetylene as an alternative fuel in IC engine. Rentech symposium compendium. 2012; 1.

[34] Tira HS, Herreros JM, Tsolakis A and Wyszynski ML. Characteristics of LPG-diesel dual fuelled engine operated with rapeseed methyl ester and gas-to-liquid diesel fuels. Energy. 2012; 47: 620-629.

[35] Chandra R, Vijay VK, Subbarao PMV, and Khura TK. Performance evaluation of a constant speed IC engine on CNG, methane enriched biogas and biogas. Applied Energy. 2011; 88: 3969-3977.

[36] Yoona Seung, Hyun Lee and Chang Sik. Experimental investigation on the combustion and exhaust emission characteristics of biogas-biodiesel dual-fuel combustion in a CI engine. Fuel processing technology. 201; 92: 992-1000.

[37] Deshmukh Samir J, Bhuyar Lalit B and Thakre Shashank B. Investigation on performance and emission characteristics of ci engine fuelled with producer gas and esters of hingan (balanites) oil in dual fuel mode. International journal of aerospace and mechanical engineering. 2008; 2.3: 148-153.

[38] Agarwal Deepak, Kumar Lokesh, Agarwal and Avinash Kumar. Performance evaluation of a vegetable oil fuelled compression ignition engine. Renewable energy. 2008; 33: 1147-1156.

[39] Labeckas Gvidonas and Slavinskas Stasys. Performance of direct-injection of road diesel engine on rapeseed oil. Renewable energy. 2006; 31: 849-863.

[40] Hanbey Hazar and Huseyin Aydin. Performance and emission evaluation of a CI engine fueled with preheated raw rapeseed oil (RRO)-diesel blends. Applied energy. 2010; 87: 786-790.

[41] Nwafor OMI. Emission characteristics of diesel engine operating on rapeseed methyl ester. Renewable energy. 2004; 29: 119-129.

[42] Devana PK and Mahalakshmi NV. Study of the performance, emission and combustion characteristics of a diesel engine using poon oil-based fuels. Fuel processing technology. 2009; 90: 513-519.

[43] Acharya SK, Mohanty MK and Swain RK. Kusum oil as a fuel for small horse power diesel engine. International journal of engineering and technology. 2009; 1: 1793-8236.

[44] Demirbas Ayhan. Biofuels securing the planet's future energy needs. Energy conversion and management. 2009; 50: 2239-2249.

[45] Demirbas Ayhan. Importance of biodiesel as transportation fuel. Energy policy. 2007; 35: 4661-4670.

[46] Singh S.P and Singh Dipti. Biodiesel production through the use of different sources and characterizationof oils and their esters as the substitute of diesel: A review. Renewable and sustainable energy reviews. 2010; 14: 200-216.

[47] Ismet Celiktena, Atilla Kocaa and Mehmet Ali Arslanb. Comparison of performance and emissions of diesel fuel, rapeseed andsoybean oil methyl esters injected at different pressures, Renewable energy. 2010; 35: 814-820.

[48] Ramadhas AS, Muraleedharan C and Jayara SJ. Performance and emission evaluation of a diesel engine fueled with methyl esters of rubber seed oil. Renewable energy. 2005; 30: 1789-1800.

[49] Baiju B, Naik MK and Das LM. A comparative evaluation of compression ignition engine characteristics using methyl and ethyl esters of karanja oil. Renewable energy. 2009; 34: 1616-1621.

[50] Cheung CS, Zhu Lei and Huang Zhen. Regulated and unregulated emissions from a diesel engine fueled withbiodiesel and biodiesel blended with methanol. Atmospheric environment. 2009; 43: 4865-4872.

[51] Yu PC, Hsien YH, Hang LC and Mei CS, Effects of the biodiesel blend fuel on aldehyde emissions from diesel engine exhaust. Atmospheric environment. 2008; 42: 906-915.

[52] Agarwala Deepak, Kumar Lokesh and Agarwal Avinash Kumar. Performance evaluation of a vegetable oil fuelled compression ignition engine. Renewable energy. 2008; 33: 1147-1156.

[53] Raheman H and Ghadge SV. Performance of compression ignition engine with mahua (Madhucaindica) biodiesel. Fuel. 2007; 86: 2568-2573.

[54] Math MC. Investigation of fuel properties of restaurant waste oil methyl esters and their blends with diesel to assess their usefulness as compression ignition engine fuel. Energy for sustainable development. 2007; 9.

[55] Nabi Nurun Md, Hoque SM. Najmul, Akhter Md. and Shamim. Karanja (Pongamia Pinnata) biodiesel production in Bangladesh, characterization of karanja biodiesel and its effect on diesel emissions. Fuel processing technology. 2009; 90: 1080-1086.

[56] Karabektas Murat, Ergen Gokhan and Murat Hosoz. The effects of preheated cottonseed oil methyl ester on theperformance and exhaust emissions of a diesel engine. Applied thermal engineering. 2008; 28: 2136-2143.

[57] Banapurmatha NR, Tewaria PG and Hosmath RS. Performance and emission characteristics of a DI compression ignition engine operated on honge, jatropha and sesame oil methyl esters. Renewable energy. 2008; 33: 1982-1988.

[58] Devan PK and Mahalakshmi NV. A study of the performance, emission and combustion characteristics of a compression ignition engine using methyl esterof paradise oil–eucalyptus oil blend. Applied Energy. 2009; 86: 675-680.

[59] Devan PK and Mahalakshmi NV. Utilization of unattended methyl ester of paradise oil as fuel in diesel engine. Fuel. 2009; 88: 1828-1833.

[60] Sahoo PK, Das LM, Babu MKG and Naik SN. Biodiesel development from high acid value polanga seed oil and performance evaluation in a CI engine. Fuel. 2007; 86: 448-454.

[61] Sahoo PK and Das LM. Combustion analysis of jatropha, karanja and polanga based biodiesel as fuel in a diesel engine. Fuel. 2009; 88: 994-999.

[62] Srivastava PK and Verma M. Methyl ester of karanja oil as an alternative renewable source energy. Fuel. 2008; 87: 1673-1677.

[63] Jindal S, Nandwana BP, Rathore NS and Vashistha V. Experimental investigation of the effect of compression ratio and injection pressure in a direct injection diesel engine running on Jatropha methyl ester. Applied thermal engineering. 2010; 30: 442-448.

[64] Saravanan S, Nagarajan G, Lakshmi G, Narayana Rao and S. Sampath. Combustion characteristics of a stationary diesel engine fuelled with a blend of crude rice bran oil methyl ester and diesel. Energy. 2010; 35: 94-100.

[65] Deshmukh SJ and Bhuyar LB. Transesterified hingan (balanites) oil as a fuel for compression ignition engines. Biomass and bioenergy. 2009; 33: 108–112.

[66] Raheman H and Ghadge SV. Performance of compression ignition engine with mahua (madhuca indica) biodiesel. Fuel. 2007; 86: 2568–2573.

[67] Edgar PP, Joao A. Carvalho Jr, Luiz R. Carrocci1, Ely V. Cortez and Marco Ferreira A. Comparative study between diesel fuel and hydrated ethanol in direct burning. Proceedings of the european combustion meeting. 2009; 1-6.

[68] Wang LJ, Song RZ, Zou HB, Liu SH and Zhou LB. Study on combustion characteristics of a methanol diesel dual-fuel compression ignition engine. Proceedings of the institution of mechanical engineers, Part D: Journal of automobile engineering. 2008; 222: 619-627.

[69] Kowalewicz Andrzej and Pajączek Zbigniew. Dual fuel engine fuelled with ethanol and diesel fuel. Journal of kones internal combustion engines. 2003; 10: 1-2.

[70] Rai G.D, Non conventional energy source, Standard publishers distributors.

[71] David Chiaramonti, Oasmaa Anja and Yrjo Solantausta. Power generation using fast pyrolysis liquids from biomass. Renewable and sustainable energy reviews. 2007; 11: 1056-1086.

[72] Zhang Qi, Chang Jie, Wang Tiejun and Xu Ying. Review of biomass pyrolysis oil properties and upgrading research. Energy conversion and management 2007; 48: 87-92.

[73] Czernik S and Bridgwater AV. Overview of applications of biomass fast pyrolysis oil. Energy & fuels. 2004; 18: 590-598.

[74] Shihadeh Alan and Hochgreb Simone. Diesel engine combustion of biomass pyrolysis Oils. Energy & fuels. 2000; 14: 260-274.

[75] Evans RJ and Milne TA. Molecular characterization of the pyrolysis of biomass fundamentals. Energy Fuels. 1987; 1: 123-137.

[76] Murugan S, Ramaswamy MC and Nagarajan G. The use of tyre pyrolysis oil in diesel engines. Waste Management. 2008; 28: 2743-2749.

[77] Murugan S, Ramaswamy MC and Nagarajan G. Performance, emission and combustion studies of a DI diesel engine using distilled tyre pyrolysis oil-diesel blends. Fuel Processing Technology. 2008; 89: 152-159.

[78] Murugan S, Ramaswamy MC and Nagarajan G. A comparative study on the performance, emission and combustion studies of a di diesel engine using distilled tyre pyrolysis oil–diesel blends. Fuel. 2008; 87: 2111–2121.

[79] Hariharan S, Murugan S. and Nagarajan G., Effect of diethyl ether on tyre pyrolysis oil fueled diesel engine. Fuel. 2013; 104: 109–115.

[80] Dogana O, Celik MB and Ozdalyan B. The effect of tire derived fuel/diesel fuel blends utilization on diesel engine performance and emissions. Fuel. 2012; 95: 340-346.

[81] Arpa O, Yumrutas R and Argunhan Z. Experimental investigation of the effects of diesel-like fuel obtained from waste lubrication oil on engine performance and exhaust emission. Fuel processing technology. 2010; 91: 1241-1249.

[82] Tajima H, Takasaki K, Nakashima M, Yanagi J, Takaishi T, Ishida H, Osafune S and Iwamoto K. Combustion of used lubricating oil in a diesel engine. SAE. 2001: paper no. 2001-01-1930.

[83] Mani M and Nagarajan G. Influence of injection timing on performance, emission and combustion characteristics of a di diesel engine running on waste plastic oil. Energy. 2009; 34: 1617-1623.

[84] Mani M, Subash C and Nagarajan G. Performance, emission and combustion characteristics of a di diesel engine using waste plastic oil. Applied thermal engineering. 2009; 29: 2738-2744.

[85] Abeysundara DC, Weerakoon C, Lucas JR, Gunatunga KAI and Obadage KC. Coconut oil as an alternative to transformer oil, ERU Symposium. 2001; 1-11.

[86] Moulai H, Khelfane I, Yahiat A, Toudja T, Nacer A, Zemirli MM and Doussas F. Physico-chemical properties of power transformer oil mixtures, Mediterranean Electro technical Conference, 2010; 978-1-4244-5793-9: 1105-1110.

[87] Abou HH, Naga EI, Anis A. Salem AE and Boghdady YM. Production of a transformer oil from paraffinic base stocks. Lubrication science. 1997; 10: 77-89.

[88] Gayara El, Gohara GA, Ibrahima AM, Ibrahimb HM and Alyc AM. Transformer oils prepared from the vacuum distillates of egyptian crude paraffinic petroleum. Fuel processing technology. 2008; 89: 254-261.

[89] Krawiec Steve and Petro-Canada, Production of corrosive sulphur free transformer fluids, International symposium on electrical insulation, 2008; 978-1-4244-2091-9: 174-177.

[90] Krawiec Steve and Petro-Canada, Review of recent changes to mineral insulating oil specifications. Electrical insulation conference. 2009; 978-1-4244-3915-7: 363-367.

[91] Abdi S, Boubakeur A and Haddad A. Influence of thermal ageing on transformer oil properties. International conference on dielectric. 2011; ISBN 978-1-4244-1585-4: 1-4.

[92] Mak J, Sokolov V, Bassetto A, Oommen TV, Haupert T and Hanson D. Transformer fluid a power full tool for life management of aging transformer population ZTZ service.

[93] http://www.astm.org

[94] Replacements, Bureau of Reclamation and Western Area Power Administration. 1995.

[95] www.technoworld.in.

[96] Altn Recep, Cetinkaya Selim and Serdar HY. The potential of using vegetable oil fuels as fuel for diesel engines. Energy Conversion and Management. 2001; 42: 529-538.

[97] Shao J and Yan Y. Measurement of Diesel Spray Characteristics. IEEE Trans. Instrumentation and Measurements. 2008; 57: 2067-2073.

[98] Babaji Mopoulos A, Lavoie G A and Assanis DN. HCCI combustion with high levels of residual gas fraction. SAE. 2003.

[99] Lefebvre AH. Atomization and Sprays. Hemisphere, USA, 1998.

[100] Reddy C Prabhakar. Studies on water diesel emulsion-Ph.D Thesis Regional Engineering College Warangal. 1994.

[101] Mark C Sellnau, Frederic A. Matekunas, Paul A. Battiston and Chen-Fang Chang, David R. Lancaster. Cylinder pressure based engine control using pressure ratio management and low cost non-intrusive cylinder pressure sensors. SAE. 2000; Paper number: 2000-01-0932.

[102] Bari S, Yu CW, Lim TH. Effect of fuel injection timing with waste cooking oil as a fuel in a direct injection diesel engine. Proceedings of the institution of mechanical engineers Part D Journal of automobile engineering. 2004: 218: 93-104.

[103] Martyn Roberts, Benefits and challenges of variable compression ratio (VCR), Paper Number 03P-227, SAE 2002.

[104] Chauhan BC, Kumar N, Jun YD and Lee KB. Performance and emission study of preheated jatropha oil on medium capacity diesel engine. Energy. 2010; 35: 2484-2492.

[105] Holman JP. Experimental techniques. Tata McGraw Hill Publications. 2003.

[106] Rao G Lakshmi Narayana, Sampath S and Rajagopal K. Experimental studies on the combustion and emission characteristics of a diesel engine fuelled with used cooking oil methyl ester and its diesel blends. International journal of engineering and applied sciences. 2008; 4: 64-70.

[107] Heywood JB. Internal combustion engine fundamental. McGraw Hill Publications. 1988; 491-667.

[108] Kumar MS, Ramesh A, and Nagalingam B. Investigation on the use of jatropha oil and its methyl ester as a fuel in a diesel engine. Journal of the institute of energy. 2001; 74: 24-28.

[109] Agarwal D and Agarwal AK. Performance and emissions characteristics of Jatropha oil (preheated and blends) in a direct injection compression ignition engine. Applied Thermal Engineering. 2007; 27:2314-23.

[110] Pundir BP. Engine emissions–pollutant formation and advancement in control technology. Narosa publications; 2007.

[111] Fredi Jacob. Weidmann ACTI Inc.

[112] Ryan, T.W. and Bagby, M.O. Identification of chemical changes occurring during the transient injection of selected vegetable oils. SAE paper 1993; 930-933.

[113] Caresana F. Impact of biodiesel bulk modulus on injection pressure and injection timing. The effect of residual pressure. Fuel. 2011;90**:** 477-485

[114] Seppo AN, Tommi PJP and Mika JL. Effect of injection timing, EGR and EGR cooling on the exhaust particle number and size distribution of an off-road diesel engine. SAE. 1998; Paper No. 2004-01-1988.

[115] Gumus MA. A comprehensive experimental investigation of combustion and heat release characteristics of a biodiesel (hazelnut kernel oil methyl ester) fueled direct injection compression ignition engine. Fuel. 2010; 89: 2802-2814.

[116] Gumus M, Sayin C and Canakci M. Effect of fuel injection timing on the injection, combustion, and performance characteristics of a direct-injection (DI) diesel engine fueled with canola oil methyl esterifies diesel fuel blends. Energy fuels. 2010; 24: 3199-3213.

[117] Bari S, Yu CW and Lim TH. Effect of fuel injection timing with waste cooking oil as a fuel in a direct injection diesel engine. Proceedings of the institution of mechanical engineers Part D Journal of automobile engineering 2004; 218: 93-104.

[118] Kannan GR, and Anand R. Experimental evaluation of DI diesel engine operating with diestrol at varying injection pressure and injection timing. Fuel Processing Technology. 2011; 92: 2252-2263.

[119] Venkatraman M and Devaradjane G. Effect of compression ratio, injection timing and injection pressure on a DI diesel engine for better performance and emission fuelled with diesel biodiesel blend. International journal of applied engineering research. 2010; 1.

[120] Sequera AJ, Parthasarathy RN and Gollahalli SR. Effects of fuel injection timing in the combustion of biofuels in a diesel engine at partial loads. Journal of energy resources technology. 2011; 133.

[121] Nagraraja AM and Prabhukumar GP. Characterization and optimization of rice bran oil methylester for compressed ignition engines at different injection pressure. SAE. 2004; 28: 0048.

[122] Busch M. Understanding CHT and EGT. Cessna Pttots Amroeiotion. 2009.

[123] Venkanna BK, Swati B, Wadawadagi and Reddy Venkataramana C. Effect of injection pressure on performance, emission and combustion characteristics of direct injection diesel engine running on blends of pongamia pinnata linn oil (Honge oil) and diesel fuel. Agricultural engineering international The CIGR E-journal. 2009; 11: 1-17.

[124] Muralidharan K and Vasudevan D. Performance, emission and combustion characteristics of a variable compression ratio engine using methyl esters of waste cooking oil and diesel blends. Applied energy, 2011; 88: 3959-3968.

[125] Balaji TP, Vignesh, Balamurugan C, Vinayagam N and Gavaskar T. Experimental analysis and modelling of a four stroke single cylinder DI diesel engine under variable compression ratio. International journal of engineering science and technology. 2012; 4: 4029-4042.

[126] Raheman H and Ghadge SV. Performance of diesel engine with biodiesel at varying compression ratio and ignition timing. Fuel. 2008; 87: 2659-2666.

[127] Pugazhvadivu and Sankaranarayanan. Experimental studies on a diesel engine using mahua oil as fuel. Indian Journal of Science and Technology. 2010; 3: 787-791.

[128] Rao PV. Experimental investigations on the influence of properties of jatropha biodiesel on performance, combustion, and emission characteristics of a DI-CI engine. World academy of science, engineering and technology. 2011; 51: 854-867.

[129] Senthil Kumar M, Ramesh A and Nagalingam B. Complete vegetable oil fueled dual fuel compression ignition engine. SAE: Paper No: 2001; 28: 0067.

[130] Martin M and Prithviraj D. Performance of pre-heated cottonseed oil and diesel fuel blends in a compression ignition engine. Jordan journal of mechanical and industrial engineering. 2011; 5: 235-240.

[131] John BH. 1988. Internal Combustion Engine Fundamentals. McGraw Hill International 1st Edn., ISBN: 9780070286375, 779.

Resume

The author, Pritinika Behera, graduated in Mechanical Engineering from Seemanta Engineering College, Mayurbhanj in the year 2005. She did her postgraduate study in Mechanical Engineering with specialization in Thermal Engineering at the National Institute of Technology (NIT), Rourkela. Immediately after the completion of M.Tech in 2009, she continued her Ph.D at NIT, Rourkela in the Department of Mechanical Engineering. This dissertation is being submitted for the fulfilment of the Ph.D. degree

Permanent address

Pritinika Behera, c/o Shira Behera, At-Montapal, Post-Muktapur,
Via-B.sathilo, Dist-Mayurbhanj, Odisha-757025

E mail: priti.minu@gmail.com

List of publications

International Journals

1. **Pritinika Behera**, S. Murugan, (2013), "Combustion, performance and emission parameters of used transformer oil and its diesel blends in a DI diesel engine", Fuel, Elseiver publications, Vol.104, pp.47–154.
2. **Pritinika Behera**, S. Murugan, (2013), "Studies on a diesel engine fueled with used transformer oil at different fuel injection nozzle opening pressures", International Journal of Ambient Energy, Taylor & Francis publications, Accepted for publication.

International Journals [under review]

1. **Pritinika Behera**, S. Murugan, G. Nagarajan, Potential energy recovery from used transformer oil for a CI engine application, CTEP-D-13-00349, Clean Technologies end environmental policies.
2. **Pritinika Behera**, Sandip Belas Ekka and S. Murugan, Studies on the effect of higher compression ratio on the engine behaviour fueled with used transformer oil, IJEWM-53621, International journal of environment and waste management.
3. **Pritinika Behera**, Sandip Belas Ekka and S. Murugan, Studies on the effect of variable compression ratio on the engine behaviour fueled with used transformer oil, IJEWM-53621, International journal of environment and waste management.

4. **Pritinika Behera**, S. Murugan, G. Nagarajan, Dual fuel operation of used transformer oil with acetylene in a DI diesel engine, ECM-D-13-02394, Energy conversion and management.

International Conference

1. **Pritinika Behera** and S. Murugan , A Review of vegetable oils and their utilization in compression ignition engine, Vol-II, , International conference on Advances in renewable energy (ICARE) – 300, page 586-595.
2. **Pritinika Behera** and S. Murugan, Effect of nozzle opening pressure on the combustion, performance and emission parameters of DI diesel engine fueled with used transformer oil, SAE 2012 International powertrains, fuels & lubricants meeting, September 18, 2012, Malmo, Sweden, Paper Number: 2012-01-1584.
3. Sandip Belas Ekka, **Pritinika Behera** and S. Murugan, Performance and emission studies of a diesel engine with different compression ratios, International conference on alternative fuels for I. C. engines, ICAFICE – 300 at MNIT Jaipur from February 6-8, 2013, page 236-241.
4. **Pritinika Behera**, Abhishek Kumar Jha and S. Murugan, Dual fuel operation of used transformer oil with acetylene in a DI diesel engine, 1st International conference on metallurgical, manufacturing and mechanical engineering, ICMMME-23PUNMAR13-026.
5. **Pritinika Behera**, Niraj Toppo and S. Murugan, Waste management of disposed oil and characterization of used transformer oil as an energy source, International Conference on Advances in Mechanical and Energy Engineering-1135, Chennai.
6. **Pritinika Behera** and S. Murugan, Energy recovery from used transformer oil for small power generation, 4th International Conference on Advances in Energy Research, 149, 2013, IIT Bombay.

National Conference

1. **Pritinika Behera** and S. Murugan, Prospects of non-conventional energy from waste potential sources of energy, National conference on recent advances in chemical and environmental engineering, January 20-21, 2012, Page-47.
2. **Pritinika Behera**, Abhishekh Kumar Jha, S.Murugan, Characterization of used transformer oil & utilization as a fuel in CI engine, National conference on Advances in automotive engineering, 7th September, 2012.